INFORMATION TO USERS

This manuscript has been reproduced from the microfilm master. UMI films the text directly from the original or copy submitted. Thus, some thesis and dissertation copies are in typewriter face, while others may be from any type of computer printer.

The quality of this reproduction is dependent upon the quality of the copy submitted. Broken or indistinct print, colored or poor quality illustrations and photographs, print bleedthrough, substandard margins, and improper alignment can adversely affect reproduction.

In the unlikely event that the author did not send UMI a complete manuscript and there are missing pages, these will be noted. Also, if unauthorized copyright material had to be removed, a note will indicate the deletion.

Oversize materials (e.g., maps, drawings, charts) are reproduced by sectioning the original, beginning at the upper left-hand corner and continuing from left to right in equal sections with small overlaps.

Photographs included in the original manuscript have been reproduced xerographically in this copy. Higher quality 6" x 9" black and white photographic prints are available for any photographs or illustrations appearing in this copy for an additional charge. Contact UMI directly to order.

Bell & Howell Information and Learning
300 North Zeeb Road, Ann Arbor, MI 48106-1346 USA

UMI®
800-521-0600

A MECHANISTIC STUDY OF THE REACTIONS OF 1,1-DIARYLSILENES AND 1-SILASTYRENES

By

CHRISTINE JULIE ANN BRADARIC, B.Sc.

A Thesis

Submitted to the School of Graduate Studies

in Partial Fulfilment of the Requirements

for the Degree

Doctor of Philosophy

McMaster University

DOCTOR OF PHILOSOPHY (1998) **McMASTER UNIVERSITY**

(Chemistry) **Hamilton, Ontario**

TITLE: **A Mechanistic Study of the Reactions 1,1-Diarylsilenes and 1-Silastyrenes**

AUTHOR: Christine J. Bradaric, B.Sc. (McMaster University)

SUPERVISOR: Professor William J. Leigh

Number of Pages: xx, 217

ABSTRACT

The chemistry of 1,1-diarylsilenes, 1-phenylsilene and 1-methyl-1-phenylsilene has been studied using nanosecond laser flash and steady-state photolysis techniques. The silenes were generated by photochemically induced [2+2] cycloreversion of 1,1-diarylsilacyclobutane, 1-phenylsilacyclobutane and 1-methyl-1-phenylsilacyclobutane, respectively. Steady-state photolysis in the presence of alcohols, methoxytrimethylsilane, water and acetic acid yields the corresponding alkoxy-, hydroxy-, or acyloxysilane in high yield, consistent with the trapping of the silene by ROH or silyl ether. Steady-state photolyses in the presence of acetone afford silyl enol ethers exclusively, the product of an ene reaction between the silene and acetone.

Nanosecond laser flash photolysis of air saturated hexane, acetonitrile or tetrahydrofuran solutions of the silacyclobutanes leads to readily detectable transient absorptions in the 310-330 nm range which have lifetimes of 2-4 μs and have been assigned to the corresponding silenes. Increasing phenyl substitution at the silenic silicon atom results in red-shifts in the silene absorption maxima consistent with increasing conjugation of the chromophore. The transient absorption spectrum of 1,1-diphenylsilene in THF solution is broadened and red-shifted compared to that in hexane and acetonitrile, consistent with the formation of a silene-THF complex.

Absolute rate constants for reaction of the silenes with alcohols, trimethylmethoxysilane, acetic acid and acetone have been determined by NLFP techniques. Silene quenching follows a linear dependence on quencher concentration over the range investigated in all cases and proceeds with rate constants which vary over the range 10^7-10^9 $M^{-1}s^{-1}$. The absolute rate constants for reaction with alcohols, trimethylmethoxysilane and acetic acid are slightly faster for phenyl- and methylphenylsilene than for diphenylsilene. Deuterium kinetic isotope effects for reactions of the 1-silastyrenes (1,1-diphenylsilene, 1-phenylsilene and 1-methyl-1-phenylsilene) with methanol, *t*-butanol and acetone are consistent with a primary effect and rate determining proton transfer. Acetic acid addition is not subject to a deuterium kinetic isotope effect.

Steady-state competition experiments between 1,1-diphenylsilene and various alcohols and water have been carried out. The product ratios agree with the corresponding relative rate constants for water, methanol and ethanol. Those for methanol/*t*-butanol are significantly different from the rate constant ratio but approach it at very low total alcohol concentrations.

Reactions of the 1,1-diarylsilenes with alcohols, acetic acid, acetone and trimethylmethoxysilane afford small positive Hammett ρ-values consistent with initial nucleophilic attack by oxygen on silicon. Deuterium isotope effects and Arrhenius parameters have been determined for the reactions of 1,1-di-(4-methylphenyl)silene, 1,1-

diphenylsilene and 1,1-di-(4-trifluoromethylphenyl)silene with methanol, acetone and acetic acid. Methanol and acetone additions are characterized by negative activation energies, which are suggested to result from entropy dominated proton transfer within a reversibly formed silene-nucleophile complex. The kinetic isotope effects for methanol and acetone addition decrease with increasing electron withdrawing ability of the diaryl substituent and temperature. Acetic acid addition proceeds with a positive activation energy that increases in magnitude with increasing electron withdrawing ability of the substituent. This observation is consistent with a small enthalpic barrier to complex formation.

The above results are consistent with a two-step mechanism involving reversible formation of a zwitterionic complex, followed by intramolecular proton (or $SiMe_3^+$) transfer. The latter is rate determining in all cases but acetic acid, for which it is proposed that complexation is the rate determining step for reaction. The trends in kinetic isotope, substituent and temperature effects are rationalized in terms of variations in the relative rate constants for reversion of the complex to reactants and proton transfer as a function of substituent and temperature. In the case of alcohol additions, proton transfer from the complex to a second molecule of alcohol competes with the intracomplex proton transfer pathway at high alcohol concentrations, for all cases except *t*-butanol and acetic acid.

ACKNOWLEDGEMENTS

There are a number of people I would like to thank who have made a contribution to this thesis:

First of all I would like to thank my supervisor, Professor William Leigh, without whom this work would not be possible. Willie has always made himself available for guidance, assistance and new ideas. Willie sets forth an example of excellence, hard work and dedication that is truly an inspiration to all. I am very glad that I pursued study under his supervision over the past five years, and hope our professional and personal association continues.

I would like to thank my supervisory committee Professor Michael Brook and Professor Nick Werstiuk, who gave their time and insight at my committee meetings and in this thesis.

Thanks to Mr. Brian Sayer and Dr. Don Hughes for assistance with the operation of the NMR spectrometers and Dr. Richard Smith for his assistance with the GC/MS.

Thanks to Dr. Greg Sluggett, Dr. Al Postigo, and Dr. Mark Workentin who helped me in the lab when it all began. Thanks for training me on all the instruments and great advice.

Thanks to my former and current lab-mates: Jo-Ann, Mike, Nick, Ed, Bruce and Tracy who made life in the lab lots more fun. Dr. Corinna Kerst thanks for all the discussions about my work and your friendship.

Dad, Mom and Robbie, the best family in the world. You were my first teachers and helped build the foundation upon which I stand. Thanks so much for your love and support in everything I pursue.

Finally, thanks to the love of my life, Louis. You are my destiny.

TABLE OF CONTENTS

LIST OF SCHEMES

LIST OF FIGURES

LIST OF TABLES

CHAPTER 1

INTRODUCTION

1.1 Doubly Bonded Compounds Containing Silicon

Over the past ten years interests in organosilicon and, more recently, organogermanium chemistry have focused on the study of the unsaturated analogues of alkenes containing silicon or germanium, i.e., silenes (**1**), germenes, disilenes (**2**), digermenes, and silagermenes (**3**). For many years chemists believed these compounds to be too unstable to exist due to poor π-bond overlap and longer bond distances. Indeed most silenes, germenes, disilenes, etc. are short-lived reactive intermediates found in many organosilicon (organogermanium) reactions.

Scheme 1.1 **Doubly Bonded Compounds Containing Silicon or Germanium**

M, M' = Si, Ge

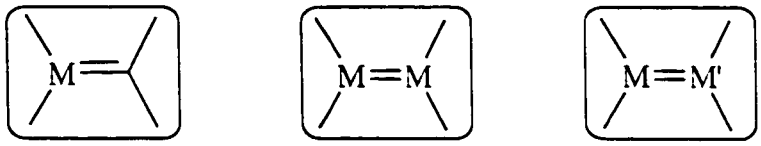

1 **2** **3**

In 1967 Gusel'nikov and Flowers reported the first indirect evidence of a transient silene, 1,1-dimethylsilene (**5**) (eq 1.1).[1] Gas phase pyrolysis of 1,1-dimethylsilacyclobutane (**4**) yielded 1,1,3,3-tetramethyl-1,3-disilacyclobutane (**6**), the head-to-tail dimer of the intermediate **5**.

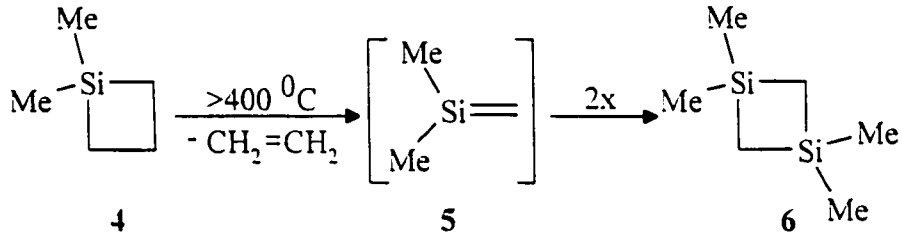

4 **5** **6** **1.1**

With this result began the investigation of these compounds in great detail.[2-5] Most known silenes, disilenes and the corresponding germanium analogues (**1-3**) are highly reactive and have been postulated as intermediates on the basis of indirect methods such as chemical trapping experiments.[2,3,5,6] More recently the application of transient spectroscopic techniques such as matrix isolation[2,7] and laser flash photolysis techniques[7-10] have allowed these reactive species to be studied by direct methods. Several stable silenes and disilenes have been reported and the factors which contribute to their stability are reasonably well established.[11-14] Current interests in our group have focused on the study of the reactions of transient silenes in solution.

1.2 Physical Properties of Silenes

In the early 1980's theoretical calculations focused on characterizing the properties of silene, $H_2Si{=}CH_2$ (**7**). The reasons for the much higher reactivity of silenes become apparent from a comparison of the calculated physical properties of (**7**) and ethylene (**8**) (Table 1.1). The ground-state molecule is a singlet and is calculated to be planar.[15-17] The Si=C equilibrium bond length is calculated to be about 1.705 Å [16], which should be compared to the experimental value of 1.702 Å obtained from X-ray analysis of the stable silene 1,1-dimethyl-2-(trimethylsilyl)-2-(di-tert-butylmethylsilyl)-silene.[20]

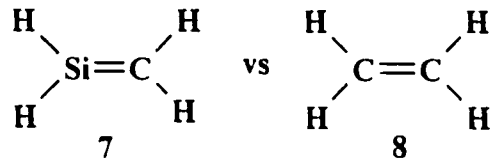

7 **8**

Table 1.1 Calculated Physical Properties of Silene (**7**) and Ethylene (**8**).[a]

	$H_2C=CH_2$	$H_2Si=CH_2$
Bond Length (A)	1.33	1.70
Dipole Moment (D)	0	0.84
π-Bond Energy (kcal/mol)	65	38
$\nu_{X=C}$ (cm^{-1})	1640	985
λ_{max} (nm)	165	258
π-IP (eV)	10.5	8.8

[a] Data from reference 2.

The calculated π-bond energy in **7** (as defined by the height of the barrier to cis-trans isomerization) is 38 kcal/mol using a MCSCF/3-21G basis set. By contrast, ethylene (**8**) has a π-bond energy of 65 kcal/mol.[21] Silene's ground-state calculated dipole moment is 0.84 D, corresponding to charges of about -0.6e on carbon and +0.5e on silicon.

The effects of substituents directly bonded to silicon and carbon on calculated silene geometries, charge distribution, and relative thermodynamic stability have been investigated by Apeloig and Karni.[11] They proposed that the polarity of the π-bond is the most important factor affecting silene reactivity i.e., substituents which increase the natural polarity of this bond, $C^{\delta-}$-$Si^{\delta+}$, lead to shortening of the bond and enhanced reactivity. The calculations indicate that π-donor substituents at silicon and π-acceptors

at carbon accomplish both these tasks. Thus, π-acceptors (e.g. CN, NO_2) bonded to carbon (or silicon) increase (or decrease) the positive π-charge at silicon relative to **7**. π-Donors, (e.g. OH, $OSiH_3$) exert the opposite effect. Hyperconjugative substituents such as CH_3- or $SiMe_3$- were predicted to induce a milder effect.[11]

Later, Nagase and coworkers examined the addition of water and HCl to $H_2Si{=}CH_2$, $Me_2Si{=}CH_2$, $F_2Si{=}CH_2$ and $H_2Si{=}CH(OH)$ using ab initio calculations at the HF/6-31G*//3-21G level.[22] These calculations were consistent with the results of Apeloig *et al.* and predicted the following order of reactivity towards water addition: $H_2Si{=}CH(OH) < H_2Si{=}CH_2 < F_2Si{=}CH_2$.

Multiple substitution with sterically bulky substituents generally leads to enhanced kinetic stability of the Si=C bond; a number of tetrasubstituted silenes survive in solution or as solids at room temperature and can be handled easily by the standard methods of organic chemistry using vacuum line techniques.[5]

Silenes exhibit dramatic red-shifts in their UV absorption maxima compared to alkenes. This difference is thought to be due to the smaller separation between the highest occupied molecular orbital (HOMO) and the lowest unoccupied molecular orbital (LUMO) of silene.[2] For example, silene (**7**) has an absorption maximum, λ_{max} = 258 nm *versus* ethylene (**8**) whose λ_{max} = 165 nm. Silenes substituted with simple alkyl groups exhibit absorption maxima in the 240-260 nm range but as the number of vinyl or aryl substituents increase, so do the absorption maxima (Table 3.2).[2,5]

1.3 Thermal and Photochemical Reactions Yielding Silenes

Silenes are formed in a number of thermal and photochemical reactions of organosilicon compounds. Typical routes include thermal or photochemically induced cycloreversions,[1,23] electrocyclic reactions,[24] rearrangements[20,25-27] and elimination reactions.[6,28] Photochemical [2+2] cycloreversions of silacyclobutanes and 1,3-sigmatropic shifts in aryl- and vinyldisilanes have been the two methods of silene generation employed by our group for time-resolved spectroscopic studies of their reactivity.[8-10,29,30]

1.3.1 Silenes from Cycloreversion of Cyclic Organosilicon Compounds

By far the most convenient thermal and photochemical route to silenes is the [2+2] cycloreversion of silacyclobutanes. Simple transient silenes bearing small substituents such as H, Me and Aryl are typically generated in this manner (eq 1.2).[1,3,5,7] Silenes have also been generated by retro-Diels-Alder reaction of silabicyclo[2.2.2]-octadiene derivatives (eq 1.3).[31-33] Reactions of silenes with ketimines yield the [2+2] and [2+4] cycloadducts which have been used as storable sources of silenes such as $Ph_2Si{=}C(TMS)_2$ and $Me_2Si{=}C(TMS)_2$ (eq 1.4).[6]

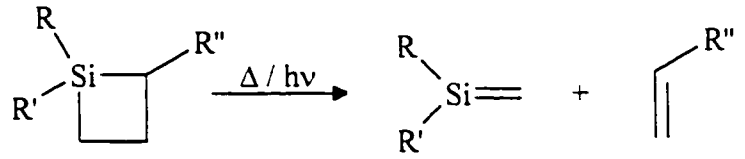

1.2

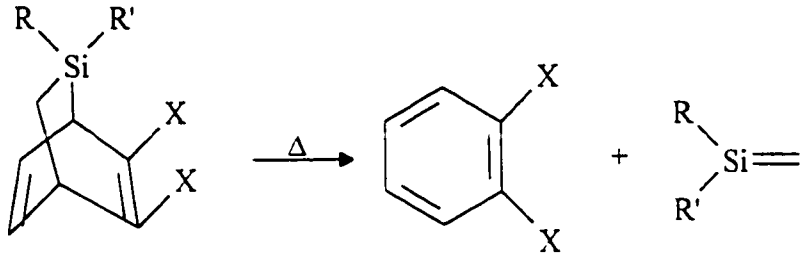

1.3

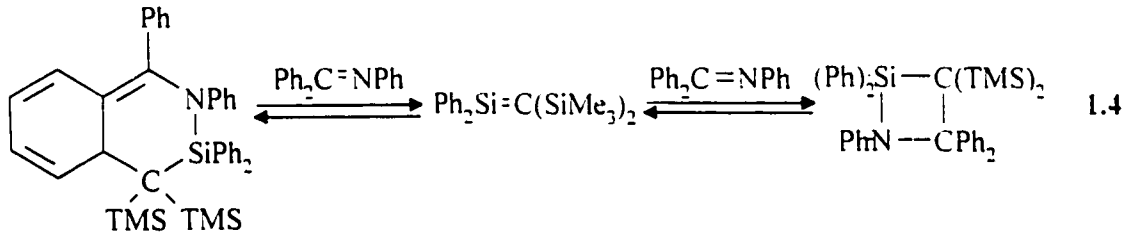

1.4

1.3.2 Silenes from Photochemically Induced 1,3-Sigmatropic Shifts

In 1972, Boudjouk and Sommer reported that irradiation of pentaphenylmethyldisilane led to products consistent with the formation of 1,1-diphenylsilene (**12a**).[34] In 1992, Leigh and Sluggett examined the photochemistry of a series of aryldisilanes and found products consistent with dehydrosilylation leading to simple silenes, 1,3-silyl migration leading to the formation of silahexatrienes, and silyl radical formation (eq 1.5).[35] The product distributions were found to be dependent on the steric bulk at the silicon atom and the solvent. Formation of simple silenes requires that one silicon be substituted with a methyl group and the other have a bulky substituent,

while silyl-migration to yield a silahexatriene is favoured when the migrating group is a relatively small trialkylsilyl moiety. Silyl radical formation begins to compete when both substituents bear radical stabilizing substituents. A variety of other 1,3,5-silahexatrienes have also been generated in this manner from the photolysis of 1,1,1-trialkyl-2,2,2-triphenylsilanes ($Ph_3Si\text{-}SiR_3$; SiR_3 = $SiMe_3$, $SiEt_3$, $SiMe_2{}^tBu$).[36]

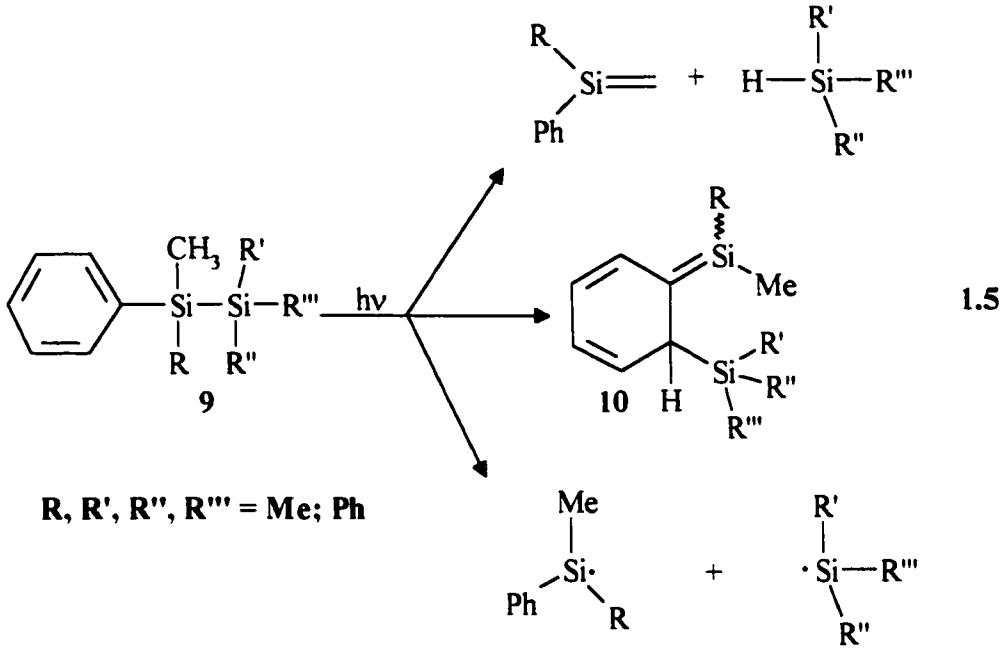

Brook and coworkers have described acyldisilanes as convenient photochemical precursors to stable silenes.[3,5] Photolysis of acyldisilanes (eq 1.6) and acylpolysilanes (eq 1.7) results in a 1,3-silyl shift from silicon to oxygen yielding a silene. The stability of the silenes depends on the steric bulk of R.[13,14] When R is 1-adamantyl, mesityl, triethylmethyl or 1-methylcyclohexyl, the silenes are stable at room temperature for weeks or longer.

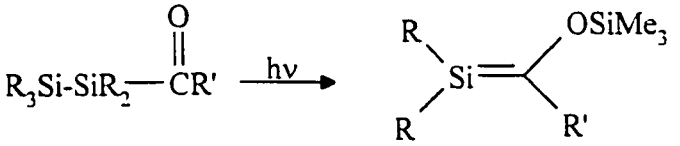

1.6

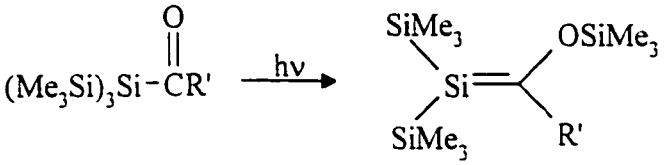

1.7

Upon irradiation of vinyldisilanes a 1,3-shift of a silyl group from silicon to the sp^2-hybridized carbon occurs with the formation of a silene (eq 1.8).[37] Silenes generated in this manner are not stable and, in the absence of a trap undergo head-to-tail dimerization.

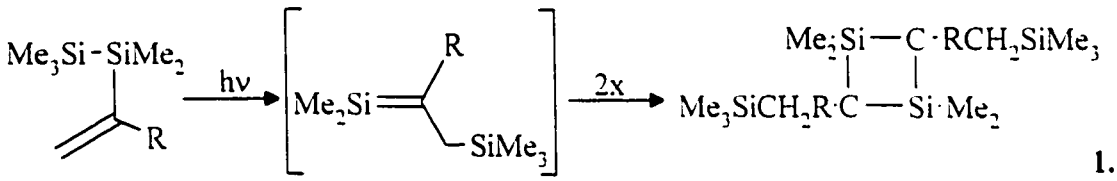

1.8

1.3.3 Thermal or Photochemical Isomerizations of Silylcarbenes

Photolysis or thermolysis of disilyldiazoalkanes[20,25] leads to disilylcarbenes [26,27] (eq 1.9) which undergo thermal 1,2-silyl rearrangement to the carbenic center, yielding a silene. A number of silenes have been generated by the photolysis of disilyldiazoalkanes bearing a variety of groups which include R = COMe, H and CO_2Et (eq 1.9).[20,25] In the cases where R = CO_2R', the silenes further rearrange to an alkoxyketene (eq 1.10).[26,27]

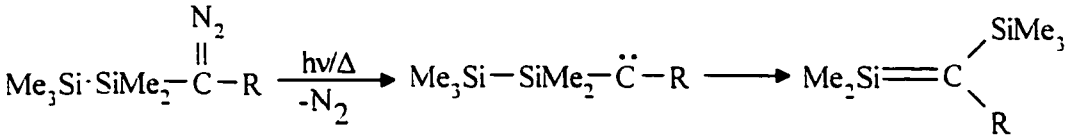

1.9

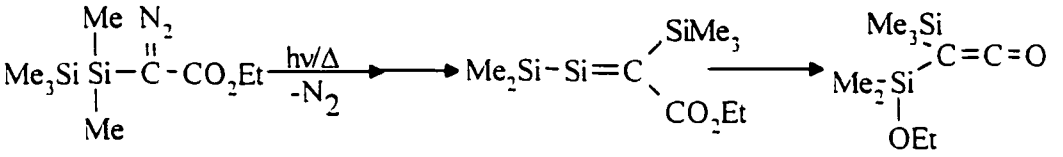

1.10

1.3.4 Thermally Generated Silenes by Salt Elimination Reactions

Jones *et al.* in 1977 first demonstrated that silenes could be generated thermally by salt-elimination reactions (eq 1.11).[28] Addition of *t*-butyllithium to the carbon-carbon double bond of vinylchloro- or fluoro-silanes, followed by loss of lithium halide, results in the formation of silenes as shown in the example below.[28]

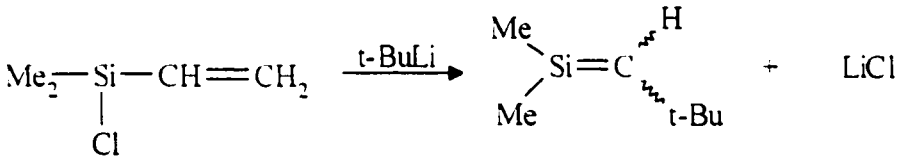

1.11

In the 1980's Wiberg established the conditions for silene generation from 1,2-salt elimination from adjacent silicon and carbon atoms (eq 1.12).[6] Thermolysis of a molecule containing a metal (typically lithium) attached to carbon and a leaving group (i.e. halide, sulfide or phosphate) bonded to silicon results in the formation of silene and a

salt. They described conditions for preparation of a number of silenes in this general manner, including the stable silene shown in the example below.[6]

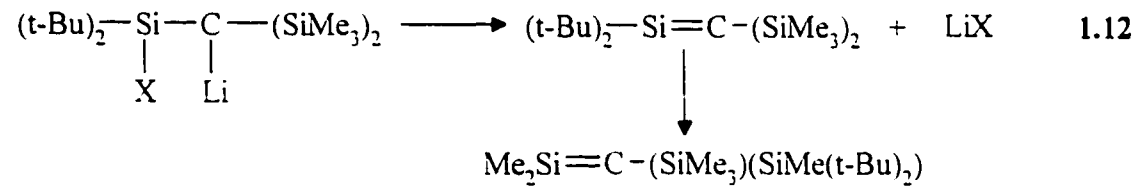

1.12

1.4 Silene Reactions

The major obstacle in isolating silenes is believed to be their high reactivity towards nucleophilic and electrophilic additions, and dimerization to disilacyclobutanes. Some factors which contribute to the higher reactivity of the silene π-bond in comparison to alkenes are the polarization of the bond, the weaker bond strength and longer bond length. Due to their much higher reactivity, silenes are involved in many reactions which are uncharacteristic to alkenes. The following sections discuss the typical reactions of silenes, with emphasis on the mechanisms of silene dimerization and reactions with alcohols and carbonyl compounds.

1.4.1 Silene Dimerization

Almost all silenes dimerize or oligomerize in the absence of external trapping agents.[2] The head-to-tail regiochemistry which is most commonly observed is consistent with the polarization of the silicon-carbon double bond.[1,2,38,39] The head-to-tail dimerization of silene (7) is calculated to be exothermic by 76 kcal/mol and have an activation energy of 5.2 kcal/mol.[11] Head-to-head dimerization is also observed, although to a lesser extent because this regioisomer is calculated to be 20 kcal/mol less stable than the head-to-tail dimer.[10] Silenes which do not dimerize contain very bulky substituents (e.g. Ad, Mes, *t*-Bu, $OSiMe_3$) attached to at least one end of the Si=C double bond and are considered "stable silenes."[3,5,14] Steric effects are presumed to hinder the process.

The mechanism of dimerization has been the subject of many theoretical studies.[11,17,40,41] Several groups have suggested that head-to-tail dimerization occurs in a concerted manner, even though it is forbidden on the basis of orbital symmetry selection rules.[17] Recently, Grev *et al.* have been able to calculate transition states leading to concerted formation of silene dimers. The presence of heteronuclear bonds has been suggested to relax orbital symmetry restrictions to dimerization.[40] However, the debate continues with the results of Bernardi *et al.* [41]who have reported that dimerization via a biradical intermediate provide a lower energy pathway than concerted $\pi 2s + \pi 2s$ cycloaddition (eq 1.13).

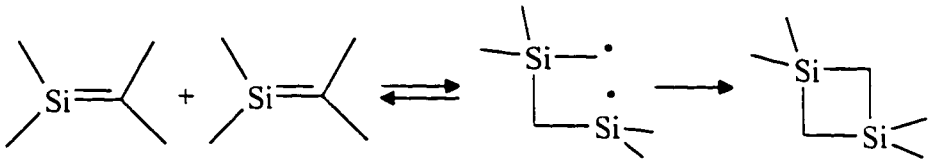

1.13

Head-to-head dimerization has been observed in silenes which bear substituents that decrease the natural polarity of the double bond.[5,11] Silenes of the type $(TMS)_2Si{=}C(OTMS)R$ undergo head-to-head dimerization exclusively to yield 1,2-disilacyclobutanes. Linear dimers formed via ene type cycloaddition are also observed if R is an alkyl group which contains an allylic hydrogen.[12] Experimental evidence supports a biradical mechanism for dimerization (eq 1.14). For example, a strong ESR signal is observed during the photolysis of the acylsilane, $(Me_3Si)_3SiCOCMe_3$, which is identical to the signal produced when the head-to-head dimer is dissolved in pure solvent.[13]

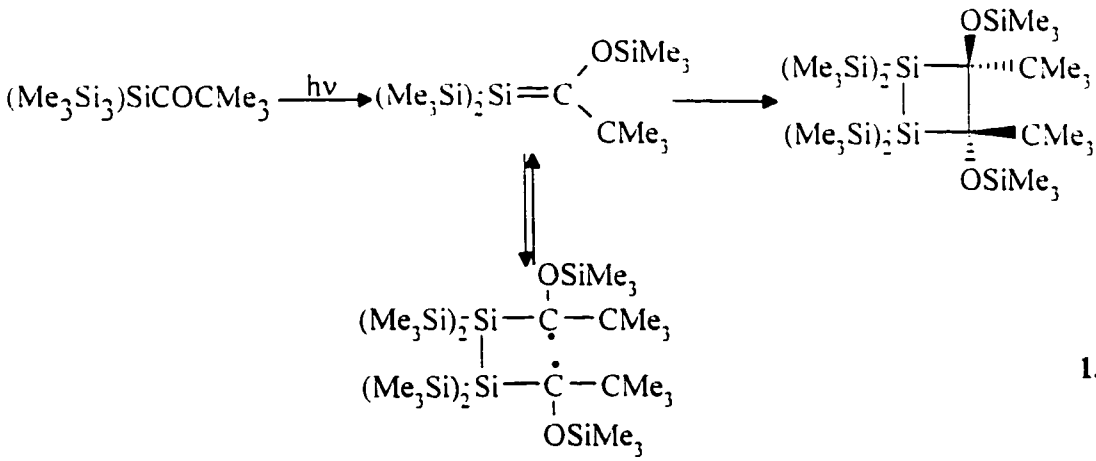

1.14

Activation parameters have been reported for the head-to-head linear dimerization of 1,1-bis(trimethylsilyl)-2-methyl-2-(trimethylsiloxy)silene to give an acyclic disilane (eq 1.15) in cyclohexane solution. The silene dimerizes with an Arrhenius activation

energy of 0.2 kcal/mol and a log(A) of 7 $M^{-1}s^{-1}$. The authors concluded that the reaction occurs via a highly ordered transition state and suggested two possible mechanisms. The first proposed mechanism involves a biradicaloid which disproportionates intramolecularly while the other is a concerted bimolecular ene type mechanism.[7]

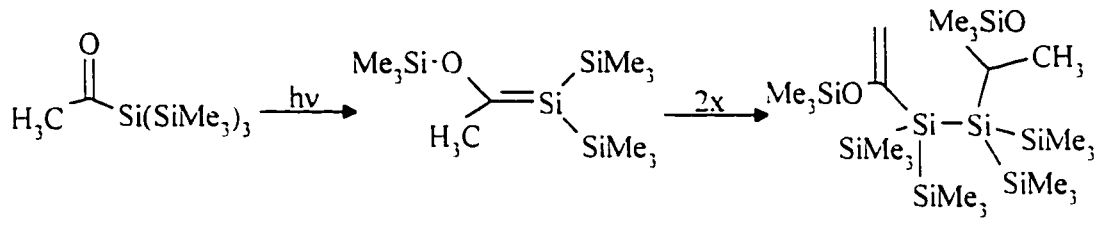

1.15

1.4.2 Reactions of Silenes with σ-Bonded Compounds

Silenes react with many σ-bonded nucleophiles including water, alcohols, hydrogen and alkyl halides, amines and silyl ethers (eq 1.16).[2,3,5,6,42] The most commonly employed transient silene trap is methanol, and the mechanism of its addition has been the subject of considerable interest.[6,9,24,29,30,43-45]

Scheme 1.2 Reactions of Silenes with σ-Bonded Nucleophiles

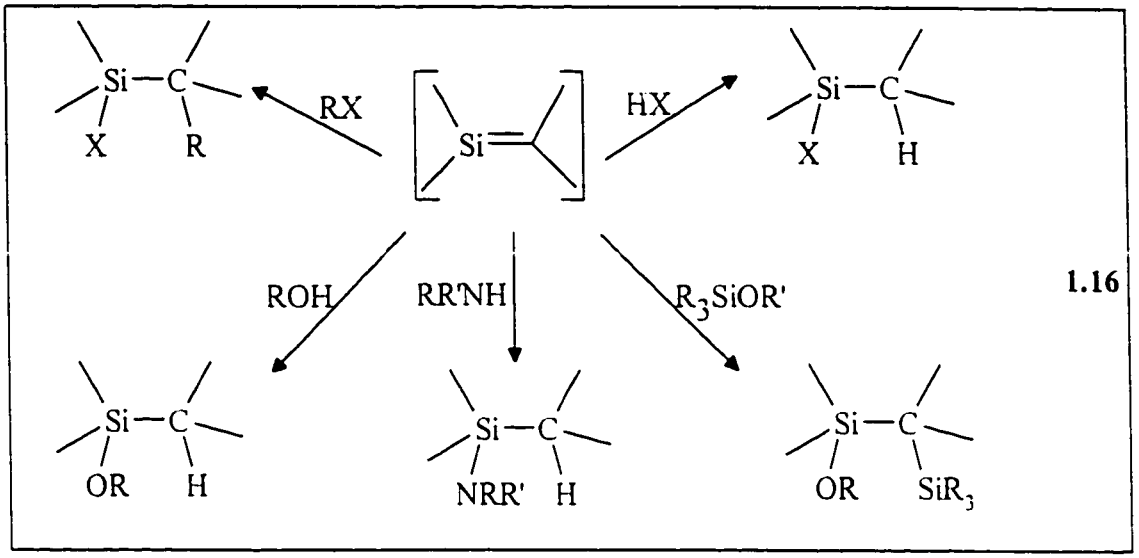

1.4.3 Mechanism of Alcohol Additions to Silenes

In the early eighties Wiberg studied the relative rates of addition of various alcohols to 1,1-dimethyl-2,2-bis(trimethylsilyl)silene[9] and found the following order of increasing reactivity PhOH < cyclohexanol < 1-pentanol < *t*-BuOH < i-PrOH < EtOH < MeOH. Thus, the rate of reaction increases with increasing nucleophilicity of the alcohol and acidity plays a secondary role. A similar conclusion was reached for the relative rates of reaction of a series of amines. In a competition experiment to determine the effect of steric bulk on addition, it was found for the equally sterically hindered nucleophiles *t*-$BuNH_2$ and *t*-BuOH, that the more nucleophilic amine reacted faster. They also concluded that methanol and methanol-Od react with the same rate. A two-step

mechanism involving initial nucleophilic attack by oxygen on silicon forming a silene-alcohol complex, followed by fast proton transfer to carbon, was proposed (eq 1.17).

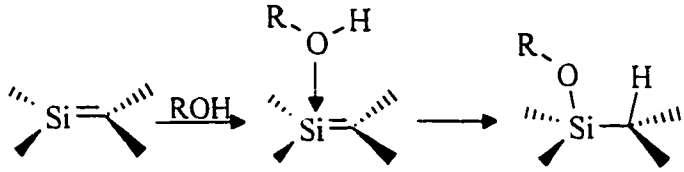

1.17

A number of studies on the stereochemistry of alcohol additions to stable and transient silenes have been reported. Jones *et al.* showed that thermolysis of the anthracene [2 + 4] cycloadduct of (*E*)- and (*Z*)-1-phenyl-1-methyl-2-neopentyl-2-(trimethylsilyl)silene in the presence of methanol gave exclusively the *syn*-addition product (eq 1.18).[32] Since the extent of decomposition of the anthracene cycloadduct was independent of methanol concentration, the authors concluded that methanol addition to silenes is stereospecific.

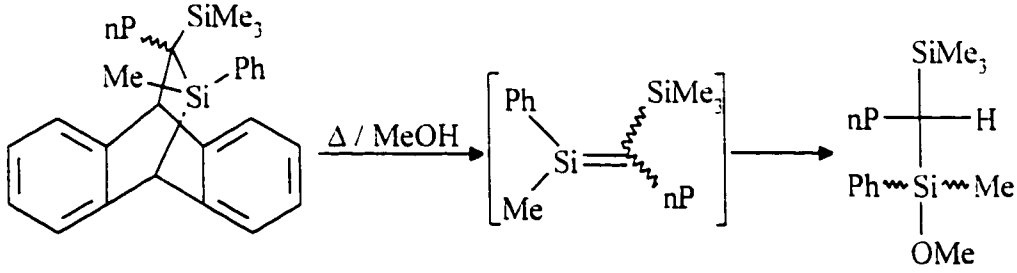

nP = neopentyl

1.18

However, these results contradicted reports on the addition of methanol to stable silenes generated from the photolysis of acylsilanes. When a single silene geometric isomer was treated with methanol, a 3:1 ratio of diastereomers was obtained, implying nonstereospecific alcohol addition (eq 1.19).[46]

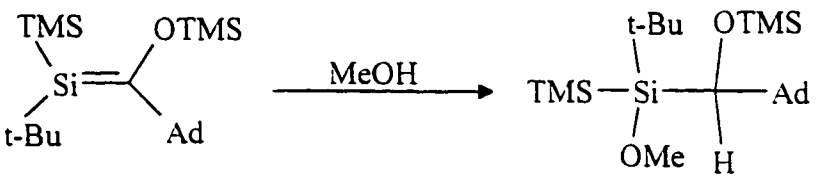

1.19

Studies on the mechanism of alcohol addition to silenes continued with Kira *et al.* who examined the stereospecificity of addition of various alcohols to a cyclic silene.[47] Alcohol addition resulted in a mixture of *syn* and *anti* adducts, whose ratio varied with alcohol concentration (eq 1.20).[47] The amount of *syn* selectivity increases in the order of methanol < *n*-propanol < *iso*propanol << *tert*-butanol and decreases with increasing alcohol concentrations for all cases but *t*-butanol, for which exclusively *syn*-addition is observed at all concentrations. On the basis of these results a mechanism involving initial formation of a silene alcohol complex, followed by competing intra- and inter-molecular proton transfer was proposed (eq 1.20). Intracomplex proton transfer yields the *syn* adduct, while intermolecular proton transfer from a second molecule of alcohol results in *anti* adduct formation.

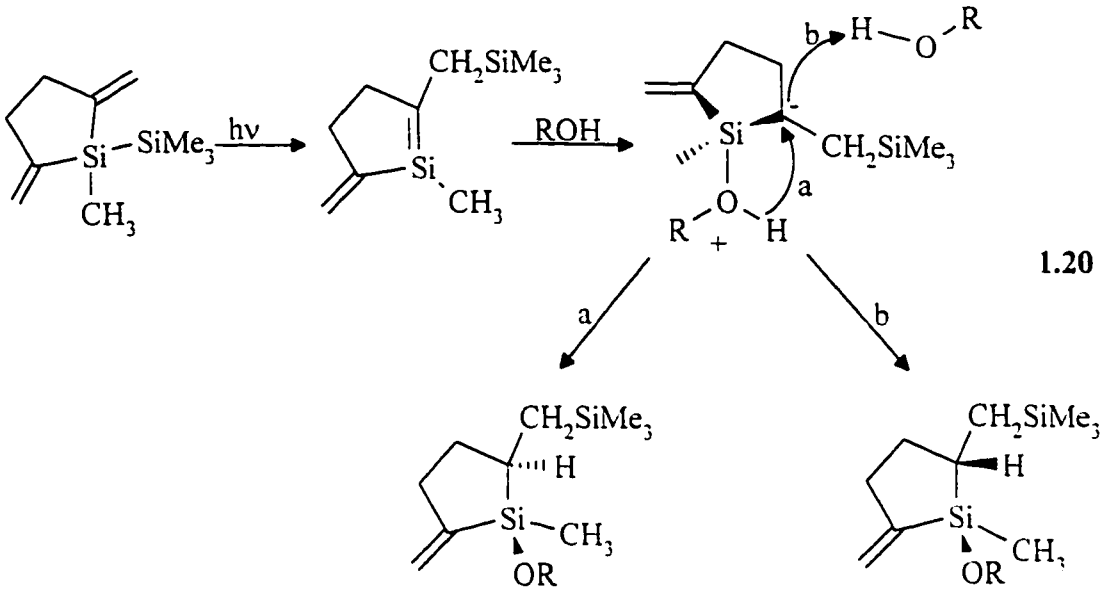

1.20

An alternative explanation for the apparent stereospecificity of addition observed by Jones was given recently.[5] It was suggested that a molecule of methanol may complex with the silicon-atom of the silene-anthracene adduct, followed by a [2+4] cycloreversion to yield anthracene and the silene-alcohol complex (eq 1.21). Since one face of the silene portion of the adduct is screened by the bulky anthracene molecule only *syn* addition is predicted.

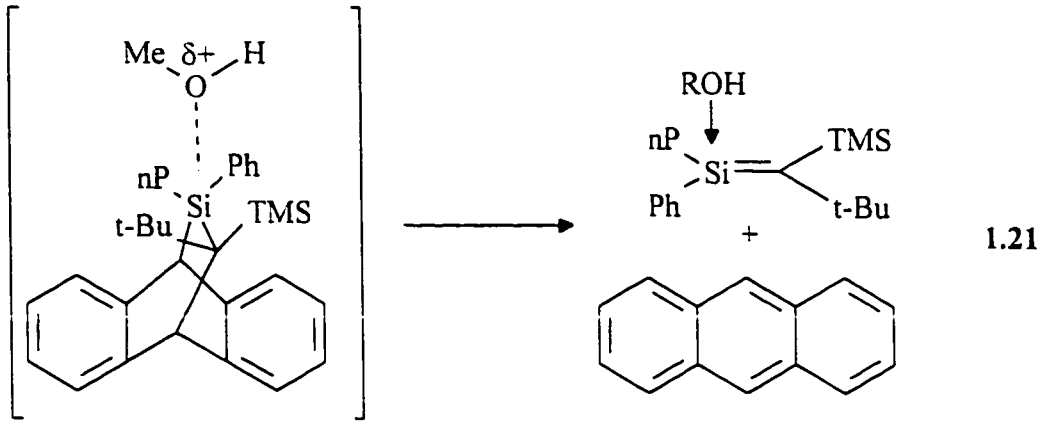

1.21

Another example of the concentration dependent silene-alcohol addition was reported by Steinmetz and coworkers.[24] Direct photolysis of 1,1-dimethyl-1-silacyclobutene in *t*-butanol yielded the (*Z*)- and (*E*)-adducts, formed from [1,4]-addition of the alcohol to the *s-cis* and *s-trans* conformers of the 1,3-silabutadiene, respectively, as well as the [1,2]-addition product (eq 1.22).

Studies of the product ratios, as a function of *t*-butanol concentration, revealed that as the alcohol concentration decreases the yield of the 1,2-adduct increases, the yield of the (E)-adduct decreases, and the yield of the (Z)-isomer remains essentially constant. The fact that the *Z*-isomer yields did not vary was interpreted to be due to a rapid equilibrium between *s-cis* and *s-trans* silabutadiene conformers.

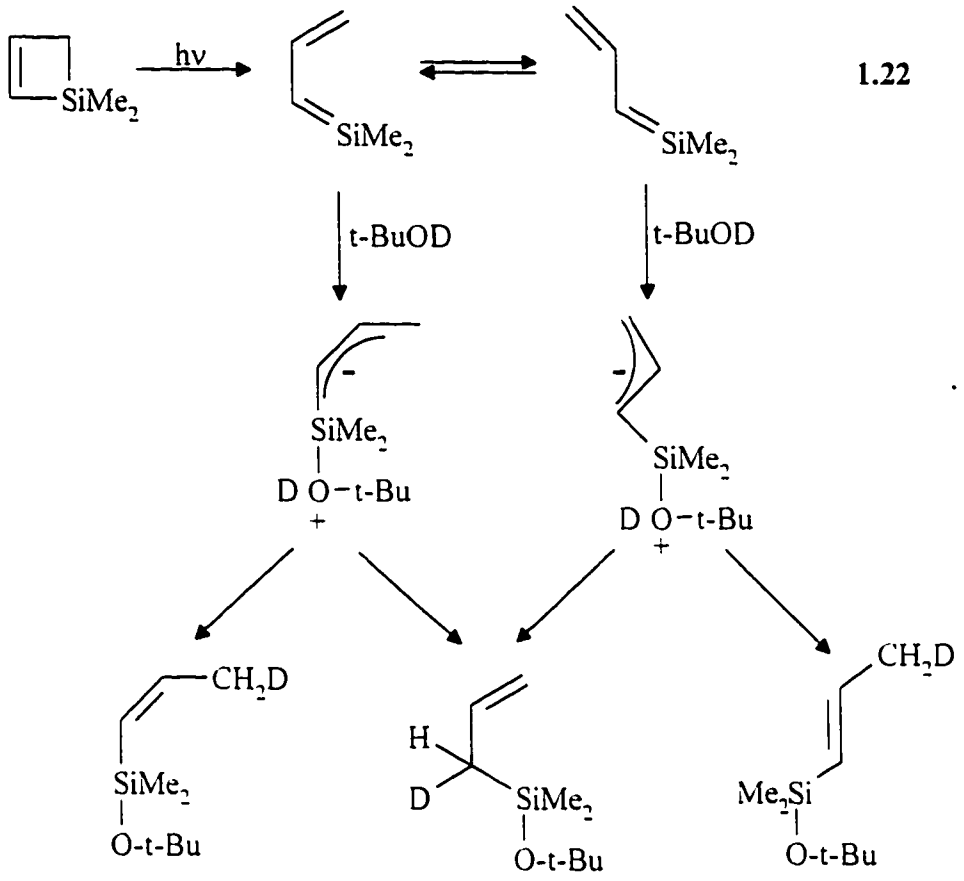

1.22

The variation in the yield of the (*E*)-isomer with alcohol concentration was attributed to a difference in the partitioning of the *s-trans* complex to products. It was proposed that proton transfer may be mediated by the alcohol, especially in the case of the (*E*)-adduct, where the distance involved is predicted to make intramolecular proton transfer difficult. Thus, the requirement of another molecule of alcohol (solvent) for (*E*)-adduct formation was added to account for the decrease in yield with decreasing alcohol concentration. The lack of variation in the yield of the (*Z*)-isomer with alcohol

concentration was attributed to the fact that this product can be formed by either intra- or intermolecular proton transfer.[24]

The most comprehensive study of alcohol additions to transient silenes was presented by Leigh and coworkers through the use of steady-state and laser flash photolysis (LFP) studies on the reactions of 1,3,5-silahexatrienes with various alcohols.[9,44] Steady-state photolysis (254 nm) of pentamethylphenyldisilane in the presence of methanol results in the formation of the [1,2]-, [1,4]-, and [1,6]-alcohol silatriene addition products (eq 1.23). The [1,2]-adduct predominates at low alcohol concentrations ([MeOH] < 0.005 M), while the [1,4]- and [1,6]-adducts predominate at higher concentrations ([MeOH] > 1 M).

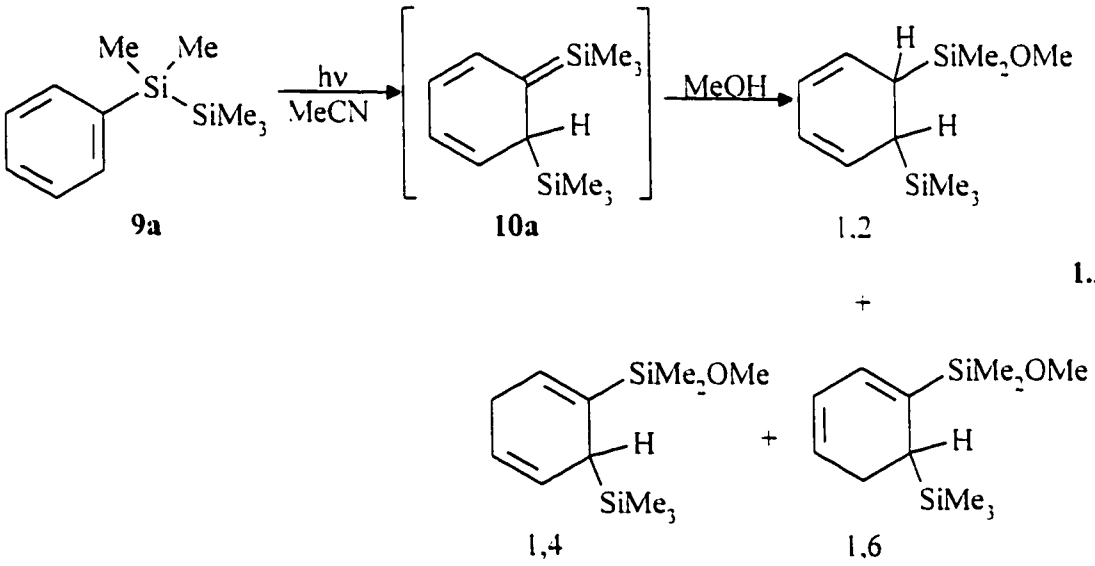

9a **10a** 1,2 **1.23**

1,4 + 1,6

Plots of the rate constant for decay of the silene *versus* alcohol concentration as determined by LFP, are curved for reactions with methanol, ethanol, water or *tert*-butyl

alcohol. These plots can be fit to a quadratic dependence of the rate constant for decay of the silatriene on alcohol concentration. For less nucleophilic and more acidic reagents, such as 2,2,2-trifluoroethanol and acetic acid, the rates are first order with respect to quencher concentration and, as a result, exhibit linear quenching kinetics. On the basis of these observations, a mechanism involving reversible formation of a zwitterionic silene-alcohol complex, followed by competing intra- and extra-complex proton transfer, was proposed (eq 1.24).[44]

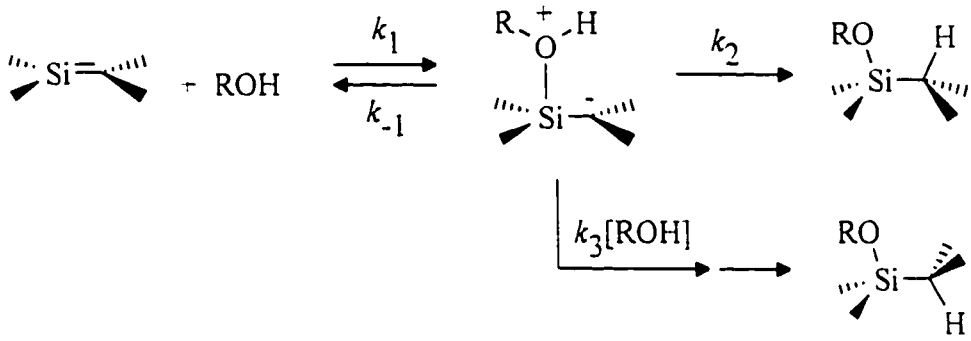

1.24

Kinetic data obtained for the reaction of the silatrienes with diols and reactions with methanol in THF suggest that the extracomplex proton transfer pathway proceeds via a general base catalysis mechanism. The solvent (THF) or alcohol deprotonates the complex in the rate-determining step.[44] For the acidic and less nucleophilic quenchers complex formation is rate-determining.[44] The corresponding rate law for decay of the silene (applying the steady-state approximation for the complex) is given in eq 1.25.

$$k_{decay} = k_o + \frac{k_1[ROH]}{(k_{-1} + k_2 + k_3[ROH])}(k_2 + k_3[ROH]) \qquad \textbf{1.25}$$

if $k_{-1} >> k_2 + k_3[ROH]$

$$k_{decay} = k_o + (k_1k_2/k_{-1})[ROH] + (k_1k_3/k_{-1})[ROH]^2$$

The rate constant ratios for intra- to extracomplex proton transfer (k_2/k_3) for reactions with methanol in acetonitrile are 0.05 M for the silatriene derived from pentamethylphenyldisilane[44]and 4.6 M for Kira's cyclic silene (eq 1.2).[47] The difference was attributed to the stabilizing effect of the cyclohexadienyl substituent at the silenic carbon which allows both pathways to compete at sufficiently low alcohol concentrations that they can be observed kinetically. It was predicted that simple and more reactive silenes of the type $R_2Si=CH_2$ (i.e., devoid of anion-stabilizing substituents) should exhibit linear alcohol-quenching kinetics with the effects of the second pathway becoming observable only at high alcohol concentrations, such as those employed by Kira and coworkers in product studies.[44]

1.4.4 Stereospecificity of Alkoxysilane Additions to Silenes

Alkoxysilanes are another class of commonly employed trap for transient silenes,[2,3] yet few studies have examined the mechanism of their addition. It is generally accepted that reaction between alkoxysilanes and silenes is a stereospecific *syn* addition.

Jones *et al.* have shown that pyrolysis of the anthracene adduct of (*E*)-1-methyl-1-phenyl-2-neopentylsilene in the presence of methoxytrimethylsilane or methoxytriphenylsilane yields the single diastereomeric adduct (eq 1.26).[31]

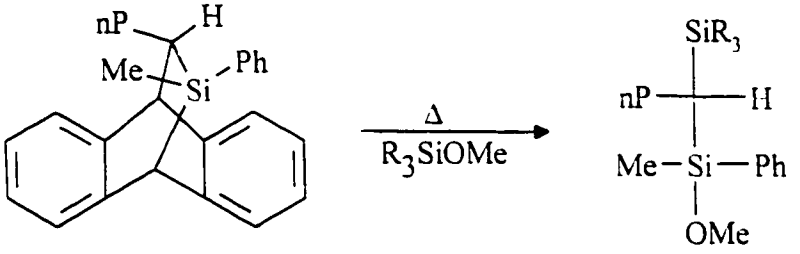

1.26

nP = neopentyl

Another example of the stereospecificity of this reaction was reported by Fink. The addition of methoxytrimethylsilane to 1-mesityl-2,3,4-tri-*tert*-butyl-1-silacyclo-1,3-butadiene (eq 1.27), generated in a 3-MP glass at 77 K by the photoisomerization of mesityl(1,2,3-tri-*tert*-butylcyclopropenyl)silylene and in the presence of excess alkoxysilane, yields only one isomer of the addition product.[48] In comparison to alcohol additions, it is unlikely that a second molecule of alkoxysilane would be involved in these reactions.

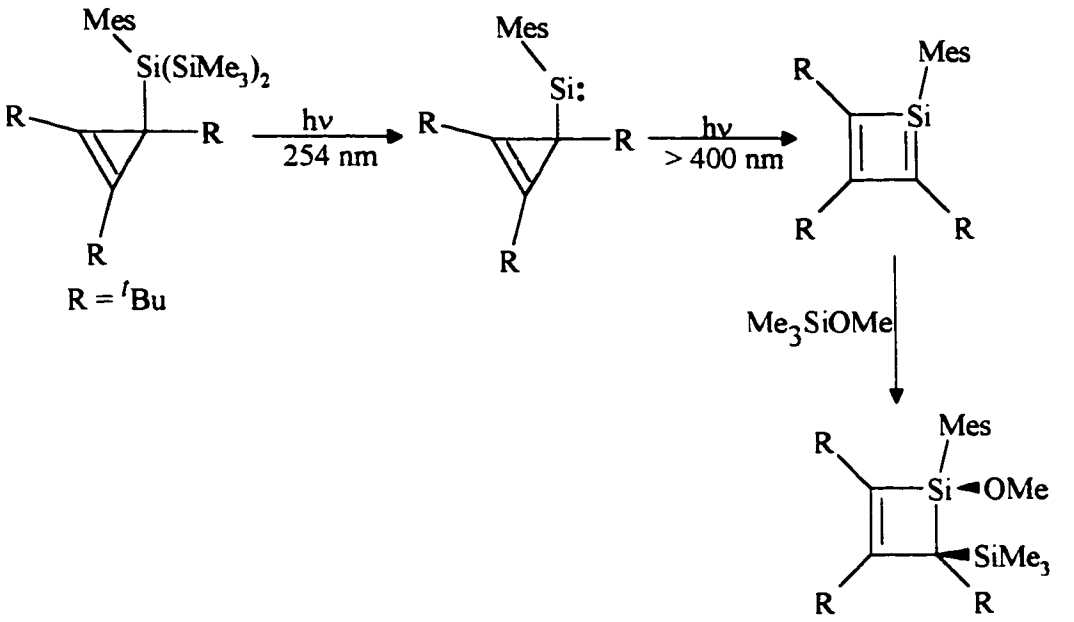

1.27

There have been few reports which described transient spectroscopic techniques to study these reactions directly. An upper limit for the rate constant for reaction of trimethylmethoxysilane with 1,3,5-silahexatrienes of $< 10^5$ $M^{-1}s^{-1}$ was reported,[49] which is about three orders of magnitude slower than those for reactions with methanol. The slower reactivity was suggested to be a result of either a difference in the rate of complex formation between the two quenchers or a difference in the rates of trimethylsilyl *versus* proton transfer.[9]

In spite of the widespread use of alkoxysilanes as trapping agents for reactive silenes there are relatively few kinetic reports on these reactions. In the early 1980's, a study on the effects of temperature on the rate constant for the reaction of 1,1-dimethylsilene with trimethylmethoxysilane in the gas-phase resulted in an Arrhenius activation energy of (1.5 ± 0.8) kcal/mol and log A of (5.3 ± 0.2) $M^{-1}s^{-1}$.[50] It was

suggested on the basis of all of the above observations that trimethylmethoxysilane undergoes 1,2-addition across silicon-carbon double bonds in a concerted manner.[24,31]

1.4.5 Reactions of Silenes with π-Bonded Compounds

Silenes also react with π-bonded compounds such as 1,3-dienes, alkynes, alkenes, azo compounds, as well as heteroatom-containing compounds such as carbonyl compounds, imines and nitriles.[2,3,5]

1.4.6 Reactions of Silenes with Alkenes

Silene reactions with dienes generate the [2+2]-, [4+2]- and ene adducts (eq 1.28), whose relative yields depend on the polarity of the silicon carbon double bond, electron density in the diene, and steric factors.[5] The effects of diene structure on the relative rates of reaction of various dienes with $Me_2Si=C(TMS)_2$ and the relative yields of Diels-Alder and ene adducts have been extensively studied.[6] It was found that the relative rates of reaction increased as the electron density in the diene increased and as steric hindrance due to diene substitution increased. Reactions with butadiene yield the [4+2]-cycloadduct exclusively, and as the diene becomes more hindered in its *s-cis*-conformation (as in cis/trans-2-4-hexadiene), the ene product predominates.

Scheme 1.3 Silene Reactions with Dienes and Alkenes

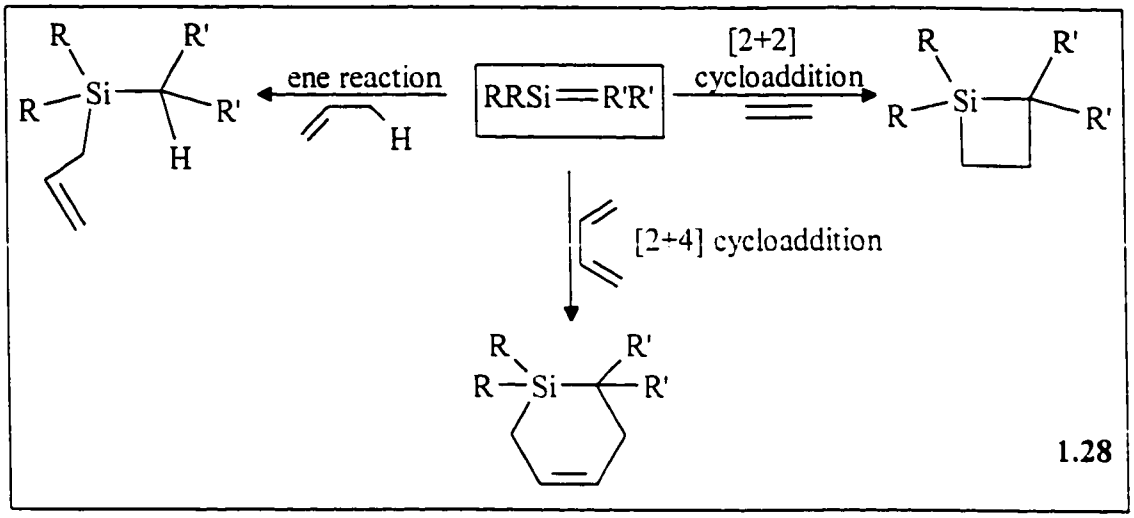

1.4.7 Mechanism for Reaction of Silenes with Carbonyl Compounds and Oxygen

Three types of addition products have been observed in the reactions of silenes with carbonyl compounds (eq 1.29). Simple silenes undergo "ene" type reactions with carbonyl compounds possessing enolizable hydrogens, which results in the formation of silyl enol ethers.[8,51-53] Aldehydes and ketones react with silenes to give the [2+2] cycloadduct 1,2-siloxetanes,[36,54] while α-β-unsaturated aldehydes and ketones react yielding 1-sila-3-oxacyclohex-4-ene isomers.[55,56]

Scheme 1.4 Silene Reactions with Carbonyl Compounds and Oxygen

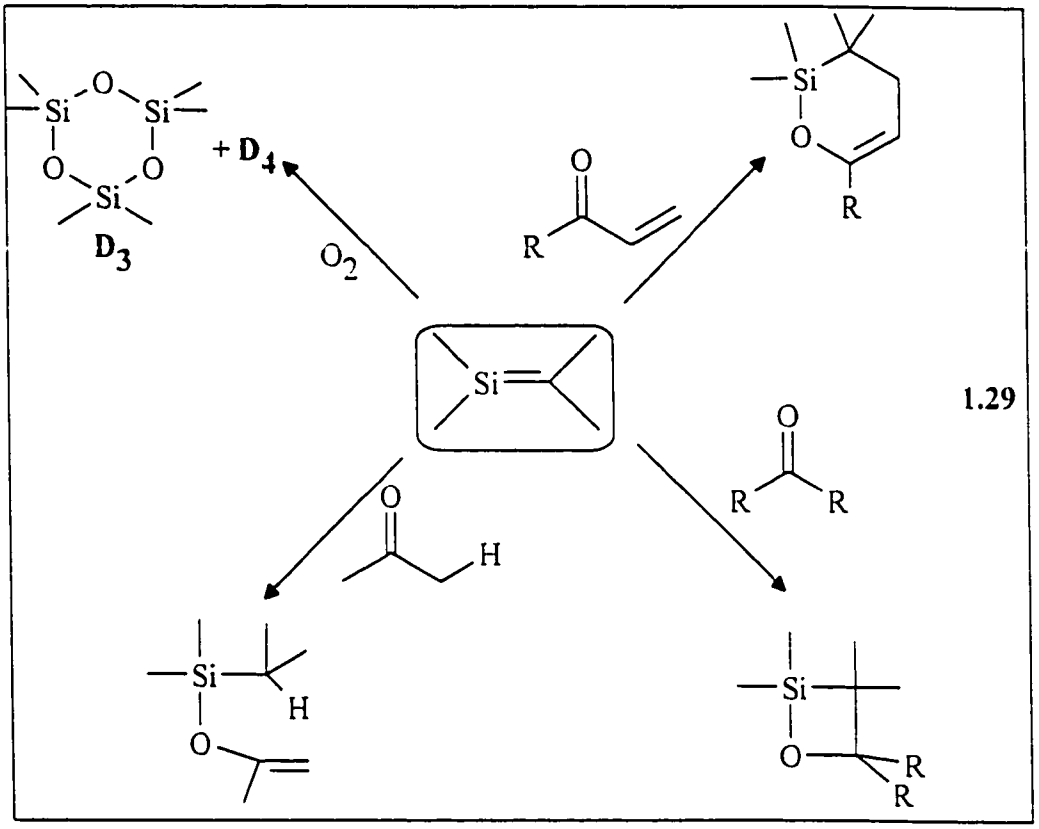

Sommer was the first to report that the trapping of pyrolytically generated silenes with a ketone yields an olefin and silanone oligomers (D_3 and D_4) (eq 1.30).[52] The reaction was postulated to proceed via a 2-siloxetane intermediate formed from formal [2+2] addition of the carbonyl compound to the silene.[52] Decomposition of the unstable 4-membered ring intermediate would result in the formation of the olefin and the highly reactive silanone which oligomerizes.

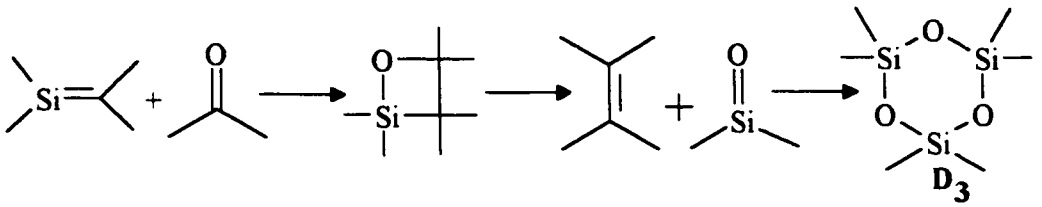

1.30

+ $\mathbf{D_4}$ + oligomers

The reaction of silenes with molecular oxygen results in the formation of cyclic siloxanes and carbonyl compounds (eq 1.31). The reaction is thought to involve a siladioxetane intermediate which undergoes decomposition to yield the corresponding carbonyl compound and silanone, the latter of which oligomerizes.

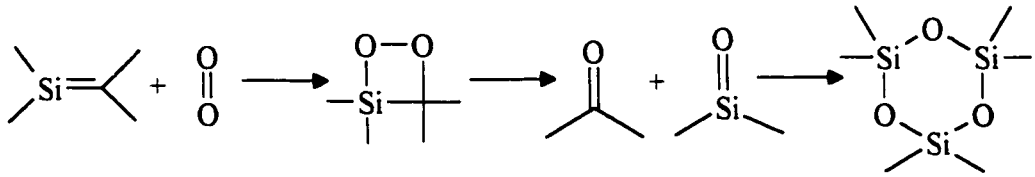

1.31

+ oligomers

Direct evidence for the formation of 1,2-siloxetanes proved elusive until recently when Brook[54] and Wiberg[6,57] independently isolated siloxetane derivatives of several stabilized silenes. These systems possess sterically bulky substituents at silicon and carbon and it is generally accepted that this factor is responsible for their stability.

There have been relatively few studies which investigate the mechanism of reaction of silenes with carbonyl compounds. The reaction is thought to involve stepwise nucleophilic attack by the lone-pair electrons on the carbonyl oxygen atom followed by proton transfer, but it is not fully established whether the mechanism is concerted or stepwise. Leigh and coworkers reported a study of the reactivity of 1,1-diphenylsilene (**12a**) towards various aliphatic ketones.[8] The addition of ketones to diphenylsilene (**12a**)

yields the corresponding silyl enol ether exclusively, with rate constants in the 10^7-10^8 $M^{-1}s^{-1}$ range in hydrocarbon and acetonitrile solutions. Reaction with acetone exhibits deuterium kinetic isotope effects of 1.9 and 1.3 in *iso*octane and MeCN solution, respectively. These isotope effects could not be conclusively assigned as primary or secondary. The absolute rate constants (and KIE's) decrease with increasing solvent polarity. It was found that the relative rates of reaction correlate with the n-M.O. energies on the carbonyl compound. A concerted asynchronous mechanism in which Si-O bond formation precedes proton-transfer was suggested (eq 1.32), since the transition state involves an eight-electron system with interaction of the silene with both the n- and π-molecular orbitals, which are orthogonal.[8]

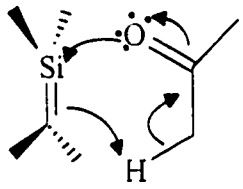

1.32

In contrast, evidence for the stepwise addition of ketones to transient 1,3,5-silahextrienes was provided through the use of kinetic and product studies. It was found that aryldisilane-derived silatrienes react with ketones to yield silyl ethers and siloxetanes, the relative yields of which vary with substitution at the silenic silicon atom, the allylic trialkylsilyl group, and the ketone.[30,36] Absolute rate constants for reaction decrease with increasing polarity of the solvent as well as increasing phenyl- substitution at trivalent silicon. Similar trends are reported for the reactions with 2,3-dimethyl-1,3-

butadiene and oxygen.[30] On the basis of these results, a 2-step mechanism was proposed involving initial attack at trivalent silicon by the carbonyl oxygen to yield a 1,4-biradical or zwitterionic intermediate which can undergo H-migration or coupling to yield silyl ether and siloxetane, respectively (eq 1.33). Hydrogen abstraction in the biradical (leading to silyl ether) requires that the allylic hydrogen be in the pseudoaxial position and the trimethylsilyl group in a pseudoequatorial position. A biradicaloid intermediate was favored over a relatively polar one, since the rate constants for reaction decreased as the polarity of the solvent increased.

Extremely bulky ketones such as di-*tert*-butyl ketone react much slower than methyl ketones and exclusively yield silyl ethers.[36] It was proposed that addition in this case occurs in a concerted fashion since attack at the carbonyl oxygen n-orbital is prevented by steric factors.

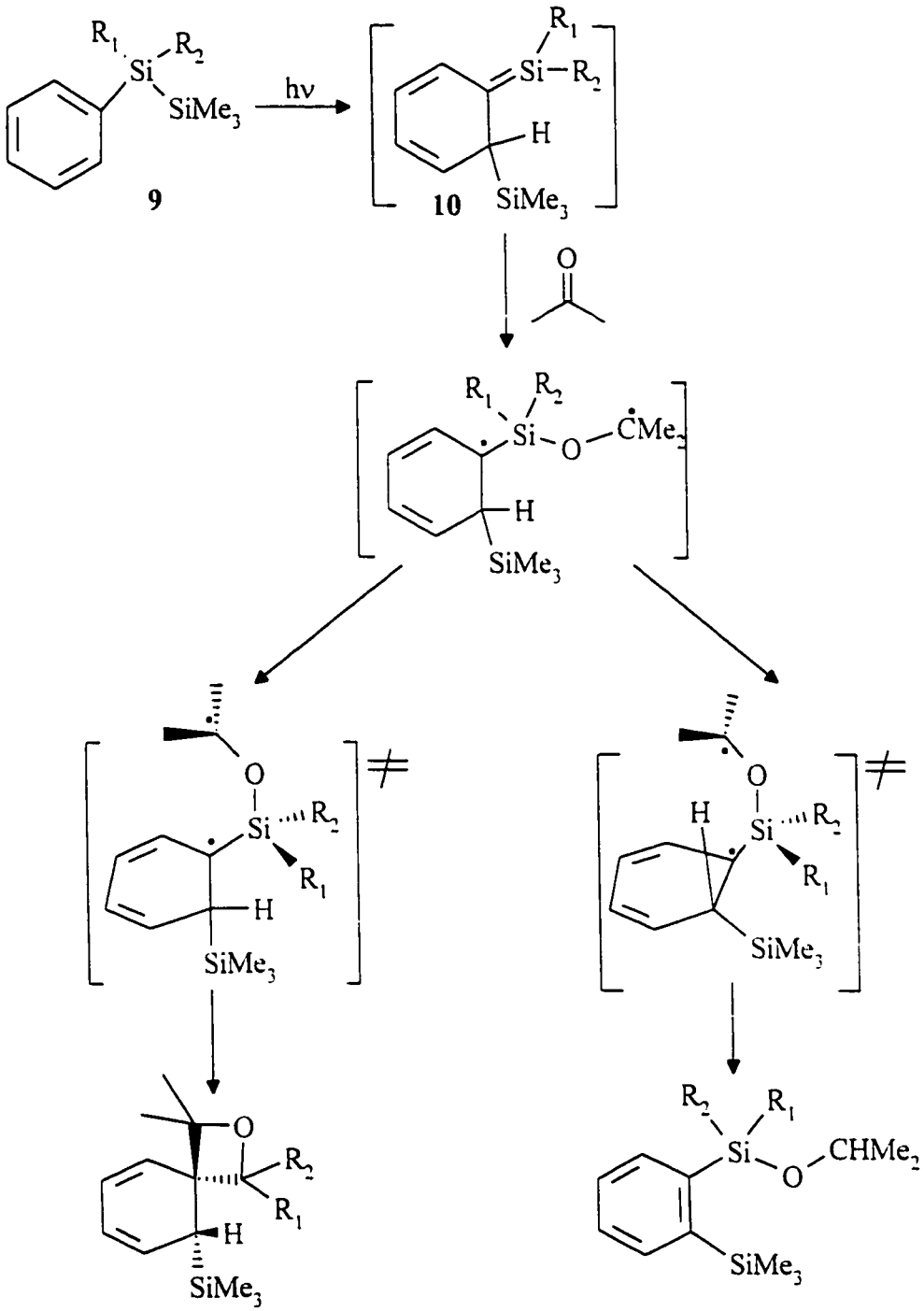

1.33

1.5 Objectives of this Work

In spite of the considerable interest in silenes over the past twenty years, there have been relatively few reports which examine the spectroscopic properties and reactivity of transient silenes using direct methods in solution. The majority of studies employ chemical trapping experiments which yield only qualitative information of about their mechanisms for reaction with nucleophiles or other reagents. Those kinetic studies which have been reported in the literature for silene reactions in solution have been the reactions of highly conjugated silenes, i.e., 1,3,5-silahexatrienes (**10**). Therefore, the goal of this work was to examine the mechanisms of addition of a variety of nucleophiles to simpler silenes which are potentially more representative of this class of compounds than those previously studied by time-resolved methods.

Theory suggests that substituents which accentuate the natural polarity of the Si=C double bond should lead to a shortening of the bond and increased reactivity toward nucleophilic addition.[11,22] There have, however, been no studies thus far which report a quantitative description of the effects of polar factors on silene reactivity. Thus, one of the goals of this study was to investigate the effects of ring substituents on the absolute rate constants for reaction of 1,1-diphenylsilene with typical silene traps such as alcohols, trimethylmethoxysilane, acetone and acetic acid. This represents the first Hammett type study for compounds containing the Si=C double bond. The effects of direct substitution at silicon on 1-silastyrene reactivity was also examined by comparing the rate constants

for reaction of 1-phenylsilene and 1-methyl-1-phenylsilene to 1,1-diphenylsilene with each of the reagents listed above.

One of the most widely studied silene reactions is the addition of alcohols. Previous kinetic[9,30,44] and product studies[32,47,58] are consistent with a mechanism involving rapid reversible formation of a silene-alcohol complex followed by competing intra- and inter-molecular proton transfer. The intramolecular pathway operates at low alcohol concentrations, while extracomplex proton transfer predominates at higher alcohol concentrations since it involves a second molecule of alcohol. Unfortunately, silene-alcohol complexes have not yet been observed directly. Indirect evidence that supports their intermediacy includes the fact that product distribution commonly varies with bulk alcohol concentration[44,47] and the isolation of silene-ether complexes.[12] In order to further elucidate the mechanism of alcohol addition and provide indirect evidence for complex formation, temperature effect studies on the rate constants for reaction of 1,1-diarylsilenes with alcohols in acetonitrile solution were undertaken. This work represents the first Arrhenius study reported for nucleophilic addition to a transient silene in solution.

Alkoxysilane addition can be viewed as analogous to alcohol addition, where the $SiMe_3$ group takes the place of the proton. The reaction proceeds with *syn* stereoselectivity but there are no investigations which offer greater detail on the mechanism. An Arrhenius study was undertaken in order to determine whether the mechanism is similar to that reported for reactions with alcohols.

To date it is still uncertain whether the reaction of carbonyl compounds with silenes is a concerted or stepwise addition. Studies on the reactions of 1,3,5-silahexatrienes have shown that these silenes undergo two modes of reaction with ketones to yield silyl ethers and 1,2-siloxetanes. This strongly suggests that the reaction is stepwise and a mechanism via a silene-ketone complex was proposed.[30] However, preliminary work on the reactions of diphenylsilene with various aliphatic ketones favour a concerted asynchronous mechanism.[8] One of the objectives of this study was to determine kinetic isotope effects and Arrhenius parameters for reaction of 1,1-diarylsilenes with acetone in polar and nonpolar solvents. This study is expected provide further insight into the reaction mechanism of simple silenes with ketones.

CHAPTER 2

RESULTS

2.1 Precursors to Simple Silenes

It is well known that direct irradiation of aryldisilanes (**9**) yields silenes by two competing pathways, as well as silyl radicals (eq 1.5). Unfortunately product distributions are dependent on silicon-atom substitution (and solvent), with simple silene formation never accounting for more than 60% chemical yield.[35]

In 1972 Boudjouk and Sommer reported that photolysis of 1,1-diphenylsilacyclobutane (**11a**) in the presence of methanol-Od yielded products consistent with the formation of **12a**.[23] In attempts to study the reactivity of **12a** towards alcohols Leigh and coworkers utilized **11a** as the precursor to **12a**.[59] Unfortunately, in the synthesis of **11a** biphenyl, which has triplet-triplet absorptions (λ_{max}=360 nm) overlapping with **12a**, is formed as a coproduct and the presence of this compound, even in trace amounts leads to complications in transient spectroscopic studies.

In 1980, Jutzi and Langer reported that photolysis of 1,1,2-triphenylsilacyclobutane (**26**) in methanol yields styrene and **13a** (eq 2.1), consistent with the formation of 1,1-diphenylsilene (**12a**).[38] Initial studies performed by our group on the

reaction of simple silenes with carbonyl compounds began by employing **26** as the photochemical precursor to **12a**.[8]

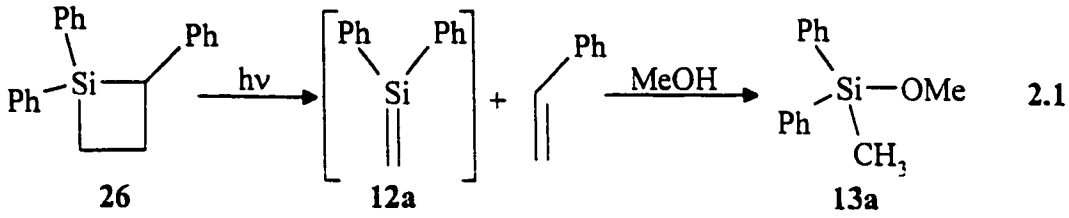

2.1

However, it was found that in acetonitrile solution **26** undergoes a dark reaction with methanol to yield the acyclic methyl ether **27** (eq 2.2)[8], making it an unsuitable precursor for nanosecond laser flash photolysis (NLFP) studies of silene reactivity towards alcohols.

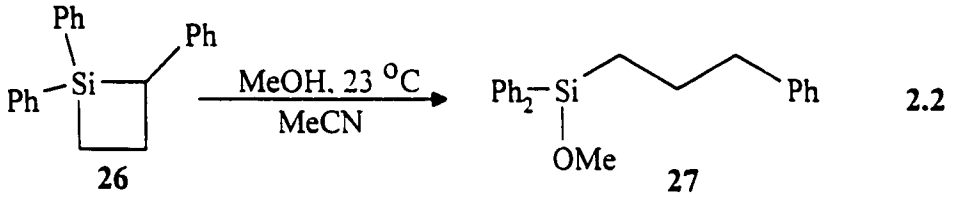

2.2

Thus, 1,1-diarylsilacyclobutanes are by far the best precursors to 1,1-diarylsilenes due to their thermal stability towards alcohols. Work began by determining the best method for purification of **11a**. It turned out that the most convenient and efficient method for complete removal of biphenyl is column chromatography.

Silacyclobutanes **11a-f** and **22a-b** were identified as being straightforward to synthesize and chosen as the photochemical precursors to 1,1-diarylsilenes (**12a-f**) and 1-silastyrenes (**23a-b**), respectively (eq 2.7-2.8). This section reports the synthesis and purification of **11a-f** and **22a-b**.

2.2 Synthesis of 1,1-Diarylsilacyclobutanes (11a-f) and 1-Phenylsilacyclobutanes (22a-b)

The 1,1-diarylsilacyobutanes **11a-f** were synthesized from 1,1-dichlorosilacyclobutane and the appropriate arylmagnesium bromide, according to the method published for **11a** (eq 2.3).[60] The silacyclobutanes (**11a-f**) were obtained as clear, colourless oils in 50-90 % yields after purification by column chromatography. Each contained < 0.01 % of the corresponding 1,1-biaryl derivative (determined by gas chromatography) after purification.

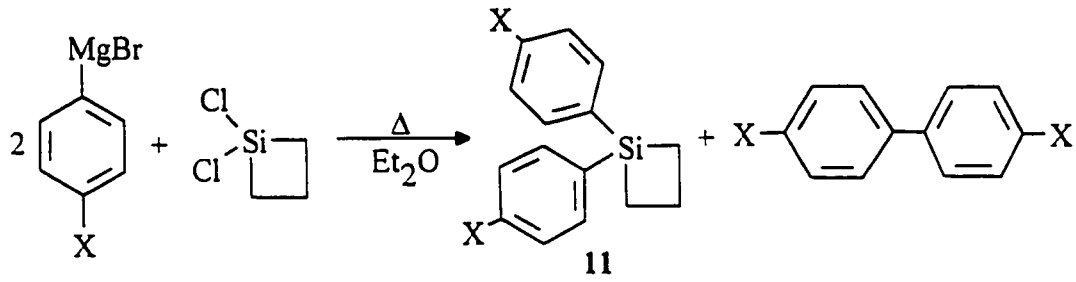

a. X = H **d.** X = Cl
b. X = Me **e.** X = CF_3
c. X = F **f.** X = OMe

2.3

1-Phenylsilacyclobutane (**22a**) was prepared by the reduction of 1-phenyl-1-chlorosilacyclobutane as reported by Bertrand and coworkers (eq 2.4).[61] The compound was obtained in 74 % yield after distillation and exhibited spectroscopic and analytical properties similar to the reported data.

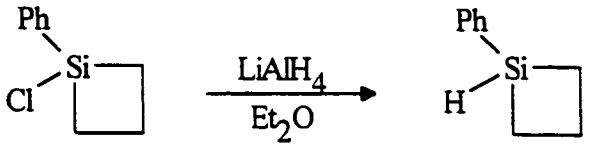

22a **2.4**

1-Methyl-1-phenylsilacyclobutane (**22b**) was synthesized from the reaction of 1-chloro-1-phenylsilacyclobutane with methylmagnesium bromide (eq 2.5).[60,62] After purification by column chromatography, the compound was obtained as a clear, colourless oil in 82 % yield. The silacyclobutane **22b** exhibited spectroscopic and analytical properties in agreement with those reported.

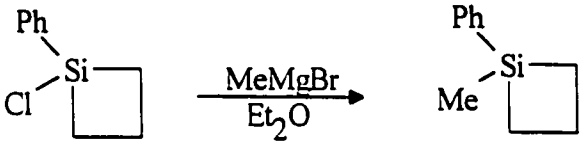

22b **2.5**

2.3 Steady-State Trapping of 1,1-Diarylsilenes (12a-f) and 1-Silastyrenes (23a,b)

Photolysis (254 nm) of silacyclobutanes **11a-e** and **22a-b** in the presence of methanol, acetone or trimethylmethoxysilane results in the formation of the silene-nucleophile addition products. This section summarizes the experimental results and conditions employed for steady-state trapping of silenes **12a-e** and **23a-b** in either hexane or acetonitrile solution at room temperature.

Steady-state irradiation of **11a** (0.05M) in hexane containing each of methanol, ethanol, *t*-butanol, or *i*-propanol (0.1 M), respectively, at 23 °C results in the formation of

the corresponding alcohol addition products (**13a-16a**) in > 90 % chemical yields (eq 2.6).[29,63] Photolysis of **11a** in the presence of water yields diphenylmethylsilanol as identified by GC/MS.[63] The photolyses were carried out to 65 % conversion of **11a**, and the products were identified on the basis of spectroscopic data after isolation by semi-preparative gas chromatography. The corresponding alkoxysilanes is also obtained from photolysis in acetonitrile, along with **17a** due to reaction with residual water in the solvent. Photolysis of **11a** in the absence of an externally added trapping reagent produces **17a**, as well as a higher molecular weight compound in high (>80 %) yield and several other minor products. The major product formed under these conditions is assigned to the head-to-tail dimer, 1,1,3,3-tetraphenyl-1,3-disilacyclobutane (**19**), on the basis of a very high GC retention time. The acyloxysilane **18a** could not be isolated because of its thermal instability and was identified on the basis of its GC/MS spectrum.[63]

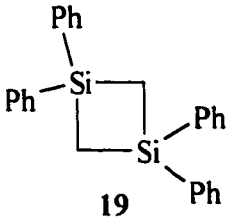

19

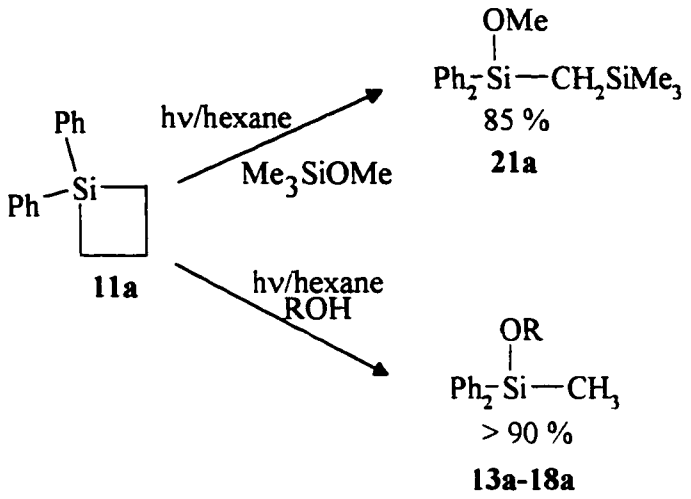

2.6

13a. R = Me **16a**. R = ^{i}Pr
14a. R = Et **17a**. R = H
15a. R = ^{t}Bu **18a**. R = Ac

The quantum yield for photolysis of **11a** was determined by potassium ferrioxalate actinometry, using 0.05 M air-saturated solutions of **11a** in hexane containing 0.1 M methanol, and 254 nm excitation light. The results of triplicate determination led to $\Phi_{\text{-11a}} = (0.21 \pm 0.03)$.[29]

Direct irradiation (254 nm) of a hexane solution containing **11a** (0.018 M) and trimethylmethoxysilane (1.15 M) at 254 nm results in the formation of 1,1-diphenyl-1-methoxy-3,3,3-(trimethylsilylmethyl)silane (**21a**) in 83 % chemical yield (eq 2.6) and ethylene. The photolysis was carried out to high conversion (60%) and no other products were observed to be formed in significant yield by NMR and GC. The silene-alkoxysilane adduct **21a** was isolated from the crude photolysate by semi-preparative GC, and identified by NMR spectroscopy.[64]

Similarly, irradiation of air-saturated hexane solutions of **11b-e** (0.007-0.013 M) in the presence of 0.05 M methanol (eq 2.7) results in the formation of the corresponding methoxysilane in greater than 85 % chemical yield, consistent with the trapping of silenes **12b-e**. Photolyses were carried out to 50 % conversion and no other products except ethylene were detected in > 5 % yield by GC. Products **13b-e** were isolated from the crude photolysate by semi-preparative GC and fully characterized. Photolysis of a hexane solution **11f** (0.02 M) in the presence of methanol (0.05 M) yields the corresponding alkoxysilane in very low chemical yield (12 %), as determined by GC (Table 2.1).

Table 2.1. Product Yields[a] from the Photolysis (15 minutes; 4 x 254 nm lamps) of 0.02 M Hexane Solutions of Silacyclobutanes **11a-f** and **22b** in the Presence of 0.05 M Methanol, 0.05 M Trimethylmethoxysilane[b] or 0.05M Acetone.

Silacyclobutane	Conversion	Alkoxysilane **13** and **21a**	Enol Ether **20**
11a	30 %	95 %	81
11b	23 %	95 %	84
11c	18 %	95 %	90
11d	38 %	78 %	76
11e	20 %	95 %	87
11f	90 %	12 %	-
11a[b]	23 %	83 %	-
22b	20 %	98 %	60 %

[a] Determined by GC analysis relative to the disappearance of silacyclobutane using dodecane as the internal standard. Errors are estimated to be ± 5 %.

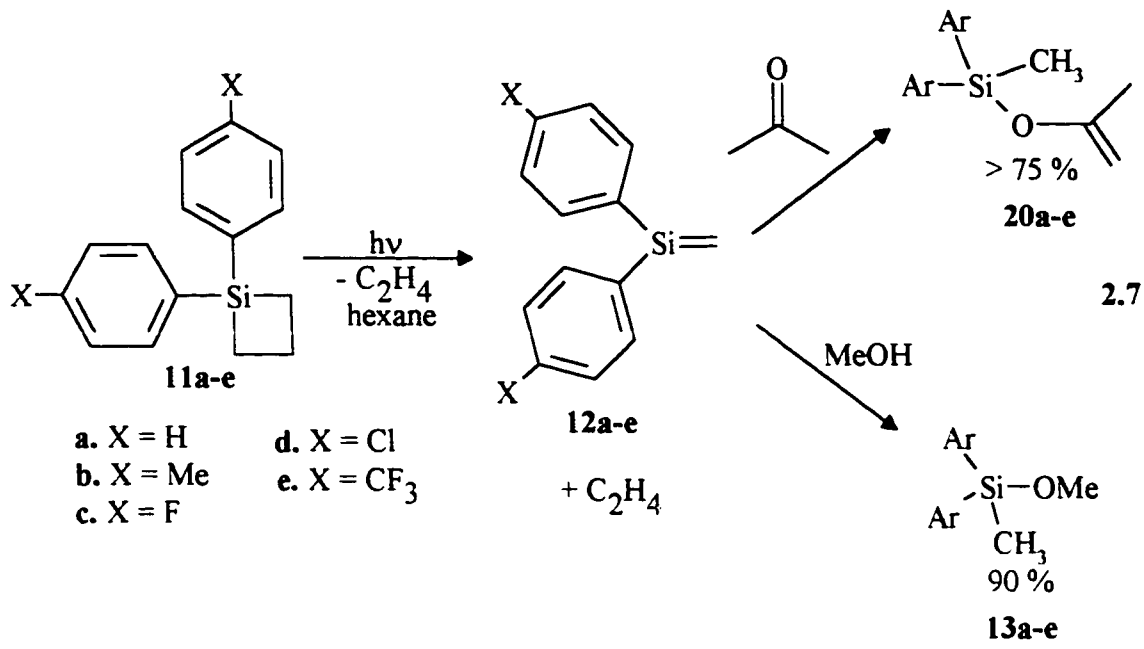

Steady-state photolyses (254 nm) of 0.02 M air-saturated solutions of **11a-e** in hexane containing 0.05 M acetone to *ca.* 20 % conversion yields the corresponding silyl enol ethers (**20a-e**) shown in eq 2.7 in > 75 % yield and C_2H_4. The enol ethers (**20a-e**) are photochemically and hydrolytically reactive, so characterization of these compounds was carried out by NMR and GC/MS of the crude photolysates. The NMR spectra of the crude photolysis mixtures shown in Figures 6.1-6.5, show two singlets δ = 3.95-4.0 range, assigned to the vinylic protons, and singlets in the range of δ = 1.72-1.80 and δ = 0.60-0.70, assigned to the C-CH_3 and Si-CH_3 protons, respectively. These spectral features are similar to those of **20a** observed in the NMR spectra of the crude photolysis of methylpentaphenyldisilane in the presence of acetone.[49]

Steady-state irradiation (254 nm) of **22a** (0.1 M) and **22b** (0.1 M) in air saturated hexane solutions in the presence of methanol (0.1 M) or acetone (0.1 M) results in the

formation of the corresponding methoxysilane (**24a-b**) or silyl enol ether (**25a-b**) (eq 2.8). Alkoxysilane formation occurs with high chemical yields (> 90 %), while enol ether formation is quite low (60 %). The products were identified after 10 % conversion by GC coinjection of the crude photosylate with authentic samples, synthesized by reaction of the appropriate chlorosilane with either trimethylorthoformate or methanol.

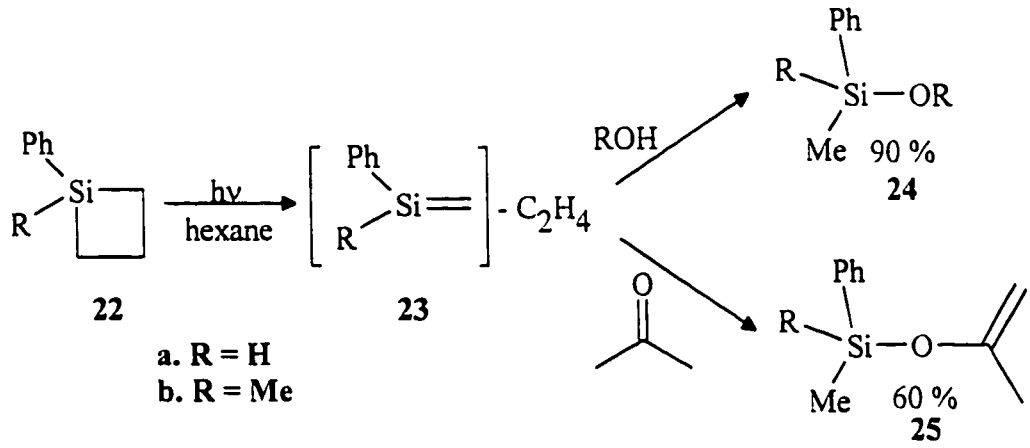

22 **23**

a. R = H
b. R = Me

2.8

Steady-state photolysis of hexane solutions of **11a-e** and **22b** in the presence of either methanol, acetone or trimethylmethoxysilane at constant photolysis time (15 min; 4 x 254 nm lamps) indicates that the conversion of silacyclobutane and product yields do not vary appreciably throughout the series (Table 2.1). On the other hand, photolysis of compound **11f** under the above conditions, led to much higher conversion of the silacyclobutane and a corresponding low yield of **13f**.

2.4 1,1-Diphenylsilene

The following chapters summarize the results of the effects of substituent on the kinetics of the reactions of 1,1-diarylsilenes (**12a-e**) and 1-silastyrenes (**23a-b**) with each of the traps discussed above. 1,1-Diphenylsilene (**12a**) serves as the parent compound to which absolute rate constants, kinetic deuterium isotope effects and Arrhenius parameters for reactions of 1,1-diarylsilenes (**12b-e**) and 1-silastyrenes (**23a-b**) with alcohols, acetic acid, trimethylmethoxysilane, and acetone are compared. These experiments were carried out using a combination of steady state and nanosecond laser flash photolysis (NLFP) techniques.

2.4.1 Steady-State Competition Experiments

Steady-state competitive trapping experiments were performed to establish the reactivities of **12a** with water, ethanol and *t*-butanol relative to methanol in acetonitrile solution. Acetic acid was not employed in these experiments due to the instability of the acyloxysilane (**18a**) under these conditions. A typical competition experiment involved irradiation (254 nm; 23 °C) of solutions of **11a** (0.0027 M) in dry acetonitrile containing 0.027 M methanol and varying amounts (0.02-0.1 M) of either water, ethanol or *t*-butanol. HPLC grade acetonitrile was used in these experiments and contained < 0.05 M water, as determined by measuring the lifetime of **12a** (by LFP) in the absence of

quencher, and the bimolecular rate constant for quenching of **12a** by water (7.6×10^8 $M^{-1}s^{-1}$). Formation of the corresponding adducts were monitored by GC as a function of alcohol concentration and plotted according to eq 2.9. In all cases, plots of the product ratio *versus* alcohol concentration ratio were linear affording the proportionality constants (C_{ROH}) listed in Table 2.2. The constants (C_{ROH}) are directly proportional to the ratio in rate constants (determined by LPF) if the reactions are governed by a rate law in which the order in alcohol concentrations are the same; Table 2.2 also contains ratios of absolute rate constant ratios determined by NLFP.

$$\frac{[Ph_2Si(CH_3)OMe]}{[Ph_2Si(CH_3)OR]} = C_{ROH}([MeOH]/[ROH]) \qquad \textbf{2.9}$$

Additional experiments were performed with *t*-butanol, since the initial relative rate ratios determined by steady-state techniques were not in agreement with those determined by NLFP. Two sets of experiments were performed at a constant [*t*-BuOH]/[MeOH] ratio of either 2.4 or 3.2, but with the bulk alcohol concentration varying between 0.006-0.093 M. The photolyses were carried out to 15-20% conversion and the concentration of **11a** in these experiments was *ca.* 10% of the methanol concentration. The proportionality constant values were calculated from the measured adduct ratios and the alcohol concentration ratios (eq 2.9) and are plotted against $[MeOH]_{total}$ concentration in Figure 2.2b. The results shown in Figure 2.2b indicate that $C_{t\text{-}BuOH}$ is concentration dependent. The constant obtained at high alcohol concentrations ([MeOH] = 0.027M; [*t*-BuOH] =

0.02-0.1M) is $C_{t\text{-BuOH}}$ =15.0 ± 0.8, while at low alcohol concentrations ([MeOH] = 0.0014 M; [*t*-BuOH] = 0.0046 M) $C_{t\text{-BuOH}}$ is equal to 4.9 ± 0.2.

Figure 2.1. Steady-state product ratios for photolysis of **11a** in the presence of methanol, water and ethanol. a. ($Ph_2Si(Me)OMe$)/($Ph_2Si(Me)OH$) *versus* [MeOH]/[H_2O] ratio; b. ($Ph_2Si(Me)OMe$)/($Ph_2Si(Me)OEt$) *versus* [MeOH]/[EtOH].

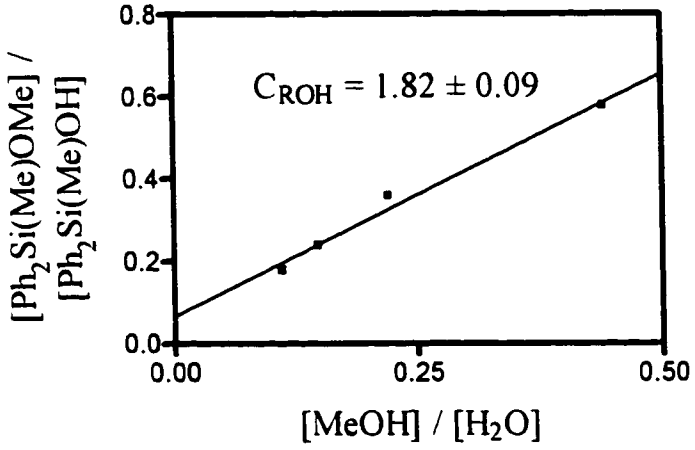

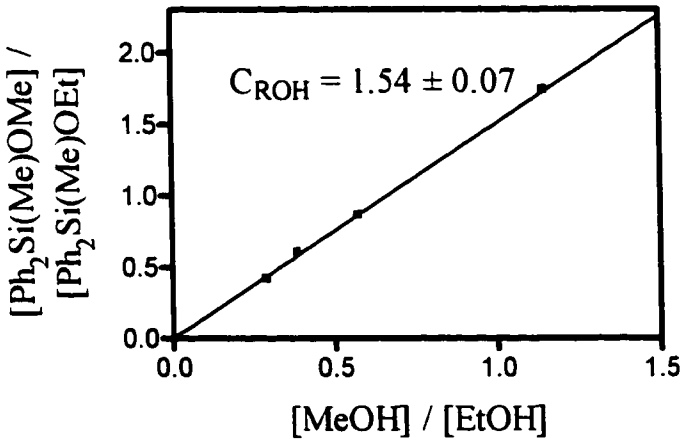

Figure 2.2. Steady state product ratios from photolysis of acetonitrile solutions of **11a** in the presence of methanol and *t*-butanol: a. $Ph_2Si(Me)OMe$ / $Ph_2Si(Me)OC(CH_3)_3$ *vs.* [MeOH]/[*t*-BuOH], for photolyses of $2.7x10^{-3}$ M solutions of **11a** containing 0.027 M methanol and varying concentrations (0.0-0.1 M) of *t*-butanol; b. $C_{t\text{-BuOH}}$ *vs.* [MeOH], from photolysis of solutions **11a**, MeOH, and *t*-BuOH at various methanol concentrations, but similar [MeOH]/[*t*-BuOH] ratios (■, 2.4; □, 3.2).

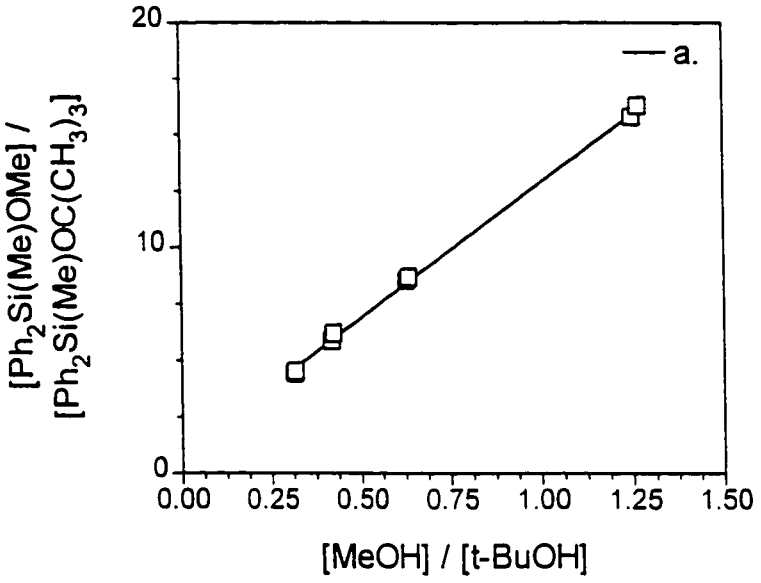

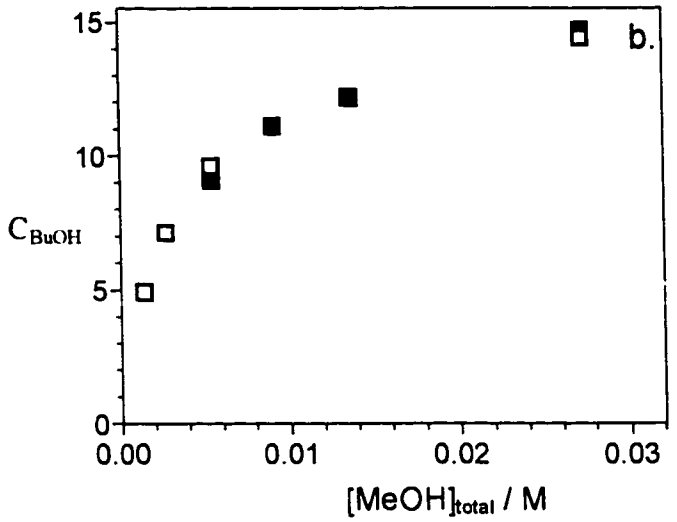
15
10
5
0
C_{BuOH}
0.00
0.01
0.02
0.03
$[MeOH]_{total}$ / M
b.

Table 2.2. Proportionality Constants (C_{ROH}) from Steady-State Competition Trapping of 1,1-Diphenylsilene (**12a**) with Water, Ethanol and *t*-Butanol[a], and Rate Constant Ratios (k_{ROH}/k_{MeOH}) in Acetonitrile at 23 °C determined by NLFP.

ROH	C_{ROH}[a]	k_{MeOH} / k_{ROH}
H_2O	1.82 ± 0.09	2.0 ± 0.2
EtOH	1.54 ± 0.07	1.5 ± 0.2
t-BuOH	15.0 ± 0.8[b]	5.5 ± 0.4
t-BuOH	4.9 ± 0.2[c]	5.5 ± 0.4

[a] C_{ROH} values were determined from the slopes of product ratio ([**13a**] / [**14**,**15**,**17**]) *versus* alcohol concentration ratio of the two alcohols according to eq 2.9. Errors are reported as twice the standard deviation of the least squares slope.

[b] [MeOH] = 0.027M; [*t*-BuOH] = 0.02-0.1M

[c] [MeOH] = 0.0014 M; [*t*-BuOH] = 0.0046 M

2.4.2 Nanosecond Laser Flash Photolysis Studies of 1,1-Diphenylsilacyclobutane

NLFP experiments employed a flow system and air saturated solutions of **11a** (*ca.* 6.5 x 10^{-3} M) in hexane, dried acetonitrile, or dried THF. The pulses from a KrF excimer laser (248 nm, ≈16 ns, 70-100 mJ) were employed for excitation, and a microcomputer-controlled the transient detection system.[65] The acetonitrile was distilled from calcium hydride and dried by repeated passage through an activated alumina column, while the THF was dried and distilled from sodium. The dried acetonitrile contained 0.0005-0.001 M water, as calculated from the lifetime of **12a** in the absence of quencher and the bimolecular rate constant for quenching of **12a** by H_2O (7.6 x 10^8 $M^{-1}s^{-1}$; Table 2.3). The time-resolved UV absorption spectra recorded 0.5-1.0 μs and 0.2-0.5 μs after laser flash photolysis of a 0.0065 M solution of **11a** in hexane, acetonitrile and tetrahydrofuran, respectively, are shown in Figure 2.3. Representative decay traces recorded at monitoring wavelengths of 325 nm (hexane, MeCN), and 350 nm (THF) are shown in Figure 2.3 as inserts. The UV spectra in hexane and MeCN are similar to those reported from NLFP of 1,1,2-triphenylsilacyclobutane under similar conditions,[8] and are assigned as due to 1,1-diphenylsilene (**12a**) (λ_{max} = 325 nm). The transient absorption spectra of **12a** recorded in THF is quite different from that obtained in either hexane or acetonitrile solution. The spectrum is broadened and red-shifted (λ_{max} = 350 nm) compared to those recorded in hexane or MeCN, and is attributed to complexation of the silene with solvent (THF).

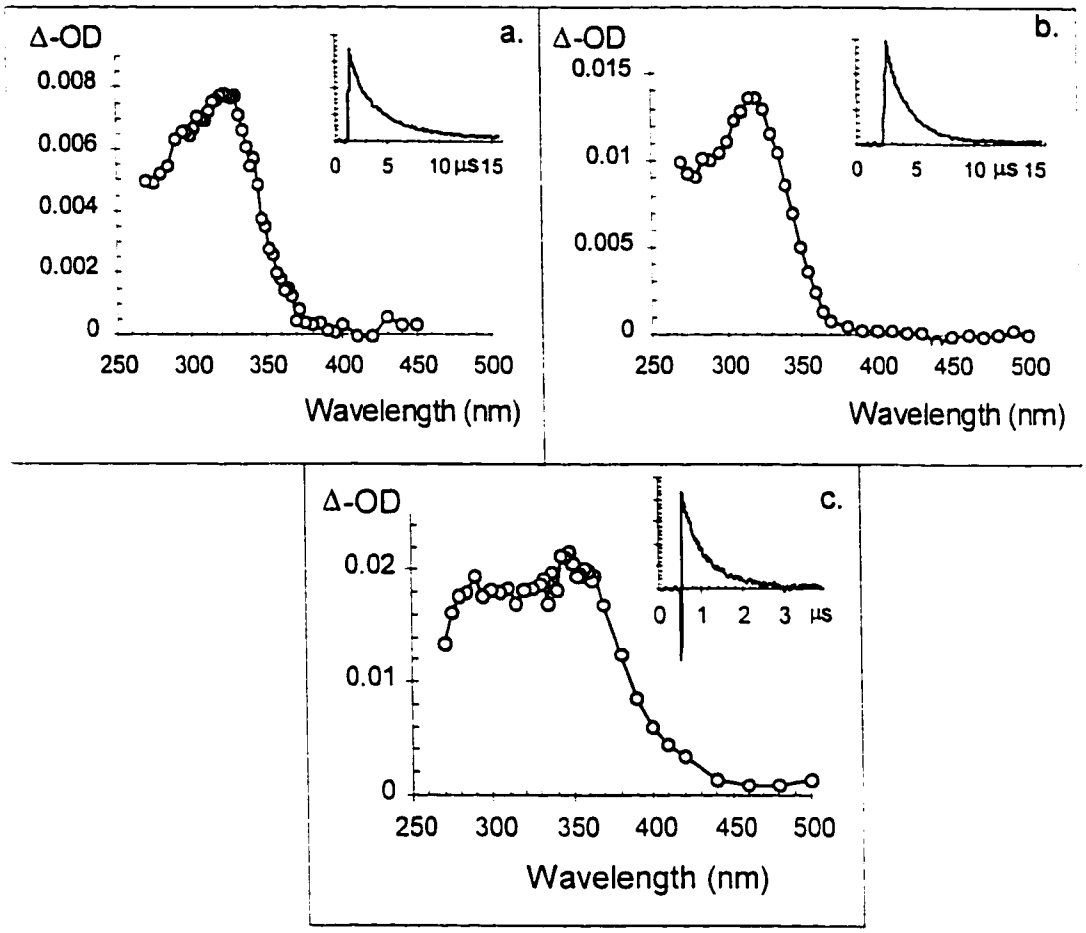

Figure 2.3. Absorption spectra of 1,1-diphenylsilene (**12a**) recorded by nanosecond laser flash photolysis (248 nm) of air-saturated solutions of **11a** (0.006 M) in (a) hexane, (b) acetonitrile, and (c) tetrahydrofuran at 23 °C.

2.4.3 Reactivity of 1,1-Diphenylsilene Towards Alcohols and Acetic Acid

In hexane or dried acetonitrile solution, **12a** decays with mixed first and second order kinetics over a 2-3 μs range. Addition of water, alcohols (methanol, ethanol, *i*-propanol, *t*-butanol), acetic acid or the O-deuterated isotopomers of each of these quenchers results in a shortening of the lifetime of the transient and a change in silene decay to clean pseudo-first order kinetics. The initial yield of the transient is unaffected by the addition of the quenchers, and at the end of a quenching experiment there are not any new transient absorptions observed in the spectrum. Plots of decay rate constant (k_{decay}) *versus* concentration of added quencher (Q) were linear and were analyzed according to eq 2.10 (where k_q is the bimolecular rate constant for quenching of **12a** by Q, and k_d^0 is the pseudo-first order rate constant for decay in the absence of added Q). Representative quenching plots for the reaction of **12a** with methanol and methanol-Od in acetonitrile are shown in Figure 2.4.

$$k_{decay} = k_d^0 + k_q[Q] \qquad \textbf{2.10}$$

The bimolecular rate constants for quenching of **12a** by the alcohols, water and acetic acid, as well as the k_H/k_D values calculated from the rate constants for reaction by the corresponding deuterated isotopomers are listed in Table 2.3.

Figure 2.4. Plots of k_{decay} *versus* methanol (■) and methanol-Od (▲) concentration (MeOL), from laser flash photolysis of 1,1-diphenylsilacyclobutane (**11a**) in acetonitrile solution at 23 °C. The concentration of water in the solvent is estimated to be ≈ 0.0005 M.

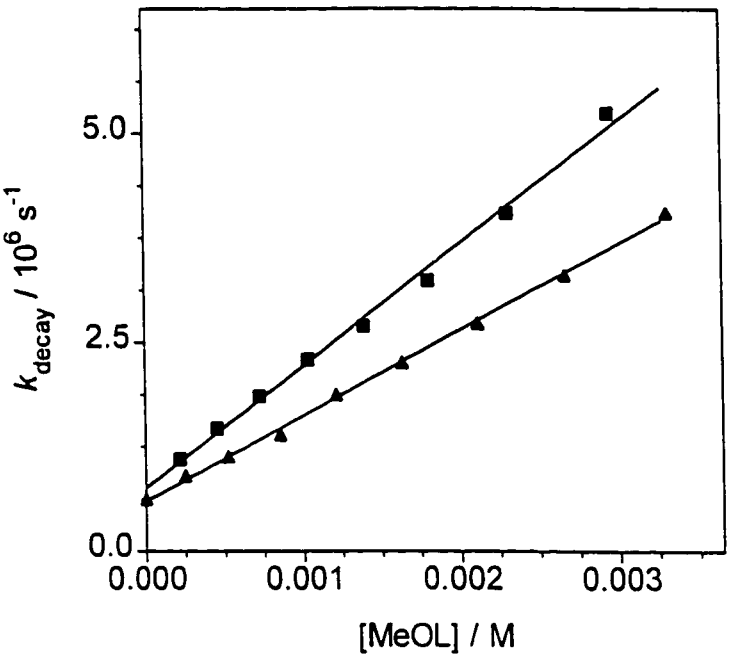

Table 2.3. Rate Constants and Kinetic Isotope Effects (KIE's) for Reactions of 1,1-Diphenylsilene (**12a**) with Water, Various Alcohols and Acetic Acid in Acetonitrile Solution Containing 0.0005 M water at 23 °C.[a]

ROH	k_q / 10^9 M^{-1} s^{-1}	k_H/k_D[b]
MeOH	1.2 ± 0.1	1.5 ± 0.1
EtOH	1.0 ± 0.1	1.8 ± 0.1
H_2O	0.76 ± 0.09	1.4 ± 0.2
^{t}BuOH	0.22 ± 0.02	1.6 ± 0.3
HOAc	1.2 ± 0.1	1.1 ± 0.1

[a] Errors are reported as twice the standard deviation of least squares analysis of decay rate-concentration data according to eq 2.10.

[b] Errors are reported as calculated relative errors.

[c] Absolute rate constant ratios (k_{MeOH}/k_{EtOH} and k_{MeOH}/k_{H2O}) are not consistent with relative and absolute rate ratios listed in Table 2.2 due to the higher quality reagents employed in the above experiments.

Absolute rate constants for reaction of **12a** with methanol, *t*-butanol and acetic acid were also determined in hexane and THF solution and are listed in Table 2.4. For all three quenchers, the reaction rate constants decrease from hexane to THF solution.

Table 2.4. Bimolecular Rate Constants for Reaction of 1,1-Diphenylsilene (**12a**) with Methanol, *t*-Butanol and Acetic Acid in Hexane, Acetonitrile and Tetrahydrofuran Solution at 23 °C.[a]

	$k_q / 10^9\ M^{-1}s^{-1}$		
Solvent	MeOH	*t*-BuOH	AcOH
Hexane	2.9 ± 0.2	0.40 ± 0.07	3.1 ± 0.3
MeCN	1.2 ±0.1	0.22 ± 0.02	1.2 ± 0.07
THF	0.31 ± 0.03	0.024 ± 0.002	0.33 ± 0.02

[a] Errors are reported as twice the standard deviation of least squares analysis of decay rate-concentration data according to eq 2.10.

2.4.4 Arrhenius Studies of the Reaction of 1,1-Diphenylsilene with Methanol, *t*-Butanol and Acetic Acid

In order to determine activation parameters for reaction of **12a** with methanol, *t*-butanol and acetic acid in acetonitrile solution, absolute rate constants were determined at various temperatures between -20 and 55 °C by NLFP.[45] Arrhenius plots for quenching by the three compounds are shown in Figure 2.5. Table 2.5 lists the corresponding Arrhenius activation energies (E_a) and pre-exponential factors (log A). Methanol and *t*-butanol both react with negative activation energies, i.e., reaction rates increase with decreasing temperature, while acetic acid adds with a positive activation energy.

Figure 2.5. Arrhenius plots for reaction of 1,1-diphenylsilene (**12a**) with methanol (■), *tert*-butanol (●) and acetic acid (◆) in air-saturated acetonitrile solution, and for methanol addition to **12a** in hexane (○) solution.

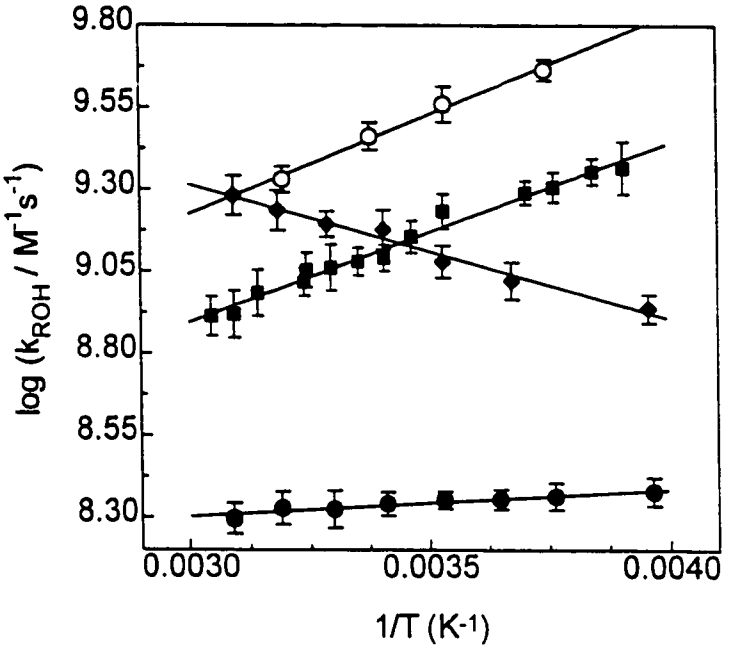

Table 2.5. Arrhenius Activation Energies (E_a), Pre-Exponential Factors (log A), and Rate Constants (296 K) for the Addition of Methanol, Methanol-Od, *tert*-Butanol and Acetic Acid to 1,1-Diphenylsilene (**12a**) in Acetonitrile Solution and for Addition of Methanol to **12a** in Hexane Solution.[a]

ROH	E_a / (kcal/mol)	log (A / $M^{-1}s^{-1}$)	k_{ROH} / 10^9 $M^{-1}s^{-1}$ [c]
MeOH	-2.5 ± 0.2	7.3 ± 0.2	1.26 ± 0.05
MeOd	-3.2 ± 0.3	6.5 ± 0.2	0.71 ± 0.08
t-BuOH	-0.4 ± 0.1	8.1 ± 0.1	0.22 ± 0.02
AcOH	+1.9 ± 0.2	10.5 ± 0.2	1.44 ± 0.05
MeOH[b]	-2.8 ± 0.2	7.4 ± 0.3	2.86 ± 0.20

[a] Errors are reported as twice the standard deviation of from linear least squares analysis of the data shown in Figure 2.5. Rate constants employed for calculation of Arrhenius activation parameters were corrected for thermal expansion of the solvent.

[b] In hexane solution.

[c] Interpolated from Arrhenius data.

The effect of temperature on the KIE for reaction with methanol was also examined and the corresponding Arrhenius plot is shown in Figure 2.6. 1,1-Diphenylsilene (**12a**) reacts with methanol-Od with an activation energy of -3.2 kcal/mol, a slightly more negative value than that observed for methanol. The deuterium kinetic isotope effect for methanol addition increases with increasing temperature from 1.4 at -17 °C to 2.3 at 55 °C.

Figure 2.6. Arrhenius plot for the addition of 1,1-diphenylsilene (**12a**) to methanol (■) and methanol-Od (●) in acetonitrile solution.

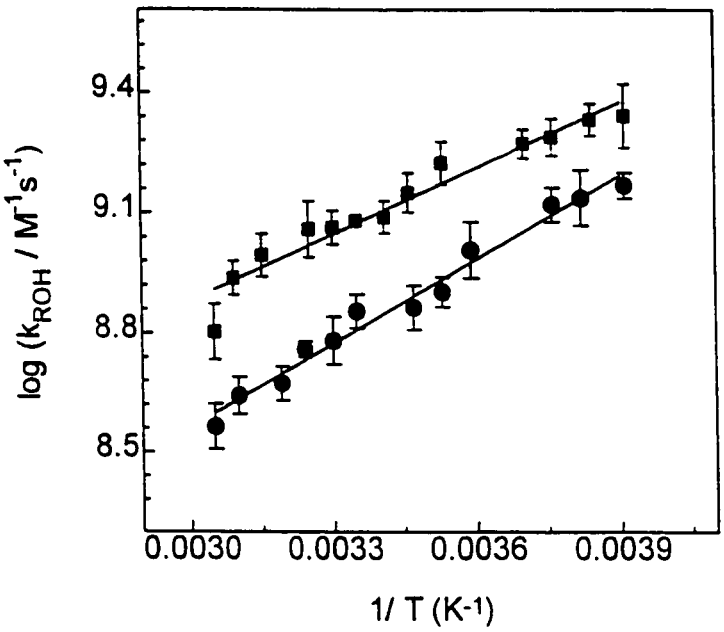

2.4.5 Substituent Effects on Diphenylsilene Reactivity Towards Alcohols

This section summarizes the effects of aryl-substitution on the absolute rate constants and activation parameters for reactions of 1,1-diphenylsilene derivatives (**12a-e**) with alcohols and acetic acid in acetonitrile solution.[10]

Nanosecond laser flash photolysis (248 nm) experiments were carried out in a similar fashion to those for **11a**. The transients **12b-e** absorb in the spectral region 350 nm - 280 nm ($\lambda_{max} \approx 325$ nm) (see Appendix), and decay on the microsecond time scale with mixed first- and second-order kinetics. The transient UV absorption spectra, lifetimes, and reactivity towards the addition of common silene traps are similar to those presented for **12a**. Figure 2.7 shows a representative absorption spectrum obtained after correction for minor residual absorption, along with typical decay traces, recorded at a monitoring wavelength of 325 nm for **12e** in acetonitrile solution. As in the case of **12a**, the lifetimes and intensities of the signals of **12b-e** are unaffected by saturation of the solutions with either nitrogen or oxygen.

LFP of **11f** results in absorptions in the entire 280-600 nm range, with only weak absorption maxima in the 290-320 nm range (Figure 2.7(b)). The intensity of the absorptions are unaffected by saturation of the solutions with nitrogen, oxygen or the addition of methanol.

Addition of methanol, t-butanol, acetic acid or water results in a reduction in the lifetimes of the transients **12a-e** and a change in decay kinetics to pseudo-first order.

Plots of the rate of decay (k_{decay}) *versus* concentration of added quencher according to eq 2.10 were linear in all cases. Typical plots are shown in Figure 2.8 for quenching by methanol. Bimolecular rate constants for the reactions of **12a-e** with the three reagents listed above in MeCN are listed in Table 2.6. Similar experiments were carried out using MeOD, *t*-BuOD, and acetic acid-Od. The k_H/k_D-values calculated from the data are included in Table 2.6 as well.

Figure 2.7. (a) Transient UV absorption spectrum obtained from laser flash photolysis of 0.0036 M **11e** in air-saturated hexane solution. (b) Transient UV absorption spectrum obtained from laser flash photolysis of 0.0028 M **11f** in air-saturated hexane solution.

(a)

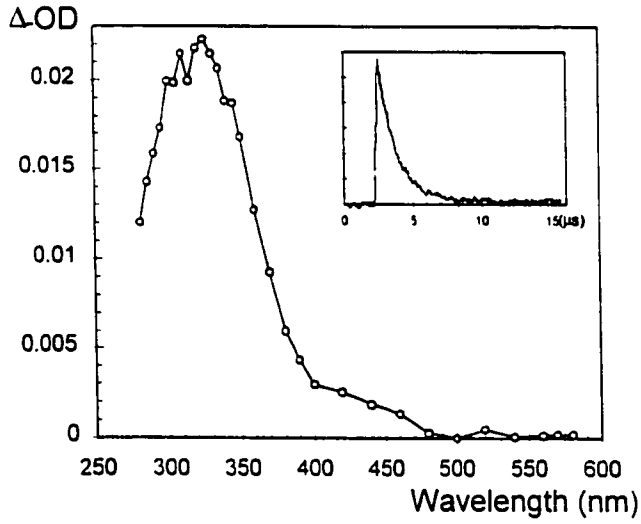

(b)

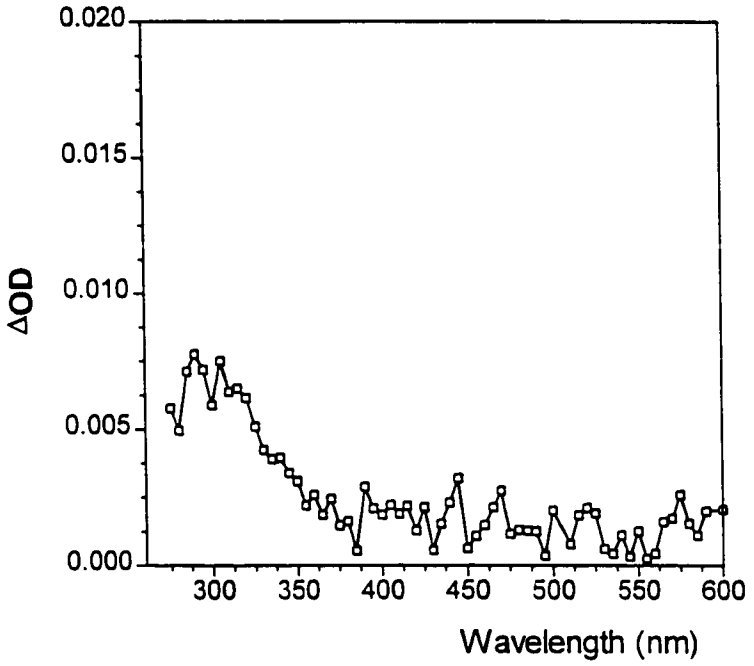
0.020
0.015
0.010
0.005
0.000
ΔOD
300
350
400
450
500
550
600
Wavelength (nm)

Figure 2.8. Plots of k_{decay} *versus* [MeOH] from laser flash photolysis of air-saturated, MeCN solutions of **11b** (■), **11c** (◆), **11d** (▲) and **11e** (●) in the presence of methanol at 23 °C.

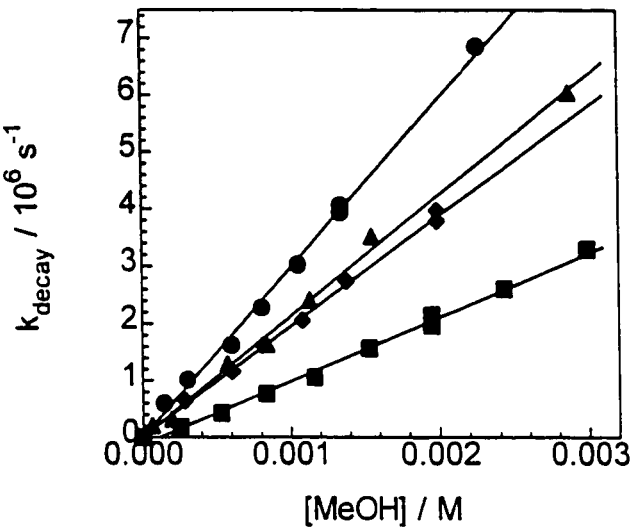

Table 2.6. Initial Lifetime (τ_o)[c], Absolute Rate Constants (k_q), and KIE's for the Reaction of 1,1-Diarylsilenes (**12a-e**) with Methanol, *t*-Butanol and Acetic Acid in Acetonitrile Solution at 23 °C.[a]

(p-X-Ph)$_2$Si=CH$_2$ (**12a-e**)	τ_o (μs)	k_q (MeOH) / 10^9 $M^{-1}s^{-1}$	k_q (t-BuOH) / 10^9 $M^{-1}s^{-1}$	k_q (AcOH) / 10^9 $M^{-1}s^{-1}$
CH_3	4.7 ± 0.4	1.10 ± 0.06	0.13 ± 0.01	1.41 ± 0.05
		(k_H/k_D = 1.9 ± 0.1)	(k_H/k_D = 1.9 ± 0.2)	(k_H/k_D = 1.2 ± 0.1)
H	3.0 ± 0.3	1.50 ± 0.10	0.22 ± 0.02	1.50 ± 0.20
		(k_H/k_D = 1.5 ± 0.1)	(k_H/k_D = 1.6 ± 0.1)	(k_H/k_D = 1.1 ± 0.1)
F	2.1 ± 0.2	1.89 ± 0.08	0.33 ± 0.02	1.75 ± 0.20
		b	b	b
Cl	2.1 ± 0.2	2.13 ± 0.10	0.39 ± 0.02	1.98 ± 0.20
		b	b	b
CF_3	1.8 ± 0.2	2.99 ± 0.16	0.75 ± 0.04	2.34 ± 0.40
		(k_H/k_D = 1.0 ± 0.1)	(k_H/k_D = 1.7 ± 0.2)	(k_H/k_D = 1.1 ± 0.1)

[a] Errors are reported as twice the standard deviation of least squares analysis of decay rate-concentration data according to eq 2.10.

[b] Not determined.

[c] Reported as the intercepts of the decay rate-concentration data according to eq 2.10.

Plots of log (k_q) versus 2σ, where k_q is the second-order rate constant for the addition of methanol, *t*-butanol or acetic acid to the diarylsilenes (**12a-e**) (Figure 2.9), yield the first Hammett plots for reaction of a transient silene. For all three quenchers, the reaction rates increase with increasing withdrawing ability of the aryl- substituent, while the kinetic deuterium isotope effects decrease. Hammett ρ-values of (0.31 ± 0.02), (0.55 ± 0.04), and (0.17 ± 0.01) for methanol, t-butanol and acetic acid addition, respectively (in acetonitrile) are obtained from the slopes of these plots. Three point Hammett plots (Figure 2.10) obtained for the deuterated analogues yield reaction constants of (0.50 ± 0.12), (0.57 ± 0.20) and (0.19 ± 0.02), for MeOD, *t*-BuOD and AcOD addition, respectively.

Figure 2.9. Hammett plots for the reaction of 1,1-diarylsilenes (**12a-e**) with methanol (□), *t*-butanol (◆) and acetic acid (▲) in acetonitrile solution.

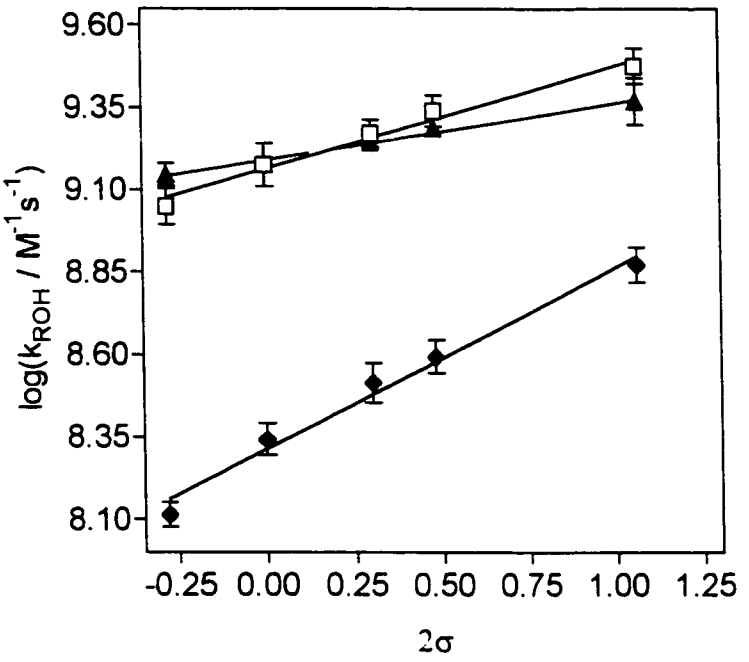

Figure 2.10. Hammett plots for the reaction of 1,1-diarylsilenes (**12a-e**) with methanol-Od (□), *t*-butanol-Od (◆) and acetic acid-Od (▲) in acetonitrile solution.

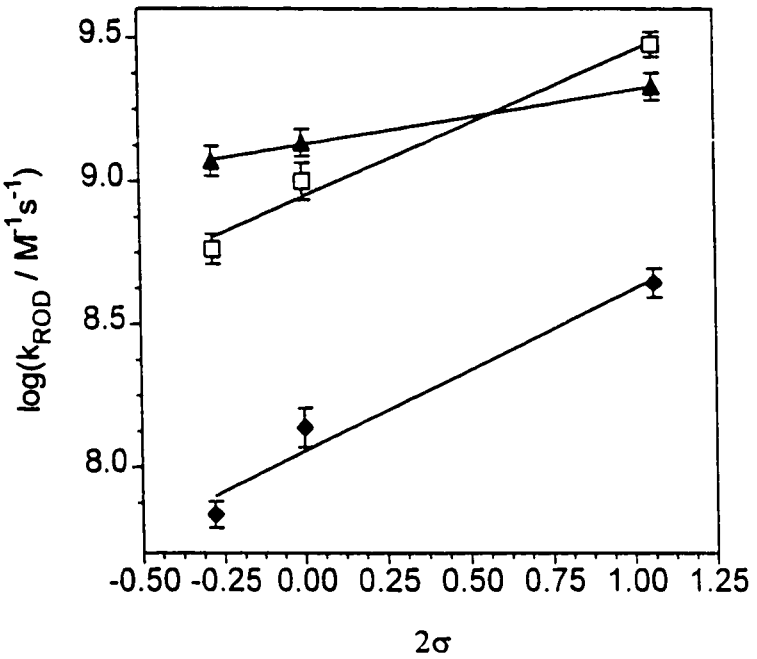

In order to examine substituent effects on the activation parameters for the above reactions, absolute rate constants for reaction of silenes **12b** and **12e** with methanol and **12e** with acetic acid were determined at several temperatures between -20 and 55 °C in acetonitrile solution. The corresponding Arrhenius plots are shown in Figures 2.11-2.12 along with those for the parent compound **12a**. Arrhenius plots for quenching **12a-b** by methanol are linear, while that for **12e** curves downward at 13 °C. For acetic acid quenching the Arrhenius plots are linear in both cases. Linear least-squares analysis of the data (all the data points for **12b** with MeOH and **12e** with acetic acid, and only those for temperatures above 13 °C for reactions of **12e** with methanol, yield the Arrhenius

parameters listed in Tables 2.7. The diarylsilenes **12a,b,e** react with methanol with negative activation energies which increase in absolute magnitude with decreasing reaction rate. Acetic acid reacts with **12a,e** with a positive activation energies, with the more reactive silene exhibiting the larger activation energy.

Figure 2.11. Arrhenius plots for reaction of methanol with 1,1-diarylsilenes **12b** (X=Me; ◆) **12a** (X =H; □) and **12e** (X = CF_3; ●), in acetonitrile solution.

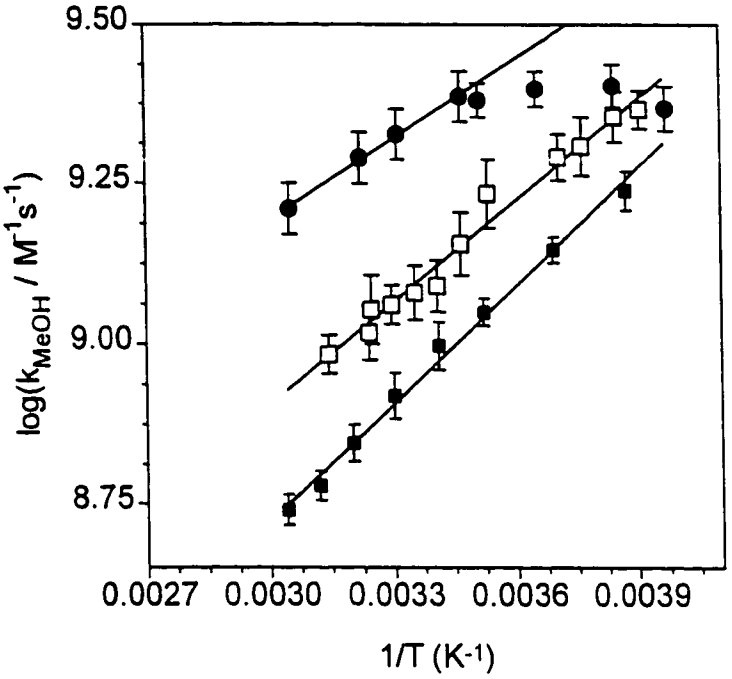

Figure 2.12. Arrhenius plot for quenching of 1,1-diarylsilenes **12a** (X=H; □) and **12e** (X=CF_3; ●) by acetic acid in acetonitrile solution.

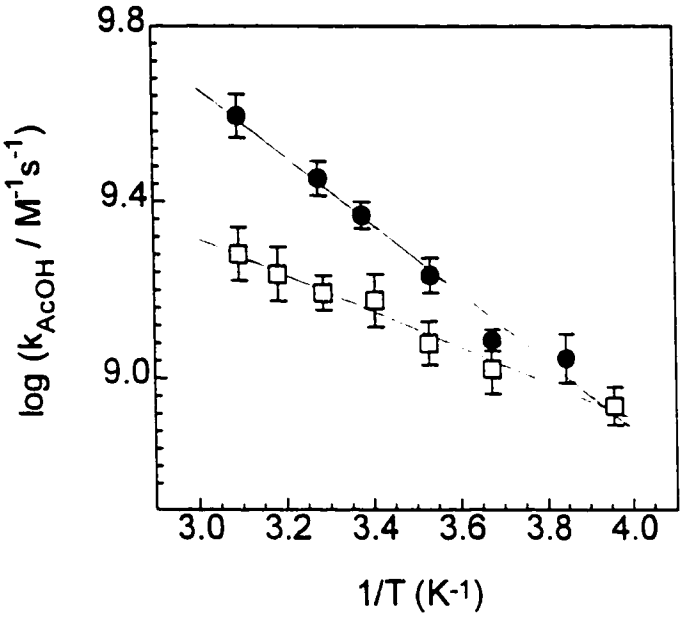

Table 2.7. Arrhenius Activation Energies (E_a) and Pre-exponential Factors (log A) for the Addition of Methanol and Acetic Acid to 1,1-Diarylsilenes (**12a,b** and **e**) in Acetonitrile Solution.[a]

	MeOH		AcOH	
X (**12a,b,e**)	E_a / (kcal/mol)	log (A / $M^{-1}s^{-1}$)	E_a / (kcal/mol)	log (A / $M^{-1}s^{-1}$)
X =Me	-2.7 ± 0.2	6.9 ± 0.2	b	b
X = H	-2.5 ± 0.3	7.3 ± 0.2	1.9 ± 0.2	10.5 ± 0.16
X = CF_3	-1.9 ± 0.2	7.9 ± 0.1	3.5 ± 0.5	12.0 ± 0.19

[a] Errors are reported as twice the standard deviation of from linear least squares analysis of the data shown in Figures 2.11-2.12. Rate constants employed for calculation of Arrhenius activation parameters were corrected for thermal expansion of the solvent.

[b] Not determined.

Addition of 0.5 M methanol to nitrogen-saturated acetonitrile or hexane solutions of **11a-e** was sufficient to reduce the lifetimes of **12a-e** to $\tau < 100$ ns and allowed detection of weak transient signals with $\lambda_{max} = 360$ nm. Qualitatively, the signal intensity of the *para*-chloro compound (**12d**) was the greatest. These transients decayed with pseudo-first order kinetics and had lifetimes in the 500-1000 ns range which were sensitive to the presence of oxygen or 1,3-octadiene. Plots of the rate of decay of these transients *versus* diene concentration were linear (eq 2.10), and afforded quenching rate constants in the range of (3-4) x 10^9 $M^{-1}s^{-1}$ in hexane solution at 23 °C. On the basis of the above observations, the transients are assigned to the silacyclobutane (**11a-e**) triplet

states. In the absence of methanol, addition of 0.01 M 1,3-octadiene to nitrogen-saturated solutions of **11a-e** resulted in no change in the initial absorbance (yield) or lifetime of **12a-e** (at 325 nm), indicating that the formation of the silene does not involve the triplet state of **11a-e**.

2.5 Reaction of 1,1-Diarylsilenes with Trimethylmethoxysilane

Nanosecond laser flash photolysis experiments were performed with trimethylmethoxysilane in the same manner as described above for alcohol additions. Addition of trimethylmethoxysilane to hexane solutions of **11a-e** resulted in reduction of the lifetimes of silenes (**12a-e**) and plots of rate of decay (k_{decay}) *versus* alkoxysilane concentration (eq 2.10) were linear (Figure 2.13). Absolute rate constants for reaction of **12a-e** with Me_3SiOMe are in the 10^7 $M^{-1}s^{-1}$ range (Table 2.8). The resulting Hammett plot shown in Figure 2.14 yields a ρ-value of (1.3 ± 0.1) for the reaction of **12a** with trimethylmethoxysilane in hexane solution.

Absolute rate constants for reaction of 1,1-diphenylsilene (**12a**) with trimethylmethoxysilane in hexane were determined between -14 and 55 °C, and the corresponding Arrhenius plot is shown in Figure 2.15. Linear least squares analysis of these data affords a Arrhenius activation energy of -(4.2 ± 0.4) kcal/mol and log A of (4.2 ± 0.3) $M^{-1}s^{-1}$.

Figure 2.13. Plot of k_{decay} *versus* [Me_3SiOMe] from laser flash photolysis of air-saturated hexane solutions of **11a** (X = H; ▲), **11b** (X = Me; ■), **11c** (X = F; □), **11d** (X = Cl; ◆) and **11e** (X = CF_3; ●) in the presence of trimethylmethoxysilane at 23 °C.

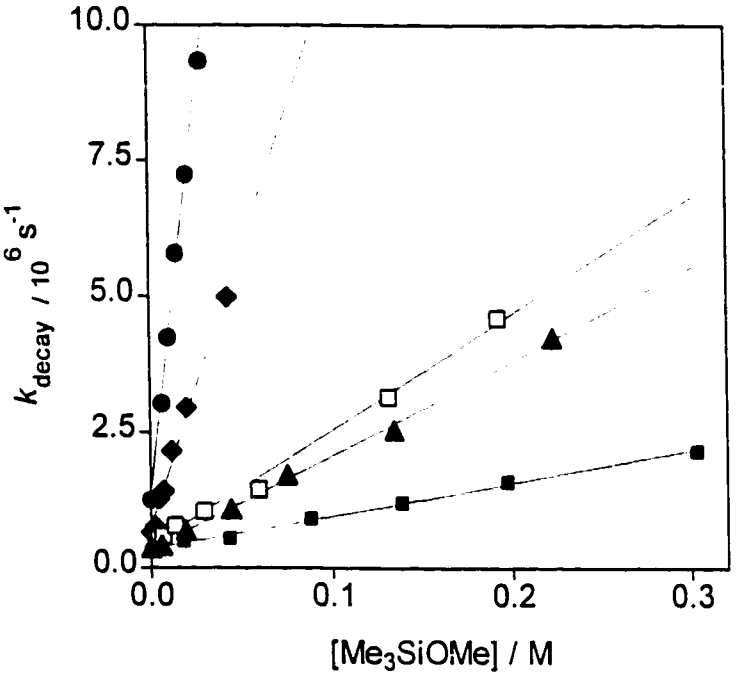

Figure 2.14. Hammett plot for the addition of trimethylmethoxysilane to the 1,1-diarylsilenes (**12a-e**) in hexane solution at 23 °C.

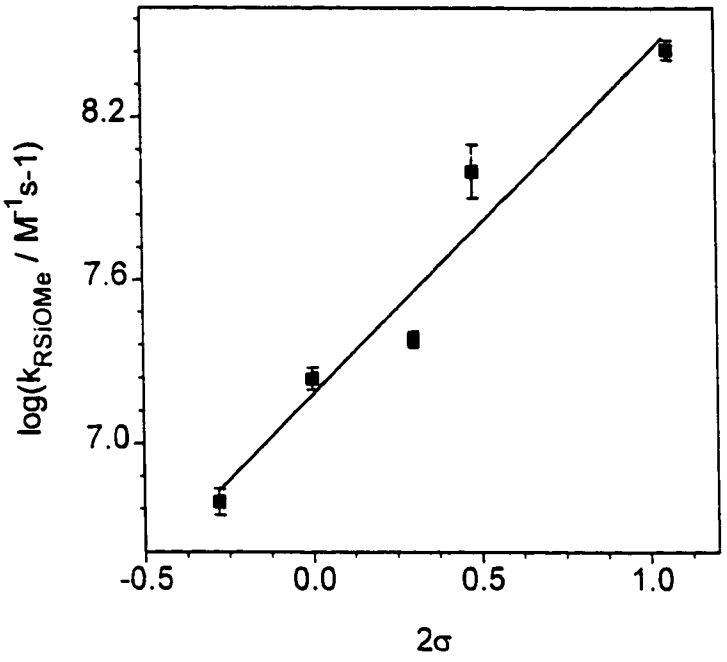

Table 2.8. Absolute Rate constants (k_q) for the Reaction of 1,1-Diarylsilenes (**12a-e**) with Trimethylmethoxysilane in Hexane Solution at 23 °C.[a]

$(p\text{-X-Ph})_2\text{-Si=CH}_2$ (**12a-e**)	$k_q / 10^7\ M^{-1}s^{-1}$
CH_3	0.61 ± 0.03
H	1.73 ± 0.07
F	2.40 ± 0.07
Cl	10.2 ± 1.0
CF_3	27.9 ± 1.0

[a] Errors are reported as twice the standard deviation of from linear least squares analysis of decay rate-concentration data according to eq 2.10.

Figure 2.15. Arrhenius plot for reaction of trimethylmethoxysilane with 1,1-diphenylsilene (**12a**) in hexane solution.

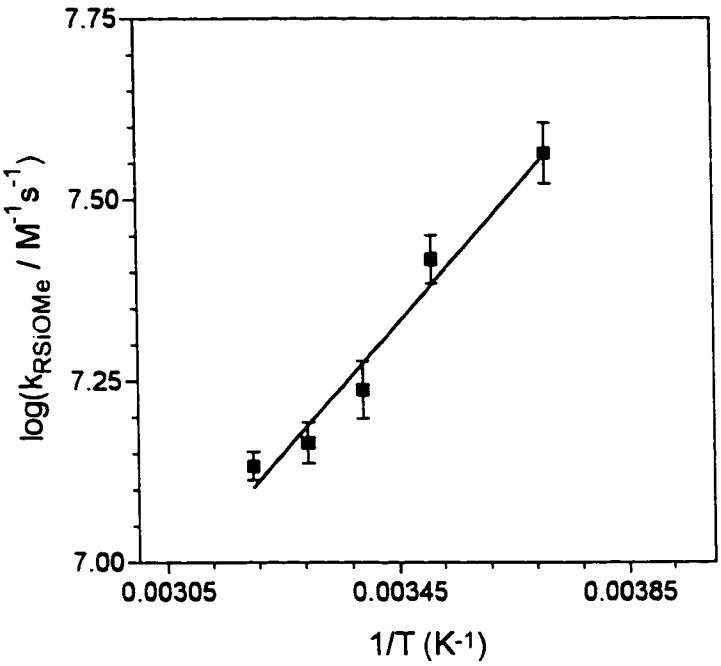

2.6 Reactions of 1,1-Diarylsilenes with Acetone

The lifetimes of transients **12a-e** are shortened by the addition of acetone or acetone-d_6 in hexane, *iso*octane or acetonitrile solution.[66] Plots of k_{decay} *versus* quencher concentration (eq 2.10) are linear in all cases and representative plots for silene quenching by acetone are shown in Figure 2.16. The bimolecular rate constants increase by a factor of two as the solvent polarity decreases from MeCN to *iso*octane or hexane. Quenching rate constants for reaction of **12a-e** with acetone and KIE's in *iso*octane and acetonitrile solution are listed in Table 2.9. The reaction rates and kinetic isotope effects

decrease with increasing electron-withdrawing ability of the substituent. Hammett plots (Figure 2.17) afford ρ-values of (1.0 ± 0.2) and (1.4 ± 0.2) for acetone addition in isooctane and acetonitrile solution, respectively. Reactions with acetone-d_6 yield reaction constants of (1.1 ± 0.3) and (0.8 ± 0.4) in *iso*octane and acetonitrile solution, respectively (Figure 2.18).

Figure 2.16. Quenching plots for the reaction of 1,1-diarylsilenes **11e** (■), **11d** (▲), **11c** (○), **11b** (◆), **11a** (●) with acetone in acetonitrile solution at 23 °C.

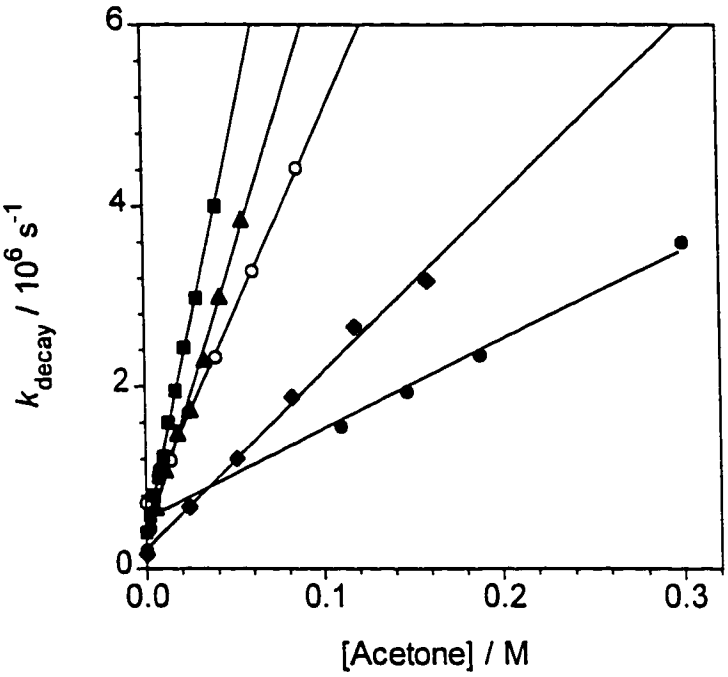

Table 2.9. Rate Constants (k_q) and KIE's[c] for the Reaction of 1,1-Diarylsilenes (**12a-e**) with Acetone in *Iso*octane and Acetonitrile Solution at 23 °C.[a]

$(p\text{-X-Ph})_2\text{-Si=CH}_2$	*Iso*octane	Acetonitrile
(**12a-e**)	k_q (Acetone) /10^8 $M^{-1}s^{-1}$	k_q (Acetone) / 10^8 $M^{-1}s^{-1}$
CH_3	1.66 ± 0.11	1.02 ± 0.14
	(k_H/k_D = 1.9 ± 0.2)	(k_H/k_D = 2.6 ± 0.2)
H	3.81 ± 0.16	1.94 ± 0.16
	(k_H/k_D = 1.9 ± 0.2)	(k_H/k_D = 2.2 ± 0.2)
F	12.9 ± 0.09	4.27 ± 0.11
	b	b
Cl	20.4 ± 2.0	6.35 ± 0.76
	b	(k_H/k_D = 2.0 ± 0.2)
CF_3	35.2 ± 2.0	8.73 ± 0.40
	(k_H/k_D = 1.4 ± 0.1)	(k_H/k_D = 1.3 ± 0.1)

[a] Errors are reported as twice the standard deviation of from linear least squares analysis of decay rate-concentration data according to eq 2.10.

[b] Not determined.

Figure 2.17. Hammett plots for quenching of 1,1-diphenylsilene (**12a**) by acetone in isooctane (▲) and acetonitrile (■) solution at 23 °C.

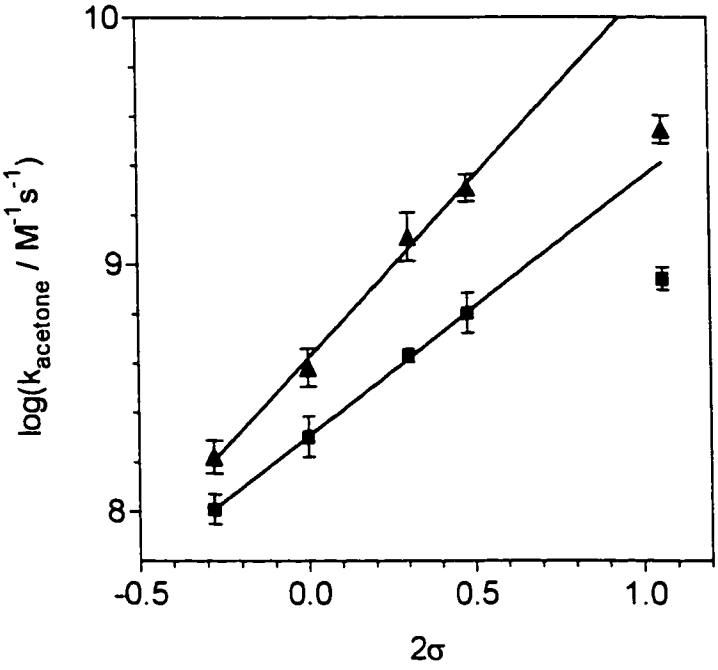

Figure 2.18. Hammett plots for quenching of 1,1-diarylsilenes (**12a-e**) by acetone-d_6 in isooctane (▲) and acetonitrile (■) solution at 23 °C.

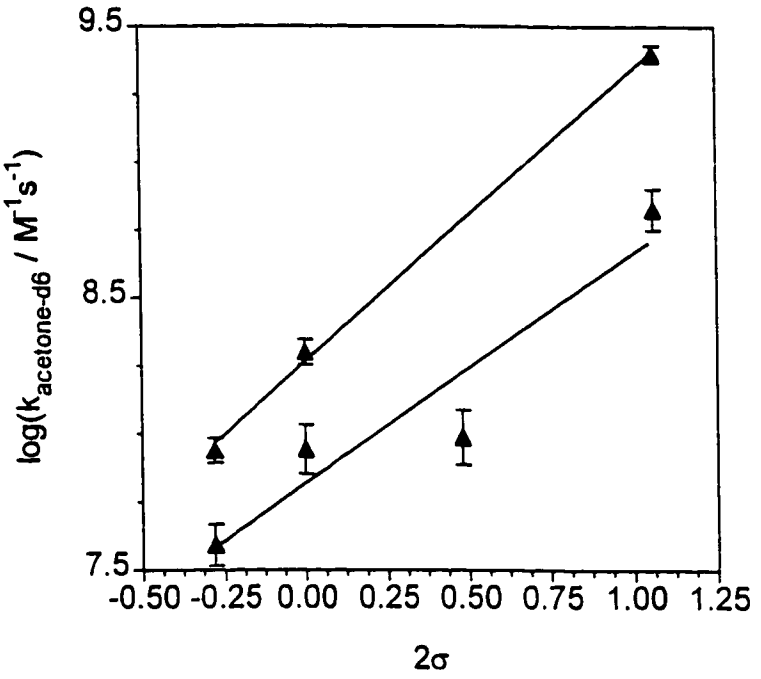

The effect of temperature on the bimolecular rate constants for reaction of acetone with **12a,b** and **12e** in acetonitrile and **12a** and **12e** in hexane solution was studied,[66] and the corresponding Arrhenius plots are shown in Figures 2.19-2.20. 1,1-Diphenylsilene reacts with acetone with activation energies of -(1.3 ± 0.1) kcal/mol and -(2.6 ± 0.2) kcal/mol in acetonitrile and hexane solution, respectively. The activation energies become more negative in absolute magnitude with decreasing electron withdrawing ability of the substituent, irrespective of solvent. Table 2.10 lists the activation parameters for the above reactions.

Figure 2.19. Arrhenius plots for reaction of 1,1-diarylsilenes **12a** (X=H; ■), **12b** (X=Me; ▲) and **12e** (X=CF_3; ▼) with acetone in acetonitrile solution.

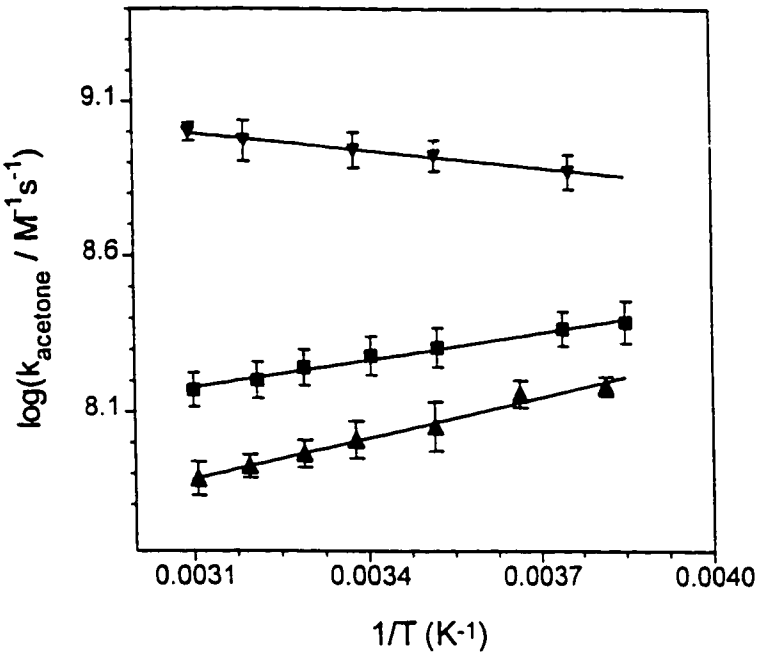

Figure 2.20. Arrhenius plots for quenching of 1,1-diarylsilenes **12a** (X=H; ■), and **12e** (X=CF_3; ▲) with acetone in hexane solution. The dotted line (---) is the Arrhenius plot of diffusion in hexane.

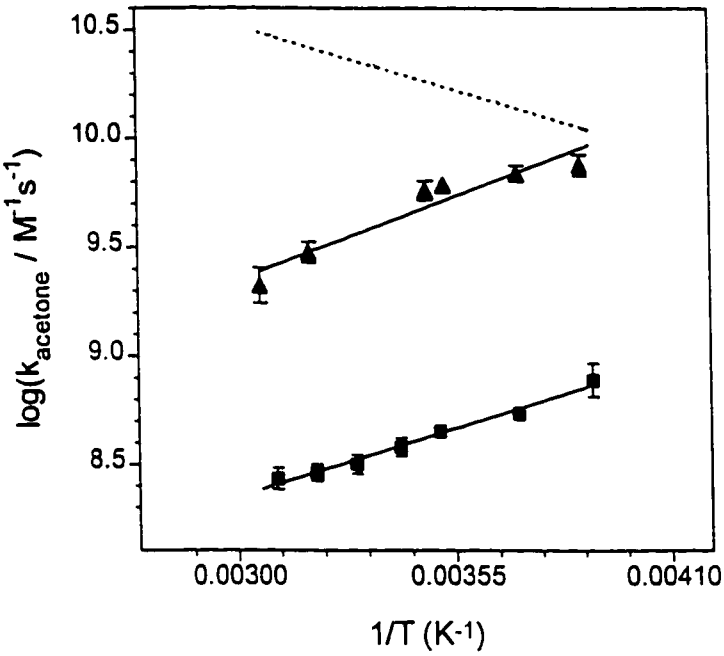

Table 2.10. Arrhenius Activation Energies (E_a) and Pre-exponential Factors (log A) for the Addition of Acetone to 1,1-Diarylsilenes (**12a,b** and **e**) in Acetonitrile and Hexane Solution.[a]

	Acetonitrile		Hexane	
X (**12a,b,e**)	E_a / (kcal/mol)	log (A / $M^{-1}s^{-1}$)	E_a / (kcal/mol)	log (A / $M^{-1}s^{-1}$)
X =Me	-2.0 ± 0.1	6.5 ± 0.1	b	b
X = H	-1.3 ± 0.1	7.2 ± 0.1	-2.6 ± 0.2	6.6 ± 0.1
X = CF_3	0.85 ± 0.05	9.6 ± 0.1	-3.2 ± 0.3	6.2 ± 0.2

[a] Errors are reported as twice the standard deviation of from linear least squares analysis of the data shown in Figures 2.19-2.20. Rate constants employed for calculation of Arrhenius activation parameters were corrected for thermal expansion of the solvent.

[b] Not determined.

2.7 A Study of the Effects of Direct Substitution at Silicon on 1-Silastyrene Reactivity

The substituent effect studies presented thus far are remote from the silenic silicon atom. The following chapter presents the effects of direct substitution at silicon on silene reactivity. The reactivity of 1-phenylsilene (**23a**) and 1-methyl-1-phenylsilene (**23b**) towards common silene traps in both nonpolar and polar solvents has been investigated by nanosecond laser flash photolysis techniques.

Nanosecond laser flash photolysis (λ_{exc} = 248 nm) of continuously flowing, air-saturated solutions of **22a-b** (0.013 M) in hexane or acetonitrile leads to weak, but readily detectable transient absorptions with $\lambda_{max} \approx 315$ nm. The absorptions decay on the microsecond time scale with mixed first- and second-order kinetics to within 10% of the pre-pulse level in scrupulously dried solvent. The transients **23a-b** exhibit similar UV absorption spectra, lifetimes and reactivity towards typical silene traps as was found for **12a**. Time-resolved UV absorption spectra were recorded for air-saturated solutions of **22a** and **22b** 0.1-0.4 μs and 1.0-1.8 μs after the laser pulse, respectively. Figure 2.21 shows the spectra obtained after subtraction for minor residual absorption, along with typical decay traces, recorded at a monitoring wavelength of 315 nm for **22a-b** in hexane solution. The residual absorption is assigned to a transient species which stable on the time scale of these experiments, and is undetectable in static UV absorption spectra of solutions of **22a-b** recorded immediately after steady-state photolysis to > 50 % conversion.

Figure 2.21. Transient absorption spectra from an air-saturated 0.013 M hexane solution of **22a** (a) and **22b** (b) after 248 nm excitation.

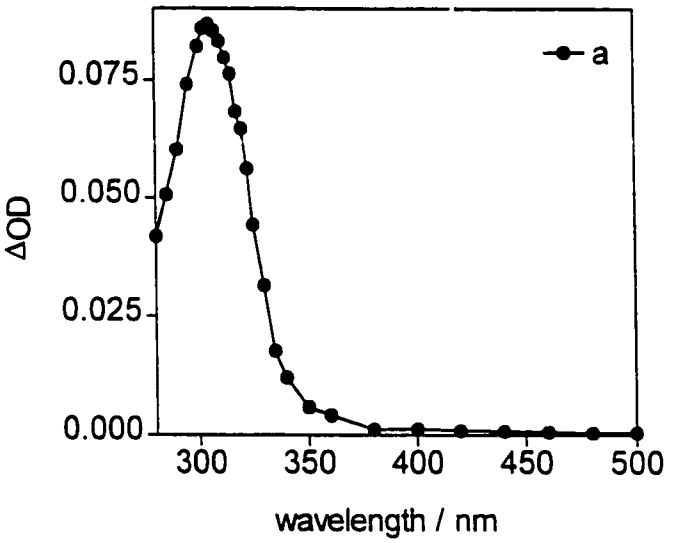

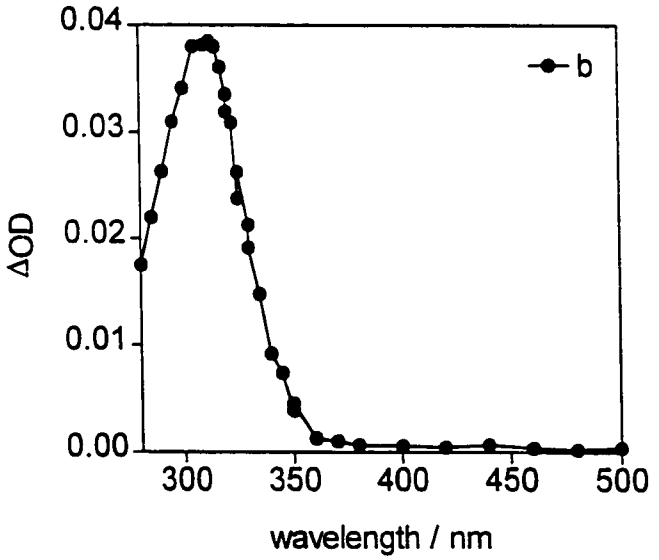

Addition of methanol, t-butanol, trimethylmethoxysilane, acetic acid, water or acetone results in a reduction in the lifetimes of **23a-b** and a change in decay kinetics to pseudo-first order. Plots of the rate constants for decay (k_{decay}) *versus* concentration of added quencher according to eq 2.10 were linear in all cases. Typical plots are shown in Figure 2.22 for quenching by methanol and methanol-Od in acetonitrile solution. Bimolecular rate constants and selected k_H/k_D values calculated from the data for reaction of the two transients in hexane and MeCN are listed in Tables 2.11-2.12, along with those for **12a**. 1-Silastyrenes **23a-b** are more reactive than **12a** towards alcohols, acetic acid and trimethylmethoxysilane in both hexane and acetonitrile solutions while the reactions of **23a-b** with acetone are slower than that of **12a**, with the reduction in reactivity being more pronounced in MeCN.

Figure 2.22. Typical quenching plots for reaction of 1-phenylsilene (**23a**) (▲) and 1-methyl-1-phenylsilene (**23b**) (■)with methanol in dry acetonitrile solution at 23 °C.

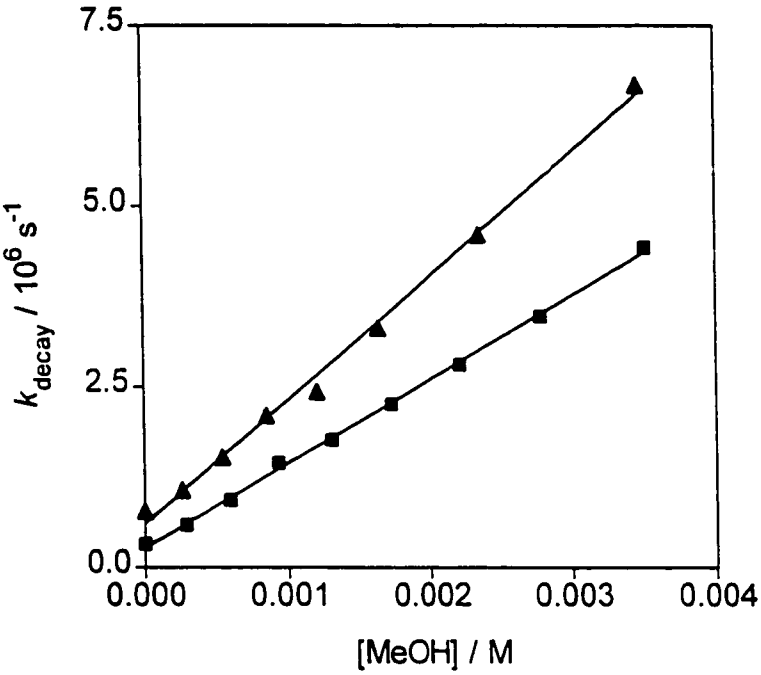

Table 2.11. Absolute Rate Constants for Reaction of 1-Phenylsilene (**23a**), 1-Methyl-1-phenylsilene (**23b**) and 1,1-Diphenylsilene (**12a**) with Various Quenchers in Air Saturated Hexane Solution at 23.0 °C.[a]

	k_q / $10^9 M^{-1}s^{-1}$		
Quencher	**23a**	**23b**	**12a**
MeOH	3.1 ± 0.1	3.3 ± 0.2	2.8 ± 0.2
t-BuOH	b	1.00 ± 0.06	0.40 ± 0.07
AcOH	b	4.8 ± 0.7	3.10 ± 0.02
Me_3SiOMe	b	0.018 ± 0.002	0.017 ± 0.007
Acetone	0.24 ± 0.01	0.36 ± 0.01	0.33 ± 0.02

[a] Errors are reported as twice the standard deviation of from linear least squares analysis of decay rate-concentration data according to eq 2.10.

[b] Not determined.

Table 2.12. Absolute Rate Constants and Kinetic Deuterium Isotope Effects[c] for Reaction of 1-Phenylsilene (**23a**), 1-Methyl-1-phenylsilene (**23b**) and 1,1-Diphenylsilene (**12a**) with Various Quenchers in Air Saturated Acetonitrile Solution at 23.0 °C.[a]

	23a		**23b**		**12a**	
Quencher	$k_q/10^9$ $M^{-1}s^{-1}$	k_H/k_D	$k_q/10^9$ $M^{-1}s^{-1}$	k_H/k_D	$k_q/10^9$ $M^{-1}s^{-1}$	k_H/k_D
MeOH	1.63 ± 0.08	1.3 ± 0.1	1.16 ± 0.02	1.6 ± 0.1	1.2 ± 0.1	1.5 ± 0.1
t-BuOH	0.67 ± 0.04	1.5 ± 0.1	0.20 ± 0.09	1.4 ± 0.1	0.22 ± 0.02	1.6 ± 0.1
AcOH	1.85 ± 0.08	1.1 ± 0.1	1.55 ± 0.04	1.0 ± 0.1	1.23 ± 0.07	1.1 ± 0.1
Acetone	0.066 ± 0.005	1.8 ± 0.3	0.048 ± 0.002	1.7 ± 0.1	0.18 ± 0.01	2.2 ± 0.2

[a] Absolute rate constants determined by nanosecond laser (248 nm) flash photolysis. Errors in rate constants are reported as twice the standard deviation from the linear least squares analysis of decay rate-concentration data according to eq 2.10.

[b] Not determined.

Absolute rate constants for quenching of **23b** by acetone in hexane and acetonitrile solution have been determined at various temperatures (-20-55 °C), and yield the Arrhenius plots shown in Figure 2.23, and activation parameters listed in Table 2.13. 1-Methyl-1-phenylsilene reacts with acetone with activation energies of -(0.83 ± 0.20) kcal/mol and -(1.9 ± 0.20) kcal/mol in acetonitrile and hexane solution, respectively.

Figure 2.23. Arrhenius plots for quenching of 1-methyl-1-phenylsilene (**23b**) by acetone in air saturated hexane (▲) and acetonitrile (■) solution.

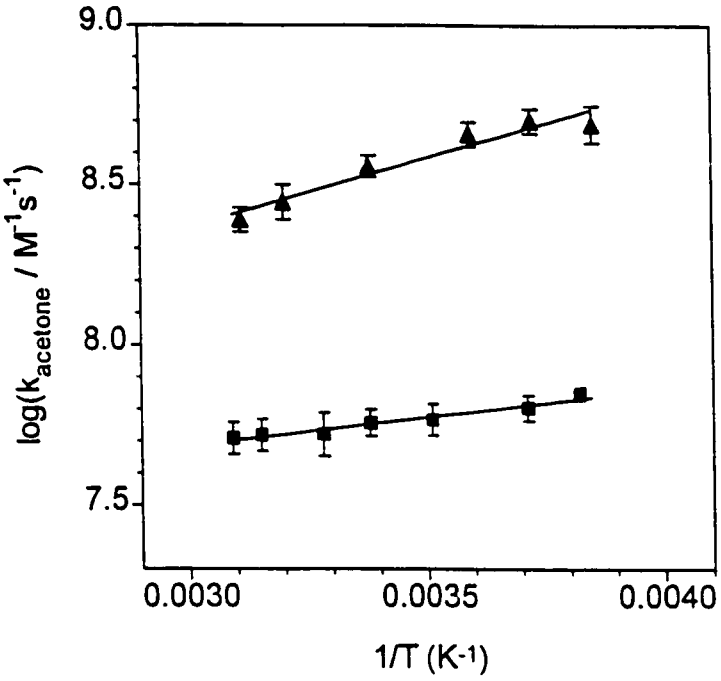

Table 2.13. Activation Parameters for the Reaction of 1-Methyl-1-phenylsilene (**23b**) with Acetone in Hexane and Acetonitrile Solution.[a]

Activation Parameter	Hexane	MeCN
E_a (kcal/mol)	-1.9 ± 0.2	-0.8 ± 0.2
log(A / $M^{-1}s^{-1}$)	7.1 ± 0.1	7.1 ± 0.2

[a] Errors are reported as twice the standard deviation of from linear least squares analysis of the data shown in Figure 2.22. Rate constants employed for calculation of Arrhenius activation parameters were corrected for thermal expansion of the solvent.

CHAPTER 3

DISCUSSION

3.1 Assignment of the Transient Observed in the Photolysis of 1,1-Diphenylsilacyclobutane

Nanosecond laser flash photolysis of **11a** in hexane, acetonitrile or tetrahydrofuran solution leads to easily detectable transient absorptions with a maximum at 325 nm and lifetimes of 3-5 μs (Figure 2.3). On the basis of a number of pieces of evidence this transient is assigned to **12a**. First, the transient UV spectra in hexane and acetonitrile solution are virtually identical to that reported from laser flash photolysis of other known photochemical precursors to **12a**: 1,1,3-triphenylsilacyclobutane[8] and methylpentaphenyldisilane[67], and are assigned to the Si=C π,π^* transitions. The transient decays with predominantly second-order kinetics in hydrocarbon solvent in the absence of added nucleophiles. This behaviour can be attributed to silene dimerization and is consistent with the formation of 1,1,3,3-tetraphenyl-1,3-disilacyclobutane (**19**), the head-to-tail dimer of **12a**, observed in the steady-state irradiation of **11a**.[29] The lifetime of the transient in all three solvents is shortened upon addition of known silene traps[2,5,6,42] such as water, alcohols, and carbonyl compounds, suggesting that the compound possesses a

Si=C double bond. Finally, steady-state photolysis of **11a** in the presence of methanol, ethanol, *t*-butanol and water affords the corresponding alkoxysilane in high chemical yield and is consistent with alcohol trapping of **12a**.

The transient UV absorption spectra of **12a** in hexane and MeCN solutions are very similar (Figure 2.3). However, the absorption spectrum in THF is substantially broadened and red-shifted in comparison to MeCN or hexane, which can be attributed to complexation of **12a** with the solvent. These types of complexes have been reported for both stable[9] and transient silenes.[30] In fact, stable silene-THF and a silene-amine complexes have been isolated and their X-ray structures indicate that the donor adducts are coordinated at the unsaturated silicon atom.[9]

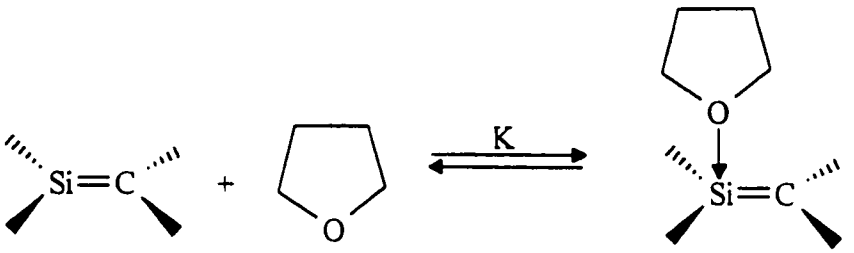

3.1

Transient silatriene-THF complexes were observed by NLFP of pentamethylphenyldisilane (**9a**), manifesting themselves by a red shift in the UV absorption spectrum from λ_{max} = 425 nm in MeCN, to λ_{max} = 460 nm in THF solution.[30] Transient spectra recorded in varying THF/MeCN mixtures have shown that the spectra at low concentrations of THF are broadened with respect to either pure MeCN or THF and that the spectral changes occur over the 1-12% THF composition range. The

spectrum recorded in 5% THF/MeCN consists of an absorption band with a maximum centered halfway between the two extremes and was interpreted as arising from equal amounts of free and complexed silatriene. With the assumption that the extinction coefficients of the free and complexed silene are similar, the equilibrium constant for THF complexation in acetonitrile solution was estimated to be *ca.* 1.6 M^{-1} (eq 3.1).[30] It was also found that increasing phenyl substitution at the trivalent silicon atom in **10** leads to a smaller equilibrium constant for complex formation, as evidenced by a smaller red-shift in the UV absorption maximum. In our case if we assign the broad absorption band for **12a** in THF to approximately equal amounts of free and complexed silene, we can estimate an equilibrium constant for a **12a**-THF complex of *ca.* 0.1 M^{-1} in pure THF.[29]

3.2 Reaction of 1,1-Diphenylsilene with Alcohols and Acetic Acid

From a mechanistic standpoint the reactions of silenes with alcohols have been by far the most thoroughly examined.[2,3,5,6,42] One of the first studies on silene-alcohol reactions was presented by Wiberg, who found that relative rates of reactivity of silenes towards alcohols depend on alcohol nucleophilicity and not acidity.[6]

On the basis of results of a study of the stereoselectivity of alcohol addition to a cyclic silene, Kira and coworkers suggested a mechanism involving initial nucleophilic attack by the alcohol oxygen atom to form a silene-alcohol complex, followed by rate-determining proton transfer (eq 1.20)[47]. Intramolecular proton transfer in the complex

results in the formation of *syn* adducts, while intercomplex proton transfer involving a second molecule of alcohol results in the formation of *anti* addition products. It was found that the relative rates of intra- to inter- molecular proton transfer decrease in the order methanol < *n*-propanol < *t*-butanol, which was suggested to parallel the acidities of the hydroxylic proton in the complexes, as approximated by the pK_a's of the protonated alcohols (Table 3.1).

Competing intra- and intermolecular proton transfer pathways leading to products was also suggested to explain the concentration dependence of the addition of *t*-butanol to 1,1-dimethyl-1,3-silabutadiene.[24] Product ratio studies revealed that as the *t*-butanol concentration decreases the yield of the (*E*)-adduct decreases, while the yield of the (*Z*)-isomer remains constant. Alcohol mediated proton transfer in the *s-trans* silene-alcohol complex yielding the (*E*)-adduct, and intramolecular molecular proton transfer in the *s-cis* complex resulting in (*Z*)-adduct formation (eq 1.22), were suggested to account for the above alcohol concentration dependencies.

Further evidence for a mechanism involving first- and second-order dependencies on alcohol concentration was provided through the use of nanosecond laser flash photolysis studies on 1,3,5-silahexatrienes (**10**).[9,30,44] It was found that plots of the rate of decay of 1,3,5-silahexatrienes *versus* quencher concentration are curved for quenchers such as water, methanol, ethanol and *t*-butanol. This result is consistent with Kira's proposed mechanism with the added requirement that formation of the silene-alcohol complex be reversible (Section 1.4.3). By assuming that the rate constant for collapse of

the complex to starting materials is faster than the rate constant for proton transfer by either pathway ($k_{-1} >> (k_2 + k_3[ROH])$), these plots can be expressed in the form of a quadratic variation in the pseudo-first order rate constant for silene decay with alcohol concentration (eq 1.25). At low alcohol concentrations, reaction occurs predominantly through the intracomplex proton transfer pathway but as alcohol concentrations increase so does the rate of the intercomplex proton transfer, since it requires a second molecule of alcohol.[44]

In contrast to the silatrienes, **12a** reacts about an order of magnitude faster (10^9 $M^{-1}s^{-1}$) and exhibits linear quenching plots for reaction with water, methanol (Figure 2.4), ethanol, *i*-propanol, *t*-butanol and acetic acid. All alcohols studied exhibit small but primary kinetic isotope effects in the 1.4 to 1.6 range, while acetic acid reacts with no significant isotope effect (Table 2.2). These results are consistent with the stepwise addition of alcohols to **12a** (eq 1.24) if the rate of proton transfer within the complex is much faster than that of the extracomplex proton transfer pathway at the much lower quencher concentrations employed for kinetic studies (i.e. $k_2 >> k_3[ROH]$ when [ROH] < 0.01M for MeOH; < 0.05 for *t*-BuOH). Under the conditions employed for LFP, the overall rate expression then reduces to eq 3.2.

$$k_{decay} = k_o + \frac{k_1 k_2}{k_{-1} + k_2}[ROH] \qquad \textbf{3.2}$$

The linear dependence of k_{decay} of **12a** on [ROH] implies that over the alcohol concentration ranges employed in the study, **12a** reacts predominantly via the

intracomplex proton transfer pathway (eq 3.3).[29] This linearity is advantageous since it allows direct determination of the second-order rate constants for reaction of **12a**. However, the linearity also masks the presence of the extracomplex proton transfer pathway, making extraction of the rate ratio k_2/k_3 impossible. Therefore steady-state competition experiments were performed. These provide an alternative method to investigate the extracomplex proton transfer pathway since under these conditions much higher alcohol concentrations can be employed.

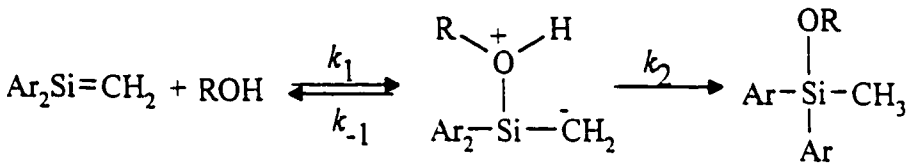

3.3

Competitive steady-state trapping experiments were performed using methanol as the standard and water, ethanol and *t*-butanol. Assuming that the reaction of **12a** with an alcohol exclusively yields alkoxysilane, the ratios of the silene-alcohol adducts formed should be directly proportional to the concentration ratio of the two alcohols. Plots of the product ratio *versus* alcohol concentration ratio (Figures 2.1 and 2.2a) yield a slope which is equal to a proportionality constant, C_{ROH}, for reaction (eq 2.9). Assuming the scheme presented in eq 3.3, this constant is equal to the expression shown in eq 3.4, and is directly proportional to the ratio in rate constants provided that addition of the two alcohols follows the same alcohol concentration dependence.

$$C_{ROH} = \frac{(k_1k_2/k_{-1} + k_1k_3/k_{-1}[MeOH])}{(k_1k_2/k_{-1} + k_1k_3/k_{-1}ROH])} \qquad \textbf{3.4}$$

Typically, steady-state competition experiments were performed at higher bulk alcohol concentrations (> 0.05 M) than used for LFP studies, to insure quantitative trapping of the silene. Plots of adduct ratios *versus* alcohol concentration ratios for methanol, ethanol, water and *t*-butanol are linear (Figure 2.1). For methanol, ethanol and water the C_{ROH} values are independent of alcohol concentration, and agree very well with absolute rate constant ratios determined by NLFP (Table 2.2). These results indicate that the contributions to product formation by the extracomplex proton transfer pathway are similar for methanol, ethanol and water and that these alcohols react via a similar mechanism.

The C_{ROH} value determined from competition experiments with methanol and *t*-butanol, at [ROH] > 0.05 M, differed significantly from the absolute rate constant ratio. However, upon further examination it was found that C_{ROH} in this case varies with bulk alcohol concentration, indicating that at least one of the alcohols is governed by a rate law containing a term of higher order in alcohol concentration (Figure 2.2). At high alcohol concentrations C_{ROH} approaches 15, which is about three times higher than the ratio of rate constants determined by NLFP. As the bulk alcohol concentration is reduced, the ratio approaches a value of (4.9 ± 0.2), which is very similar to that determined directly ($k_{MeOH}/k_{t\text{-}BuOH} = 3.7 \pm 0.5$) (Table 2.1). The plot does not level off in the low alcohol concentration range. This may be due to the presence of water in the solvent, which can

contribute to the formation of **13a** by assisting in the extracomplex proton transfer as well as form **17a**, which is observed as a coproduct in all irradiations performed in acetonitrile solution.[29]

The above steady-state competition experiments have indeed provided evidence that methanol has two possible pathways for reaction, while *t*-butanol has only one. For methanol, ethanol and water, **12a** reacts via competitive intracomplex and extracomplex proton transfer pathways, i.e. the same mechanism. For the reaction with *t*-butanol, the extracomplex proton transfer pathway is greatly reduced, which is in agreement with previous reports for methanol and *t*-butanol additions to other silenes.[44,47] At high alcohol concentrations, such as those employed in the steady-state experiments ([ROH] > 0.05 M), the methanol-adduct is disproportionately favoured over the *t*-butanol adduct, resulting in the lack of agreement between the relative and absolute rate constant ratios.

In NLFP experiments where low alcohol concentrations are employed (<0.01 M), relative rate ratios of intracomplex proton transfer pathways were observed ($k_2 >> k_3$[ROH]), since the extracomplex proton transfer pathway for methanol addition is relatively unimportant at these alcohol concentrations.

Acetic acid is the most acidic quencher examined (pK_a = 22.3, MeCN; 25 ^{0}C) and is less nucleophilic than methanol as indicated by the much higher acidity of its conjugate acid (Table 3.1).[68] The rate constant for reaction of **12a** with acetic acid is in the 10^9 $M^{-1}s^{-1}$ range, similar to methanol and ethanol addition, but acetic acid exhibits no isotope effect. These results are also consistent with the proposed two-step mechanism, if there

a change in the rate determining step from proton transfer to complex formation.[29] However, these observations alone do not allow us to completely eliminate a concerted addition mechanism. In this case the observation of a very small kinetic isotope effect could be ascribed to the fact that the reaction is strongly exergonic.[69]

The KIE's for reaction with **12a** increase slightly throughout the series H_2O < MeOH < EtOH < *t*-BuOH (Table 2.3) which suggests that the variation in rate constant ($k_{MeOH} >> k_{t\text{-}BuOH}$) can be attributed to a reduction in the rate of intracomplex proton transfer throughout the series (eq 1.24). The equilibrium constant for complex formation is also contained in the overall rate expression (eq 1.25) and is expected to increase with increasing alcohol nucleophilicity and decreasing steric bulk. The above conclusion is exactly opposite to that made by Kira, who suggested that the increase in syn-stereoselectivity in the addition of alcohols to the cyclic silene, in the order MeOH < n-PrOH < *i*-PrOH < *t*-BuOH is a result of an increase in the rate of intracomplex proton transfer, and a corresponding decrease in the rate of extracomplex proton transfer throughout the series.[47] The proposal was made on the basis that the rate of intracomplex proton transfer should increase with increasing acidity of the hydroxylic proton in the complex, and parallel the pK_a's of the protonated alcohols[47] (Table 3.1). Aqueous ROH_2^+ pK_a values were utilized for this analysis since mixtures of acetonitrile containing quite high alcohol concentrations (1-20 M) were employed for these experiments. In our system, where only millimolar alcohol concentrations are used, the ordering of protonated alcohol acidity is opposite to that in aqueous solution (Table 3.1).

Table 3.1. Conjugate Acid pK_a's for Methanol, *t*-Butanol, Water, Acetone and Acetic Acid in Acetonitrile[68] and Aqueous[21,47] Solution at 25 °C.

ROH_2^+	pK_a (MeCN)	pK_a (Water)
$MeOH_2^+$	2.3	-2.2
t-$BuOH_2^+$	3.4	-3.8
H_3O^+	2.3	-1.7[21]
	-0.1	-7.2[21]
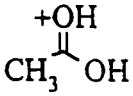	1.1	-6.0[21]

Application of the same type of analysis to our system predicts that the rate of intracomplex proton transfer should be *slower* for the silene/*t*-BuOH complex than for the silene/MeOH complex, which is consistent with the trend in the kinetic isotope effects on the absolute rate constants for reaction of **12a** with these alcohols. The actual individual rate constants of eq 1.25 may be solvent dependent. However, it seems reasonable to conclude that the relative rate of intracomplex to extracomplex proton transfer is much higher for *t*-BuOH than MeOH regardless of solvent.[29] This conclusion is made on the basis of the results obtained by Kira,[47] kinetic data obtained for the addition of alcohols to 1,3,5-silahexatrienes in hydrocarbon, acetonitrile and THF solvents,[44] and the results presented above for the steady-state competition experiments with **12a** in MeCN.[29]

Absolute rate constants for reaction of **12a** with methanol, *t*-butanol and acetic acid are solvent dependent, decreasing in the order of hexane > MeCN > THF (Table 2.4). The largest reduction in reactivity from hexane to THF solution is observed for reaction with *t*-butanol. This variation follows an order of increasing hydrogen bonding ability of the solvent, not bulk polarity, and can be attributed to increasing solvation of silene with increasing solvent Lewis basicity.[70] In the case of THF, this solvent can also act as a general base for deprotonation of the silene-aicohol complex (eq 3.5) and this would increase the second-order rate constant for reaction of methanol relative to its value in acetonitrile (eq 3.6). Such an increase in reactivity is observed for reactions of bulkier silenes, such as the silatriene derived from trimethyltriphenyldisilane (**10**), where solvation by THF is weak.[30,44] Therefore, the actual change in absolute rate constants for reaction from hexane to THF solution is a composite of a decrease in reactivity due to solvation effects plus an increase due to solvent-assisted deprotonation.

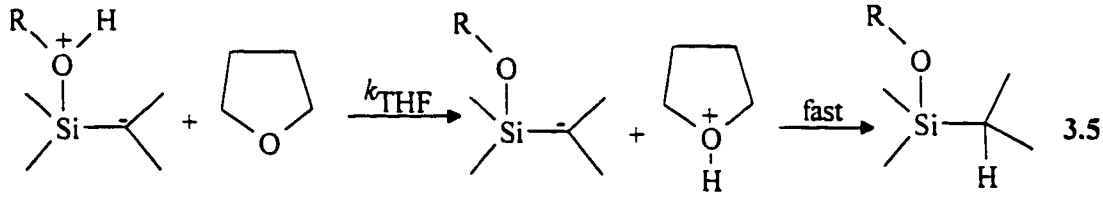

3.5

The reaction of **12a** with *t*-butanol in THF solution shows the largest reduction in rate constant in comparison to methanol or acetic acid. This result can be rationalized in terms of a difference in the importance of the extracomplex proton transfer mechanisms for the two alcohols and acid. If proton transfer in the silene *t*-butanol complex occurs

exclusively by the intramolecular pathway, then the approximate factor of ten reduction in the absolute rate constant can be attributed solely to strong solvation of the silene by the ether.

In the case of methanol addition, proton transfer can occur by both the intra- and intermolecular pathways. Solvent assisted deprotonation of the methanol-silene complex is predicted to increase the absolute rate constant in THF relative to MeCN or hexane. This predicted increase in rate manifests itself in an overall reduction in rate constant by only a factor of four, since it is still not enough to overcome the retarding effects of solvation on the silene.

Rate determining complex formation is observed for reactions of **12a** with acetic acid, thus the deprotonation step in this system is less important and is predicted to be less sensitive to solvent-assisted deprotonation. However, the nucleophilicity of the carboxylic acid is expected to increase in THF due to strong hydrogen bonding to the solvent, which should lead to enhanced reactivity in THF relative to MeCN. An overall reduction in rate constant by a factor of four is observed in this case, indicating that the enhancement in nucleophilicity of the trap is still not sufficient to overcome the strong solvation.

Thus, in spite of the fact that THF might be expected to have conflicting effects on the rate constants for the individual steps in the mechanism, the dominant factor appears to be solvation of the silene, resulting in an overall reduction in reactivity in this solvent compared to the more polar MeCN.

$$k_{decay} = k_0 + \frac{k_1}{k_{-1}} * \frac{1}{(K_{THF}[THF] + 1)} * \{k_2[ROH] + k_{THF}[THF][ROH] + k_3[ROH]^2\} \quad 3.6$$

3.3 Arrhenius Study of the Reaction of 1,1-Diphenylsilene with Alcohols and Acetic Acid

The experimental evidence presented thus far on alcohol and acetic acid addition to **12a** can be explained by a two-step mechanism involving a silene-alcohol complex (eq 3.3). Unfortunately there has of yet been no direct observation of silene-alcohol complexes. The indirect evidence which exists for their intermediacy consists of (i) the fact that product distribution quite commonly varies with alcohol concentration,[44,47] (ii) the isolation of stable silene-ether complexes,[12] and (iii) the observation of transient silene-ether complexes by LFP.[29,30]

Mechanisms of this type, involving rapid reversible formation of an intermediate that decomposes to reactants faster than to products ($k_{-1}>>k_2$), have been reported in the past and often lead to negative Arrhenius activation energies. Examples include reactions of singlet carbenes with halocarbons[71], alcohols[72-74] and alkenes[75-78] in solution, addition of alkenes to carbenium ions[79] in solution, and gas phase additions of silanes[80] and acetylenes[81] to silylenes. For example, phenylchlorocarbene reacts with tetramethylethylene in toluene solution with a rate constant of 1.5×10^9 $M^{-1}s^{-1}$, and an activation energy of -1.4 kcal/mol.[78]

One can envisage a negative activation energy by examining the reaction coordinate diagram shown in Figure 3.1 for reactions of **12** with an alcohol, ROH. A negative activation energy will result if the free energy barrier of the second step (in this case proton transfer) is dominated by a large entropic term such that the enthalpy of the transition state is lower than that of the reactants; i.e. $-\Delta H^0_{eq} >> \Delta H^{\ddagger}_2$. On the other hand, when collapse to product is much faster than reversion to reactants ($k_{-1} << k_2$), then the first step is the rate-determining step and a positive activation energy will result.

Figure 3.1 (a) Free Energy *versus* Reaction Coordinate and (b) Free Enthalpy *versus* Reaction Coordinate Diagrams for a Two Step Reaction Exhibiting a Negative Arrhenius Activation Energy

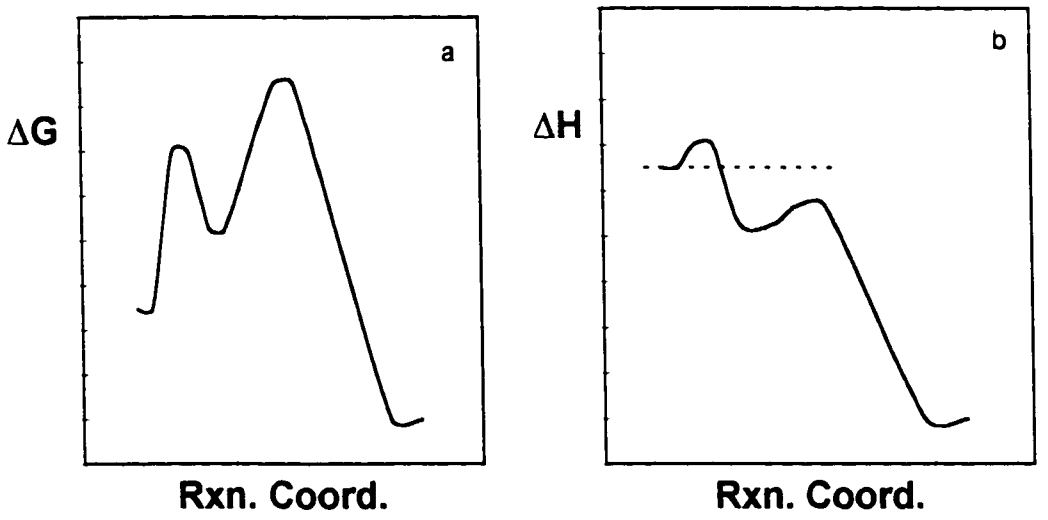

An alternative interpretation of negative activation energies has been given by Houk and Rondan[82,83] whose calculations on halocarbene cycloadditions find no evidence for complex formation and no enthalpic barrier for reaction. They predict that the reaction proceeds concertedly where the free energy of activation is dominated by a large and negative entropic term. Therefore the rate of reaction increases as the temperature decreases since the $-T\Delta S^{\ddagger}$ term decreases thereby causing a reduction in $\Delta G^{\ddagger}$. In the present study, formation of a complex is more consistent with the results presented thus far, as well as with previous theoretical,[84] spectroscopic[6,29], kinetic[9,29] and product studies[29,44,47] of the reaction.

In order to provide further evidence for the proposed two step mechanism, the temperature dependence of the absolute rate constants for reaction of **12a** with methanol, *t*-butanol and acetic acid was investigated (Figure 2.5).[45] The bimolecular rate constants for reactions of **12a** with methanol and *t*-butanol increase with decreasing temperature yielding negative activation energies, while acetic acid addition exhibits a positive activation energy (Table 2.5). The observations of negative activation energies for reaction of **12a** with the two alcohols, the primary deuterium isotope effects on the rate constants, and the results of steady-state competition experiments all provide reasonable indirect evidence for the stepwise mechanism for addition of alcohols to **12a**.[45]

In contrast to the addition of alcohols, **12a** reacts with acetic acid with a positive activation energy and kinetic isotope effect indistinguishable from unity ($k_H/k_D \approx 1.1 \pm 0.1$). These results are also consistent with the two step mechanism presented in eq 3.7, if

in this case there is a change in the rate determining step from proton transfer to complex formation.[45] Unfortunately, the above findings are also consistent with concerted acetic acid addition to **12a**, with the small isotope effect resulting from the fact that the reaction is strongly exergonic.[69,85] In general, very reactant-like transition states can afford very small primary hydrogen isotope effects.[35] Chiltz *et al.* studied the KIE's on the photochlorination of H_2, CH_4, $CHCl_3$ and C_2H_6 as a function of the heat of reaction.[86] The relatively thermoneutral reaction of CH_4 + Cl yields a k_H/k_D of 5 which should be compared to the exothermic reactions of C_2H_6 + Cl, and $CHCl_3$ + Cl which exhibit a k_H/k_D = 2.[86] Such a variation in KIE was also reported for the reactions of H_2 with halogen atoms.[87] The very exothermic addition of fluorine to H_2 exhibits a k_H/k_D = 1.9, while for the slightly endothermic addition of chlorine k_H/k_D = 9.7.

The work presented in section 3.5, on the effects of 1,1-diaryl-substitution on the rate constants and activation parameters for acetic acid addition to **12** allow us to rule out the concerted pathway. In this system, the carbonyl oxygen is the likely site of bonding to silicon due to its much higher nucleophilicity in comparison to the hydroxyl oxygen,[21] in which case proton transfer occurs via a six-membered transition state (eq 3.7).

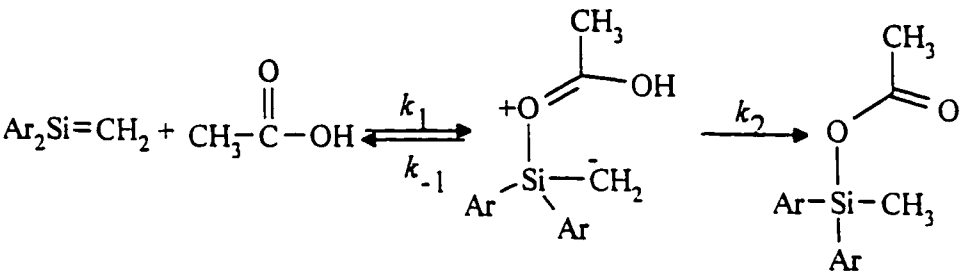

3.7

3.4 Reactivity of 1,1-Diarylsilenes and 1-Silastyrenes towards Alcohols and Acetic Acid

The investigation of the photochemistry of 1,1-diarylsilacyclobutanes (**11b-e**) through NLFP and steady-state photolysis techniques indicates that all four compounds exhibit similar photochemical behaviour to the parent compound **11a**.[10] The UV absorption maxima of silenes **12b-e** appear at 325 nm, indicating that there is no appreciable substituent effect on the absorption maxima of the diarylsilenes (Figure 2.7). All five silenes decay with pseudo-first order kinetics in dry acetonitrile and exhibit lifetimes in the 2-3 μs range. The lifetimes decrease slightly throughout the series in the order **12b** > **12a** > **12c** > **12d** > **12e**; i.e., the lifetimes shorten with increasing electron-withdrawing power of the substituent. This is consistent with an increase in bond polarity which results in an increase in reactivity towards residual water in the solvent. Plots of the rate constants for decay *versus* concentration of added quencher (methanol, *t*-butanol and acetic acid) are linear (Figure 2.8) and for all three quenchers the rate constants for reaction increase with increasing diaryl-substitution with electron withdrawing groups (Table 2.6).

In comparison to **11a-e**, NLFP of **11f** yields weak transient absorptions in the 280-320 nm range. Steady-state irradiation of **11f** in the presence of methanol yields **13f** in very low chemical yield (<12 %). These observations indicate that **11f** undergoes

[2+2] cycloreversion with much lower efficiency than the other compounds, making it an unsuitable source of **12f**.

Steady-state irradiation of **11b-e** in the presence of methanol yields the corresponding methoxysilanes (**13b-e**) in high chemical yields, indicative of the formation of silenes **12b-e**. There is no appreciable variation in the quantum yield for silene formation ($\Phi_{\text{-11a}} = 0.24 \pm 0.03$)[29] since the rates of formation of methoxysilanes **13a-e** under similar photolysis conditions do not vary appreciably throughout the series (Table 2.1).

Intersystem crossing (ISC) to yield the silacyclobutane triplet states also occurs, but only to a minor extent. Triplet formation is unrelated to the formation of **12** by [2+2] cycloreversion of **11**, so we conclude that this reaction occurs from the lowest excited singlet state of the arylsilacyclobutane. Qualitatively, the triplet yield is the largest for **12d**, presumably due to the ability of the *para*-chloro substituent to enhance ISC through a heavy atom effect.[88,89]

Silenes **12a-e** show first order dependencies of k_{decay} on alcohol concentration, which indicates that, over the alcohol concentration ranges employed, reactions occur predominantly by the intracomplex proton transfer pathways for both alcohols in all five cases (eq 3.3). The observed second order rate constants for reaction of **12a-e** with methanol and *t*-butanol increase with increasing electron withdrawing power of the diaryl-substituent (Table 2.6). The Hammett plots (Figure 2.9) afford ρ-values of +(0.31 ± 0.02) and +(0.55 ± 0.04) for methanol and *t*-butanol addition, respectively. Three point

Hammett plots obtained for the deuterated analogues yield similar reaction constants. The fact that the observed ρ-values for reactions with the above alcohols are positive is consistent with the fact that, in the reaction mechanism, nucleophilic attack by the alcohol at silicon precedes protonation at carbon.

Referring to eq 3.3, the reaction constants can be approximated by the sum of those for the complexation and proton transfer steps. The ρ-value for complexation is expected to be positive since electron withdrawing substituents should increase the polarity of the bond and make it more reactive. On the other hand the ρ-value for proton transfer should be small because this step involves charge reorganization within the zwitterionic complex. The fact that the overall reaction constant is positive for alcohol additions and essentially identical to the ρ-values obtained for reaction with their deuterated isotopomers, implies that complexation is more sensitive to polar factors.[10]

It would be interesting to compare ρ-values of this system to those obtained for the analogous reactions of alkenes. Nucleophilic addition to alkenes occurs in those compounds that are highly activated, such as in the case of Michael addition reactions.[90] Hammett studies have been reported in these types of systems for the addition of cyanide ion,[91] amines (eq 3.8)[92] and enolates[93] to substituted β-nitrostyrenes. These reactions exhibit positive ρ-values of +(0.2-1.0) for alkene-nucleophile complexation (k_1), depending on nucleophile and solvent, and are similar in magnitude to those observed here for **12** (eq 3.8).

$$ArCH{=}CHNO_2 + R_2NH \underset{k_{-1}}{\overset{k_1}{\rightleftharpoons}} ArC(R_2NH{+})HCH{=}NO_2^- \underset{H^+}{\overset{K_a}{\rightleftharpoons}} ArC(R_2N)HCH{=}NO_2^-$$

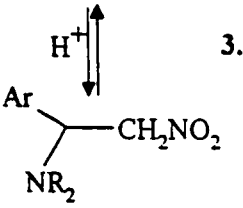

3.8

The k_H/k_D values for reactions of **12a-e** with methanol decrease with increasing electron withdrawing ability of the substituent (Table 2.6) and can be explained as arising from a variation in the relative rates of reversion of the complex to starting material (k_{-1}) and collapse to products (k_2) as a function of substitution. The overall isotope effect will be a maximum in the limit of fully reversible complex formation, i.e., $k_{-1} >> k_2$, and will decrease in magnitude to the limit of a secondary effect when $k_2 >> k_{-1}$. Thus, the reduction of k_H/k_D with increasing electron withdrawing power of the substituent can be ascribed to an increase in the k_2/k_{-1} ratio throughout the series.[10]

Since the complex has not been observed directly we have not been able to extract individual rate constants (k_1, k_{-1} or k_2). However, further inspection of the proposed mechanism (eq 3.3) reveals that the two reaction channels available to the complex should have opposing entropic requirements. Reversion of the complex to starting materials should exhibit a positive entropy of activation ($\Delta S_{-1}^{\ddagger} > 0$), while collapse to products should have a negative activation entropy ($\Delta S^{\ddagger}_2 < 0$). Therefore the two pathways will have opposing temperature dependencies and provided that a large enough temperature range can be spanned experimentally, the Arrhenius plot will be bell-shaped (Figure 3.2). The maximum negative value of E_a will be observed in the high

temperature extreme where $k_{-1} >> k_2$, i.e., when formation of the complex is fully reversible, and $k_{obs} = (k_1/k_{-1})k_2$. At the low temperature extreme where $k_2 >> k_{-1}$ complex formation is rate-determining ($k_{obs} = k_1$) and, therefore, a positive E_a will be observed.[10] It then follows that the changeover in mechanism occurs at the apex where $k_{-1} \approx k_2$, and $k_{obs} = k_1/2$. These two situations also predict a variation in the k_H/k_D from a primary one at high temperatures ($k_{-1} >> k_2$), to a secondary one where $k_2 >> k_{-1}$. The Arrhenius plots for methanol and methanol-Od addition to **12a** verify the prediction of the dependence of KIE on temperature, with an increase in k_H/k_D from (1.5 ± 0.2) at -20 °C to (2.3 ± 0.2) at 55 °C. The fact that the activation energy for methanol-Od addition is more negative than for methanol is consistent with the prediction that k_2/k_{-1} should be smaller for MeOD than for MeOH, owing to the expected primary KIE on intracomplex proton transfer.

Figure 3.2 A Hypothetical Bell Shaped Arrhenius Plot Representing a Change in the Rate Determining Step with Temperature for a Reaction Involving Two Sequential Steps

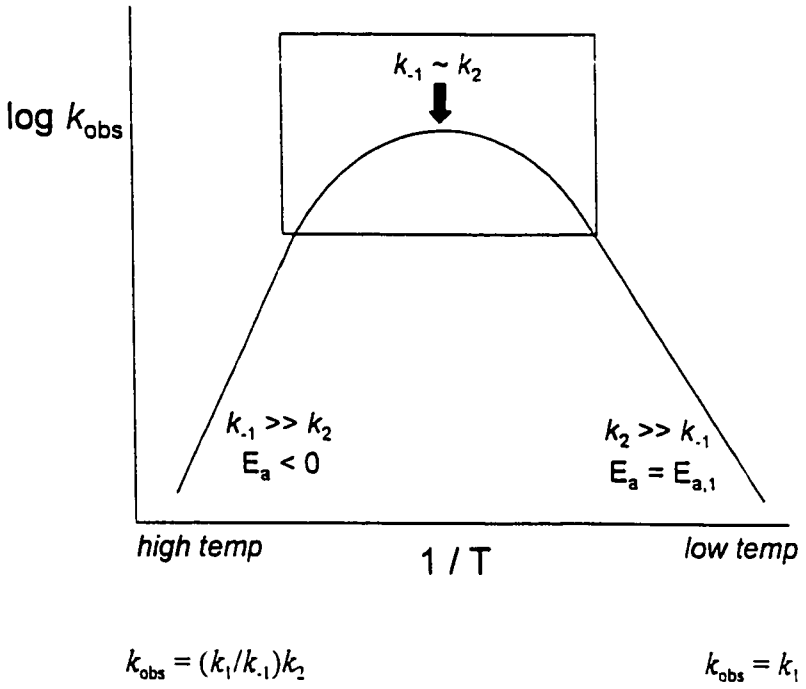

Curved Arrhenius plots have been reported in the literature for numerous reactions including cycloadditions of phenylchlorocarbene[77] or (4-trifluoromethylphenyl)bromocarbene to tetramethylethylene,[76] reaction of singlet oxygen with diphenylisobenzofuran,[94] and phosphorescence quenching of 4-carboxymethylbenzophenone by alkenes.[95] While the debate continues on the mechanism of carbene-alkene additions,[71] the observation of a curved Arrhenius plot was assigned to a change in the rate-limiting step with a change in temperature in the phosphorescence quenching of 4-carboxymethylbenzophenone by tetramethylethylene (TME) and trimethylethylene (eq 3.9). This deviation from linearity was associated with a change from reversible exciplex formation and rate determining exciplex deactivation at high temperatures to diffusion controlled exciplex formation at low temperatures.[95]

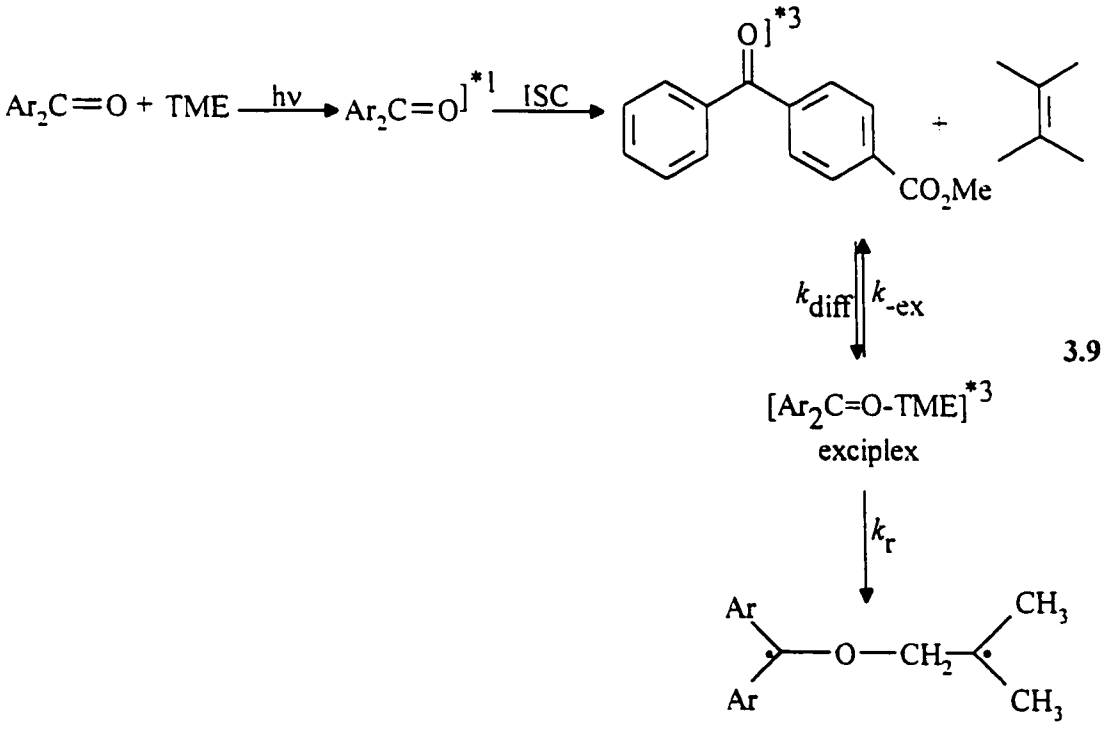

3.9

The curvature in the Arrhenius plot for reaction of **12e** with methanol (Figure 2.11) provides strong evidence for complex formation and the behaviour described above.[10] Methanol addition to **12e** above ≈13 °C exhibits a negative activation energy which indicates that at these temperatures $k_{-1} > k_2$. As the curved region of the plot is reached over the (-20 to 13) °C range, the reversibility of the first step is reduced ($k_{-1} \approx k_2$) until we reach the point where complex formation becomes rate-determining and a positive activation energy. Reaction of this silene (**12e**) with methanol exhibits no significant isotope effect at 23 °C, signifying that this temperature is within the range where the main contribution to the observed rate constant is complex formation. By comparing the activation energies for methanol addition to **12a**,**b**,**e** we observe that E_a becomes more negative with decreasing electron withdrawing ability of the substituent (Table 2.7). These results, in combination with a reduction in k_H/k_D with electron withdrawing power of the substituent, are all consistent with a successive increase in k_{-1} relative to k_2 throughout the series **12e**< **12a** < **12b**. In other words, the relative placements of the Arrhenius lines for **12a** and **12b** below **12e** signifies that we are simply observing different portions of the ideal bell-shaped Arrhenius plot that correspond to different relative magnitudes of k_{-1} and k_2. We have not extracted and compared $\Delta H^{\neq}$, $\Delta G^{\neq}$ and $\Delta S^{\neq}$ values for each compound, since we are observing different contributions of k_1, k_{-1} and k_2 along the series. Only in the limit of very high temperatures (fully reversible complex formation) and in the limit of very low temperatures (where complex formation is rate determining) are these comparisons meaningful.

One might also expect that if the reaction is not diffusion controlled, then the rate constant for complex formation (k_1) should increase with increasing electron withdrawing power of the substituent. Unfortunately, we are not able to measure k_1 since this would require measurements of rate constants at temperatures far below the ability of our present system.

We have typically observed that silenes show an enhanced reactivity towards alcohols in nonpolar compared to polar solvents.[29,30,44] The observed rate constants for reaction of **12a** with methanol and *t*-butanol are about a factor of 2-3 larger in hexane than in acetonitrile. This increase in reactivity is somewhat surprising since one would predict the more polar solvent to stabilize the silene-alcohol complex, making reactions in this solvent faster (i.e. increase k_2). By comparing the activation parameters for methanol addition to **12a** in hexane to those in MeCN we see that the E_a determined in hexane is more negative than in acetonitrile, suggesting that k_{-1}/k_2 is larger in hexane than in MeCN. A similar result is obtained for reactions of **12a,e** with acetone, and is discussed in Section 3.6. This solvent effect suggests that over the temperature range examined, the variation in k_{-1}/k_2 is solvent dependent. The reduced reactivity in acetonitrile is attributed to solvation effects on the silene causing a reduction in k_1 and, therefore, a reduction in the overall observed rate constant.

Up to this point it has been difficult to rule out a stepwise or concerted addition of acetic acid to silenes. Acetic acid reacts with a small Hammett ρ-value of +(0.17 ± 0.01) indicating that this reaction is somewhat less sensitive to polar factors than methanol or *t*-butanol. Unfortunately, this result alone does not provide us with much more insight into the mechanism for its addition. However, the fact that the more reactive silene **12e** exhibits a higher activation energy (Figure 2.12) is incompatible with a concerted mechanism, and is consistent with the two-step mechanism involving rate determining complex formation. Recall that mechanisms of this type exhibit bell shaped Arrhenius plots over a large temperature range. The high temperature extremes represent rate determining proton transfer, while at low temperatures complex formation is rate determining. The smaller apparent activation energy observed for acetic acid addition to **12a** results from the fact that over the temperature range monitored, reversion of the complex still competes with collapse to products. For **12e**, a larger k_1 and smaller k_{-1}/k_2 ratio results in a shift in the "peak" of the Arrhenius plot to higher temperatures,[10] as in the case for methanol addition. Thus, over the temperature range monitored for the two compounds different portions of the bell are being observed, i.e., a steeper temperature dependence of k_{obs} is observed for **12e**, than is for **12a**. Therefore, the Arrhenius parameters for acetic acid addition to **12e** (E_a = (3.6 ± 0.5) kcal/mol; log $A/M^{-1}s^{-1}$ = (12.0 ± 0.4)) more closely describe those for complex formation than do those for **12a** (E_a = (1.9 ± 0.2) kcal/mol; log A = (10.5 ± 0.2) / $M^{-1}s^{-1}$). The activation energy for diffusion can be calculated by using the diffusional rate constants calculated

using the modified Debye equation (k_{diff} = 8RT/3000η) and a value of η extrapolated from published temperature viscosity data.[96] This yields an E_a = (1.8 ± 0.4) kcal/mol and log A = (11.6 ± 0.5) / $M^{-1}s^{-1}$. The fact that the E_a for complex formation with **12e** is larger than that for diffusion indicates that there is a small enthalpic barrier to complex formation in excess of that of diffusion. The data of Figure 2.12 indicate that there is a much larger sensitivity to substituent at higher temperatures than at low temperatures, which is also consistent with the fact that at higher temperatures reversible complex formation is a more important contributor to k_{obs}.

It has been suggested that alcohol additions to disilenes also occur via a stepwise mechanism involving a zwitterionic intermediate.[97] Reactions of substituted phenols with tetramesityldisilene in benzene yield concave Hammett plots consistent with a change in mechanism from rate-determining nucleophilic attack by oxygen at silicon (for electron donor substituted phenols), to rate-determining electrophilic addition of the phenolic proton to silicon (for electron acceptor substituted phenols).[97] The kinetic isotope effects for reaction vary from an inverse to a primary effect with increasing electron withdrawing ability of the substituent, also consistent with a change in the rate determining step.

Based on a direct comparison to **11a**, we assign the structures of the transients observed upon flash photolysis of **22a-b** to 1-phenylsilene (**23a**) and 1-methylphenylsilene (**23b**), respectively. The transient UV absorption spectra observed for **23a,b** are essentially identical with a maximum at ≈ 315 nm (Figure 2.21). Thus,

replacement of one phenyl group with a hydrogen or methyl group causes a blue shift of ≈ 10 nm in the UV absorption spectra in comparison to that for **12a**. Silene absorptions are of π,π^* character and the effects of substitution on silene UV absorption can be understood by examining the π-system alone.[2] Since simple silenes are highly polarized, the magnitudes of the orbital coefficients on silicon and carbon are quite different in the HOMO and LUMO. A π-acceptor substituent on the silicon atom should lower the energy of the LUMO (π^* orbital) due to the large orbital coefficient on Si, whereas the energy of the HOMO (π orbital) should be only slightly lowered. This smaller HOMO-LUMO gap results in red-shifts in the UV absorption spectra of π-acceptor silenes. Similarly, a π-donor substituent on carbon should raise the HOMO without affecting the LUMO and cause a red-shift in the UV absorption. A π-acceptor substituent on carbon should cause only a small red-shift in the (π,π^*) transition since the LUMO will not be lowered much due to the small coefficient on carbon. These effects are qualitatively summarized in Scheme 3.1 and several examples are given in Table 3.2.

Table 3.2 Ultraviolet Absorption Maxima of Various Silenes.[5]

Silene	λ_{max} (nm)
$Me_2Si{=}CHMe$	255 nm
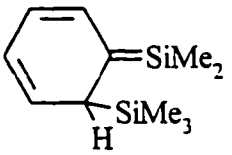	425 nm
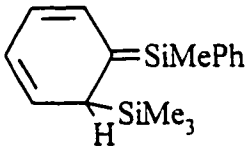	460 nm
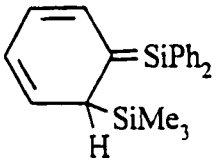	490 nm

Scheme 3.1 **Effects of π-Donor and π-Acceptor Substituents on the HOMO and LUMO Energies in Silenes**[2]

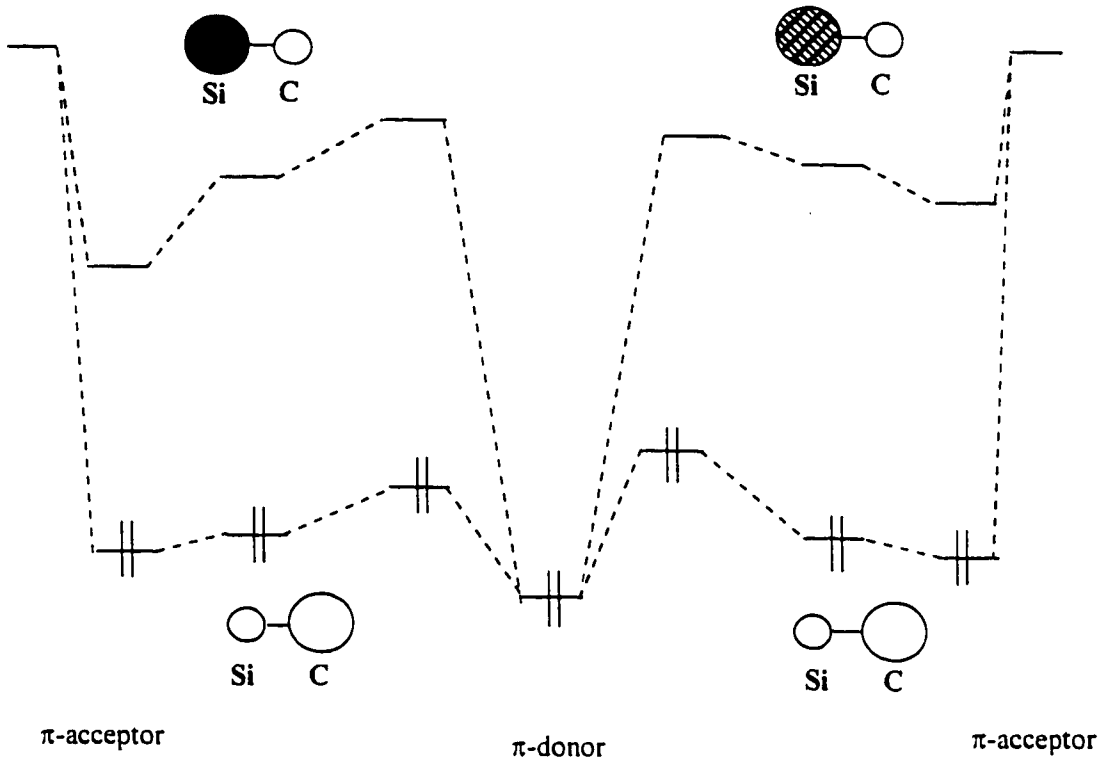

Steady-state irradiation (254 nm) of **22a** and **22b** (0.1 M) in hexane solution in the presence of methanol or acetone (0.1 M) results in the formation of the corresponding methoxysilane **24** or silyl enol ether **25**, respectively, (eq 2.8) in high chemical yields. The products were identified after 20 % conversion by GC coinjection of the crude photosylate with authentic samples and are consistent with the trapping of **23a-b** by methanol or acetone.

Indirect evidence for the formation of **23a** was previously reported in 1981 by Bertrand in a study of the steady-state trapping of **23a** with chiral alcohols.[98] Diastereomeric alkoxysilanes in 50/50 relative yields were observed in the photolysis of **22a** with borneol, menthol and isoborneol, consistent with the formation of **23a**. However, this study did not reveal any insight about the mechanism of alcohol addition since the experiments were performed at high alcohol concentrations and the dependence of product yields on alcohol concentration was not examined.

The reaction of **23a-b** with alcohols and acetic acid in hexane and acetonitrile solution (Tables 2.11-2.12) occur with rate constants in the 10^8-10^9 M^{-1} s^{-1} range. Linear quenching kinetics were observed with all quenchers and in all cases the reaction rates are approximately two times faster in hexane than in acetonitrile. As discussed above, polar solvents (like MeCN) are expected to stabilize the silene rendering it less reactive. The solvation effect is expected to be larger for the smaller silenes **23a** and **23b**, than **12a**. This is reflected in the fact that the rates of reaction of **23a-b** in hexane are *ca.* 1.5 times

faster than **12a**, while the reaction rates in MeCN show a much lower sensitivity to substitution at silicon.

The rate constants for methanol, *t*-butanol and acetic acid quenching of 1-silastyrenes **12a** and **23a-b** depend upon the degree of phenyl substitution. In both solvents, the rate constants for reaction of the silenes with the above three traps increase with decreasing substitution at silicon, while the KIE's remain essentially equal throughout the series. Similar trends were observed for the reactions of silatrienes **10** with alcohols, acetone, alkyl halides, DMB and oxygen.[30,44] These results support the general conclusion that increasing steric bulk at trivalent silicon leads to a decrease in the rate of nucleophilic attack at silicon.

Recently a substituent effect study on the reactivity of 2-[(dialkylamino)phenyl]silenes was reported.[99] Generally, 1,1-bis(trimethylsilyl)silenes generated by deprotonation and trimethylsilanolate elimination from phenyl[tris(trimethylsilyl)silyl]methanols, dimerize in a head-to-head fashion. However, it was found 2-[2-(dimethylamino)phenyl]-1,1-bis(trimethylsilyl)silene dimerizes in a head-to-tail mode, while 2-methyl-2-[4-(dimethylamino)phenyl]-1,1-bis(trimethylsilyl)silene dimerizes in a head-to-head fashion, and 2-[2-((dimethylamino)methyl)phenyl]-1,1-bis(trimethylsilyl)silene does not dimerize at all (eq 3.10). Instead, the latter silene undergoes readdition of Me_3SiOLi. These results indicate the strong influence of electronic effects on the regiospecificity of silene dimerization. The ability of the *o*-(dimethylamino)phenyl substituent to change the dimerization

mechanism was attributed to an intermolecular donor-acceptor interaction between the dialkylamino group and the silenic silicon atom. In the case of the *o*-(dimethylamino)methylphenyl substituted silene, an intramolecular donor-acceptor interaction was proposed. This interaction was suggested to be so strong that the tendency for silene dimerization is substantially reduced.[99]

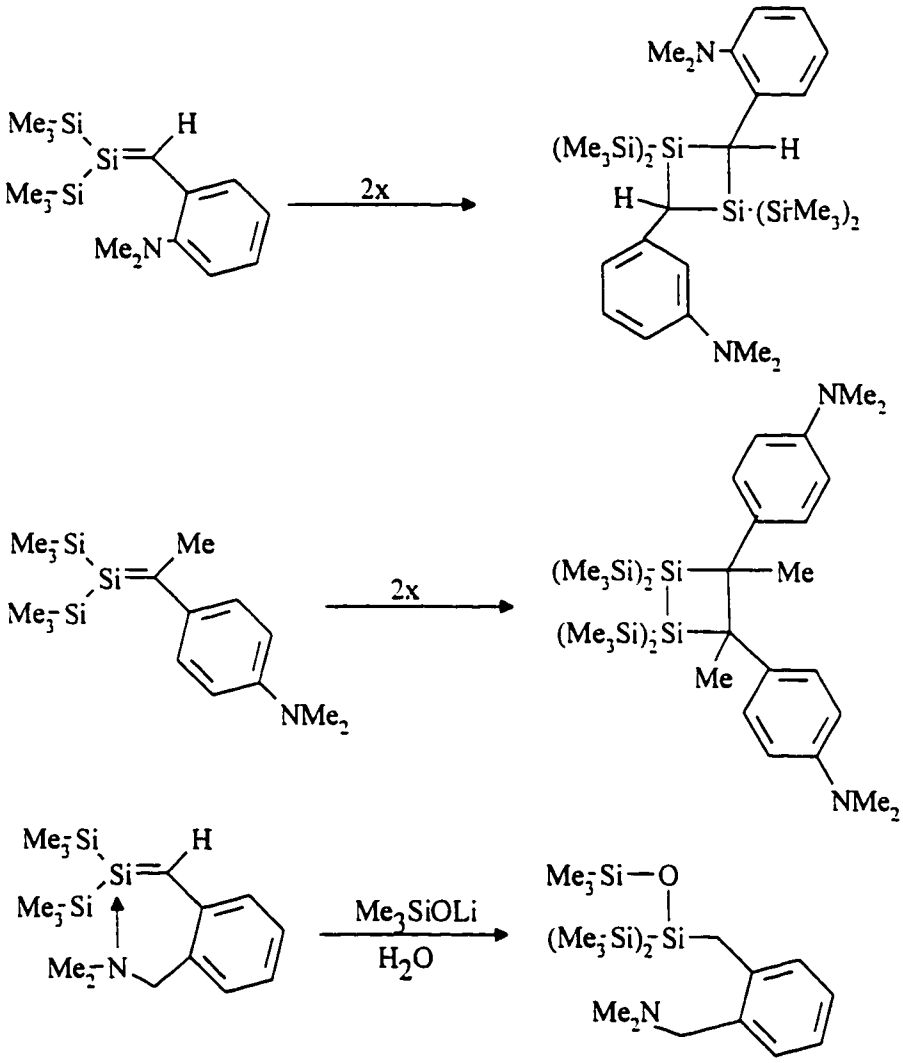

3.10

We recently reported studies of the effects of silenic substitution on the spectroscopy and reactivity of vinyldisilane derived silenes (**26-28**). Trimethylsilylmethyl substitution causes a significant reduction in overall reactivity due to the resonance electron-donor ability of the substituent which results in a reduction in positive π-charge density at the silenic silicon atom. Hyperconjugative electron-donation by the β-trimethylsilyl substitution also exerts an effect on the frontier molecular energies causing a red-shift of the lowest energy absorption bands in the UV spectra of these compounds.[100]

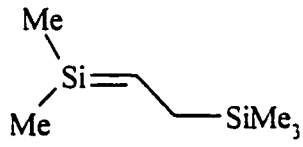

26

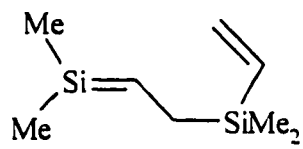

27

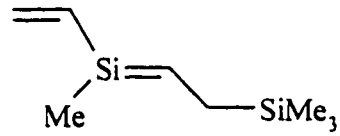

28

3.5 Reactions of Substituted 1,1-Diarylsilenes and 1-Silastyrenes with Trimethylmethoxysilane

The absolute rate constants for reaction of **12a-e** and **23b** with trimethylmethoxysilane are in the 10^7-10^8 $M^{-1}s^{-1}$ range (Table 2.8 and 2.11), about 100 times slower than those for reaction with methanol. The plots of silene decay rate *versus* Me_3SiOMe concentration were linear, indicating that addition proceeds exclusively by a mechanism which is first-order in alkoxysilane. This coupled with the fact that the reaction proceeds with *syn*-stereoselectivity[31,48] are consistent with either a concerted

mechanism or one analogous to alcohol addition, with no contribution from a catalyzed route for collapse of the complex.[31,48,101]

The rate constants for reaction of the diarylsilenes (**12a-e**) with Me_3SiOMe increase with increasing electron-withdrawing power of the ring substituent, analogous to the trend observed for reaction with alcohols. The Hammett plot (Figure 2.14) for trimethylmethoxysilane addition to **12a** in hexane affords a ρ-value of +(1.3 ± 0.2). This is significantly higher than those for addition of methanol (ρ = 0.31) or *t*-butanol (ρ = 0.55) in acetonitrile solution, suggesting that polar factors play a greater role in the reactions of alkoxysilanes. Alkoxysilanes are weaker bases than the corresponding dialkyl ethers or alcohols[102], resulting from a p_π-d_π interaction between the oxygen and silicon atoms. Alkoxysilane addition can be viewed as nucleophile-$SiMe_3^+$ addition, analogous to alcohol additions, where the $SiMe_3^+$ group takes the place of the proton. Thus, the greater sensitivity of Me_3SiOMe addition to substituent in comparison to alcohol addition, is a consequence of a reduction in nucleophilicity of the quencher.

The Arrhenius plot for trimethylmethoxysilane addition to **12a** in hexane is linear (Figure 2.14) and yields an activation energy of -(4.2 ± 0.8) kcal/mol. In this case, the negative activation energy can be explained by the involvement of a silene-Me_3SiOMe complex (eq 3.11) which reverts to free starting materials (k_{-1}) faster than $SiMe_3^+$-transfer and collapse to products (k_2) . The linearity of the plot suggests that over the temperature range investigated $k_{-1} >> k_2$. These results are also consistent with the suggestion that the slower reactivity of silenes towards alkoxysilanes than alcohols is a result of a slower rate

constant for $SiMe_3^+$-transfer in the complex than proton-transfer. The barrier for a $SiMe_3^+$ transfer is predicted to be larger since it involves breaking a Si-O bond of *ca.*127 kcal/mol,[102] in comparison to alcohol additions which involve a H^+ transfer and O-H bond breaking of *ca.* 111 kcal/mol[21], corresponding to a reduction in k_2 associated with a $SiMe_3^+$ transfer.

The negative activation energy observed for Me_3SiOMe addition to **12a** is the most negative activation energy measured to date for reactions of **12**. The observed activation energy for this type of reaction mechanism is $E_a^{obs} = E_{a,1} - E_{a,-1} + E_{a,2}$. Therefore, the more negative E_a can be interpreted as reflecting either a larger exothermicity involved in reversible silene-Me_3SiOMe complexation over silene-MeOH complexation, or a smaller enthalpic barrier to $SiMe_3^+$- than proton transfer. Semi Empirical AM1 calculations (Table 3.3) indicate that the reaction of $Ph_2Si{=}CH_2$ with Me_3SiOMe exhibits a slightly lower exothermicity for complex and product formation. Thus, the more negative activation energy cannot be rationalized in terms of a difference in exothermicity in complex formation. The suggestion that the more negative activation energy is a result of a reduction in the enthalpic barrier for $SiMe_3^+$ transfer *versus* H^+ transfer also cannot account for this difference since it would predict an overall increase in the overall rate constant, which is in fact opposite to what is observed. Therefore, the more negative E_a is a reflection of a difference in the variation of k_{-1}/k_2 for the two quenchers over the temperature ranges employed, resulting from the reduction in k_2 associated with a $SiMe_3^+$ *versus* H^+ transfer.

Table 3.3 Semi Empirical AM1 Calculated Heats of Formation.[a]

Compound	ΔH_f (kcal/mol)
$Ph_2Si{=}CH_2$	53.4
MeOH	-57.1
Me_3SiOMe	-106.6
$[Ph_2Si{=}CH_2\text{-----}MeOH]$	-5.9
$[Ph_2Si{=}CH_2\text{-----}MeOSiMe_3]$	-53.5
$Ph_2(Me)SiOMe$	-40.8
$Ph_2(CH_2SiMe_3)SiOMe$	-32.3
$\Delta H_{1,MeOH}$	-2.2
$\Delta H_{Me3SiOMe}$	-0.3
$\Delta H_{MeOH,\ rxn}$	-40.8
$\Delta H_{Me3SiOMe,rxn}$	-32.3

[a] An RMS gradient of 0.01 was used to obtain optimized geometries with Hyperchem 4.0.[103]

The rate constant for Me_3SiOMe addition to **23b** is *ca.* $1.88 \times 10^7\ M^{-1}s^{-1}$, which is slightly larger than that for **12a**. This is suggested to be a result of the lower steric bulk at silicon which is predicted to increase the rate of complexation in **23b** relative to **12a**.

In the early eighties, Arrhenius parameters for the reaction of 1,1-dimethylsilene (**5**) with trimethylmethoxysilane were determined from 459 to 516.5 °C in the gas phase, and yielded an $E_a = (1.5 \pm 0.8)$ kcal/mol and $\log A/dm^3mol^{-1}s^{-1} = (5.3 \pm 0.2)$.[50] This value

is quite different to that obtained for **12a** in solution. Assuming the two step mechanism presented in eq 3.11, one would predict that the much higher temperatures employed in this investigation should give a more negative activation energy. However, this prediction is made on the assumption that the same ideal bell-shaped plot operates in both phases.

Solvation has been shown to have large effects on acidity and basicity.[104] For example, Me_3N has a higher basicity in the gas phase than in aqueous solution (relative to NH_3) due to the electron-donating ability of the alkyl groups and the absence of hydration.[105-107] Oxygen bases show similar behavior.[106] One might predict a similar trend for Me_3SiOMe basicity. Thus, the differences in the Arrhenius activation energies can be accounted for by comparing k_1/k_{-1} in the two phases. A higher Me_3SiOMe gas phase basicity should correspond to an increase in k_1/k_{-1} relative to solution, such that $k_{obs} \approx k_1$, resulting in a positive activation energy. In solution, the negative E_a indicates that $k_{obs} = (k_1/k_{-1})k_2$, consistent with a smaller k_1/k_{-1} ratio than in the gas phase.

The present data in combination with that reported for alcohol additions and the observation of silene-ether complexes strongly suggest that the reaction of silenes with alkoxysilanes proceeds through a two step mechanism via a silene-silyl ether complex (eq 3.11). However, the two models which explain negative activation energies are easily transformed into each other by changing the magnitude of the interaction in the complex,[82,83] such that the observation of a negative activation energy for

trimethylmethoxysilane addition alone does not allow us to strictly rule out a concerted mechanism.

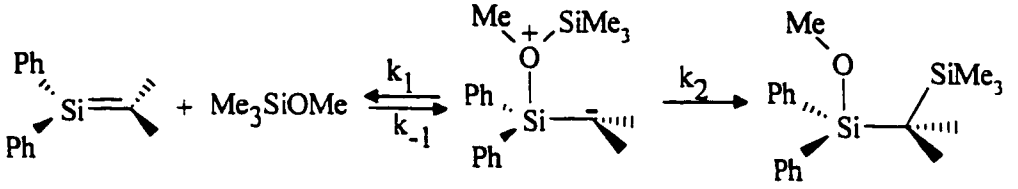

3.11

3.6 Reactions of 1,1-Diarylsilenes with Acetone

The reaction of **12a-e** with acetone in hexane yields exclusively the corresponding silyl enol ether in high chemical yields (eq 2.7). The photolyses could not be carried out to higher than 20% conversion of **11** due to the formation of secondary photolysis products. However, no other primary photoproducts were observed indicating that there is no variation in the course of the reactions of **11** with acetone as a function of aryl substitution.[66]

Plots of the rate constants for decay *versus* acetone concentration are linear (Figure 2.16) in all cases and yield rate constants in the 10^8 $M^{-1}s^{-1}$ range, approximately an order of magnitude less than the corresponding reactions with methanol. In all cases, the reaction rates decrease with increasing solvent polarity, and increase with increasing electron withdrawing power of the diaryl substituent (Table 2.9) in analogous fashion to alcohol additions. Hammett plots for reaction in acetonitrile and *iso*octane solution are curved and yield ρ-values of +(1.06 ± 0.05) and +(1.48 ± 0.16), respectively (Figure

2.16). The reaction constant observed for acetone addition in MeCN is larger than that for methanol (ρ = +0.31) or acetic acid (ρ = + 0.17) addition.

The reaction of **12** with acetone can be viewed as nucleophile-proton addition. The observation of a positive reaction constant indicates that as in ROH additions, nucleophilic addition is more sensitive to polar effects and precedes proton transfer. The conjugate acid pK_a's of acetone, methanol and acetic acid are -0.1, 2.4 and 1.1 (Table 3.1), respectively, indicating that acetone is much less nucleophilic than the other two nucleophiles. Thus, the greater sensitivity of acetone additions to substituent than methanol addition arises from the fact that the ketone is less nucleophilic.

The k_H/k_D values for reaction vary to a similar extent in both solvents (Table 2.9) from 1.3 for the most reactive silene (**12e**), to 2.7 for the least reactive one (**12b**). This effect is more consistent with a primary KIE involving rate determining α-hydrogen transfer, which is reinforced by secondary α-deuterium isotope effects.[69] A secondary effect would be compatible with a mechanism involving rate determining complex formation and fast proton transfer. Since this mechanism does not involve a change in hybridization at the carbonyl oxygen it should be relatively unaffected by isotopic substitution α- to this center. On a per deuterium basis, the isotope effect for reaction with **12a** would be $^6\sqrt{2.7}$ = 1.2. This value is much larger than would be predicted for a secondary effect,[69] and is therefore not compatible with a mechanism involving rate determining complexation and fast proton transfer.

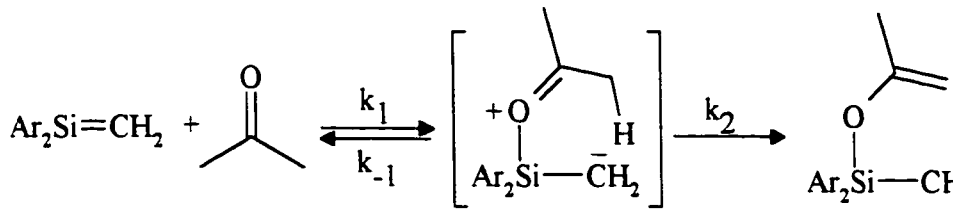

3.12

Acetone reacts with **12a** with activation energies of -(1.3 ± 0.1) and -(2.6 ± 0.1) in acetonitrile and hexane solution, respectively. This result, in combination with the substituent and kinetic isotope effects on the rate constants for reaction, provides evidence in favour of a two-step mechanism for ketone additions to silenes. The mechanism involves initial reversible association of the carbonyl oxygen and silicon atoms, followed by rate determining proton transfer of the carbonyl α-hydrogen to the silenic carbon (eq 3.12). The slower reactivity and smaller ρ-value obtained for reactions in the more polar solvent can be explained as due to a reduction in the magnitude and sensitivity to substituent of k_1/k_{-1} due to complexation of the silene with MeCN.

Activation energies for acetone addition to **12a,b,e** vary with substituent in a similar manner to that which was observed for methanol addition, i.e., E_a becomes less negative as silene reactivity increases (Table 2.10). This result can be explained in terms of variation along the series **12a,b,e** of the individual rate constants for complex formation (k_1) and reversion (k_{-1}), and proton transfer (k_2).

In acetonitrile solution, the least reactive silenes in the series, (**12a** and **12b**) react with negative activation energies of -(1.3 ± 0.1) kcal/mol and -(2.0 ± 0.1) kcal/mol, while the most reactive silene **12e** reacts with a positive activation energy of (0.8 ± 0.1)

kcal/mol. This indicates that for **12a** and **12b**, the complex reverts to reactants faster than it proceeds to products over the temperature range investigated. The fact that **12b** reacts with a more negative activation energy than **12a** indicates that the k_{-1}/k_2 ratio is larger for the 4-methyl derivative than for the parent compound. A small positive activation energy for addition to **12e** indicates that in this case proton transfer in the complex to yield product (k_2), is faster than reversion of the complex to starting materials ($k_2>>k_{-1}$) . The Arrhenius data indicates that k_{-1}/k_2 decreases in the order **12b>12a>12e**, which is also consistent with the positive Hammett ρ-value for reaction. This decrease in k_{-1} relative to k_2 with increasing electron withdrawing power of the substituent, manifests itself in a corresponding decrease in isotope effect throughout the series.

The Arrhenius data obtained for reactions of **12a,e** (Figure 2.20) in hexane suggest the same general variation in individual rate constants as was observed in acetonitrile (Figure 2.19). One important feature of the data that must be mentioned is that not only does the more reactive silene exhibit a positive activation energy, but at low temperatures the plot begins to level off and converge with the Arrhenius plot for diffusion (Figure 2.20). This behavior strongly suggests diffusion controlled and rate determining complex formation, most likely attained due to the inability of the nonpolar solvent to complex this polarized and reactive silene. The fact that the plot is so distinctly curved over this temperature range indicates that the variation in k_{-1} and k_2 is much steeper in hexane than in acetonitrile.

The curvature observed in the Hammett plots are also fully consistent with the proposed mechanism. The deviations in the plots from linearity are mainly due to the point for the 4-trifluoromethyl derivative. In acetonitrile solution the deviation of the rate constant for the **12e** point is attributed to the fact that we are comparing a positive E_a for reaction with **12e**, to negative E_a's for reactions with the other four compounds. In hexane solution, the deviation is a result of the fact that the overall rate constant for reaction with **12e** is diffusion controlled. Therefore, the curvature in the Hammett plots is a result of the different contribution of k_1, k_{-1}, and k_2 to the overall rate constant for reaction with **12e** in comparison to the other four compounds.

The variation in rate constants for reaction with acetone, as a function of silenic substitution from **12a** to **23a-b**, is opposite to that described for alcohol or trimethylmethoxysilane addition as well as the results reported previously for **10**.[9,30,44] The observed rate constants for reaction with acetone decrease with decreasing silenic substitution and the effect is more pronounced in acetonitrile solution (Table 2.11-2.12). This result came as a surprise and therefore an Arrhenius study on the addition of acetone to **23b** in acetonitrile and hexane solution was performed (Figure 2.23).

As observed for **12a**, **23b** reacts with acetone with negative activation energies of -(1.9 ± 0.2) kcal/mol and -(0.8 ± 0.2) kcal/mol in hexane and acetonitrile solution, respectively and log A of *ca.* 7.1/$M^{-1}s^{-1}$ (Table 2.13). The linearity of the plots suggest that the **23b**-acetone complex reverts to reactants faster than it proceeds to products over the temperature investigated. The Arrhenius plot in hexane does begin to show a very

slight curvature at -15 °C, but it is not nearly as pronounced as that observed for **12a**. These results suggest that the overall reduction in rate constant for reactions of **23a-b** relative to **12a** with acetone, are a consequence of a reduction in k_2 relative to k_{-1} with decreasing phenyl-substitution.

Recall that rate constants for reaction of **12a** with various carbonyl compounds show a dependence on the non-bonding MO energies on oxygen.[8] These findings suggest that the structure of the silene-acetone complex involves bonding interactions between the carbonyl n-orbital and the silenic π-bond, where the silicon atom lies in the n-orbital plane and perpendicular to the carbonyl π-system (eq 3.13). Geometric constraints limit overlap but if the enolic C-H and C=O bonds assume an angle of *ca.* 45°, the hydrogen can be transferred to the silenic carbon via a chair-like transition state (eq 3.13).

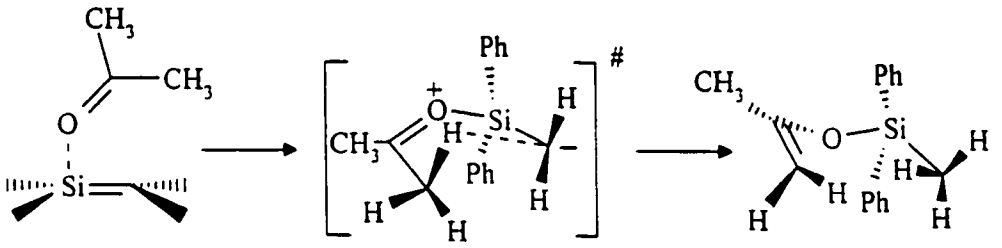

3.13

The slower reactivity of **23a-b** towards acetone can then be ascribed to steric effects on the preferred geometry for proton transfer in the complex. Transfer of a proton from the carbonyl α-carbon will be preferred when it is oriented towards the silenic carbon (eq 3.14). Increasing steric bulk at silicon should favour the conformation which places the

proton in closer proximity to the silenic carbon thereby increasing the probability for transfer.[66]

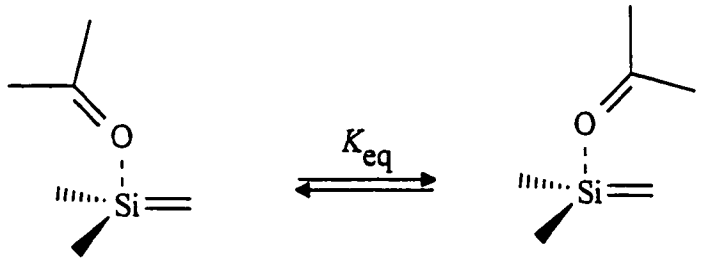

3.14

nonreactive geometry reactive geometry

Currently we are investigating the mechanisms of both ene- and [2+2]-additions of carbonyl compounds to silenes using theoretical calculations. The intermediacy of a silene-carbonyl compound complex is predicted for both reaction pathways at the semi-empirical (AM1 and PM3) and ab initio (6-31 g*) levels of theory.[108]

CHAPTER 4

SUMMARY AND CONCLUSIONS

4.1 Contributions of the Study

Although the reactions of transient and stable silenes have been investigated over the past 25 years, there has been relatively little kinetic data reported on these reactions. Prior to this work the majority of the studies focused on steady-state product studies and therefore provided only qualitative mechanistic information. The properties of reactive silenes had been investigated by low temperature matrix isolation techniques;[2] however reports which examined transient silenes through the use of time-resolved techniques in solution at room temperature were limited. The majority of kinetic data and mechanistic evidence had been obtained for reactions of conjugated silenes, the 1,3,5-silahexatrienes (**10**).

Kinetic and product studies on the reactions of highly conjugated silenes with alcohols suggest that the mechanism involves rapid reversible formation of a silene-alcohol complex, followed by rate determining and competing intra- and inter- molecular proton transfer steps to yield products. For more acidic quenchers, such as acetic acid, complex formation is rate-determining and proton transfer is fast. The mechanism was

formulated on the basis of a quadratic dependence of the pseudo-first-order rate constant for silene decay on alcohol concentration[9,30,44] and the fact that the two pathways lead to product distributions which vary with alcohol concentration.[24,44,47]

Similarly, it was proposed that reactions with carbonyl compounds proceed via a two step mechanism.[30,36] Reactions of **10** with ketones yield 1,2-siloxetanes and silyl ethers whose relative yields depend on the structure of the ketone and silatriene, consistent with a stepwise mechanism involving a zwitterionic intermediate.

The main objective of this work was to employ steady-state and nanosecond laser flash photolysis techniques to study in detail the mechanism of reaction of simple silenes with various nucleophiles in polar and nonpolar solvents. These results are compared to those previously reported for **10**. Classic physical organic methods such as Arrhenius and Hammett substituent effect studies are the first of their kind to be employed for study of silene reactivity in solution, and provide considerable insight into the mechanisms of these reactions.

1,1-Diarylsilenes (**12a-e**), 1-phenylsilene (**23a**) and 1-methyl-1-phenylsilene (**23b**) were generated by photolysis of 1,1-diarylsilacyclobutanes (**11a-e**), 1-phenylsilacyclobutane (**23a**) and 1-methyl-1-phenylsilacyclobutane (**23b**), respectively. The 1,1-diarylsilenes exhibit UV absorption maxima at 325 nm, and decreasing phenyl substitution at the silenic silicon atom results in a blue shift in the UV absorption maxima to 315 nm, for the 1-silastyrenes (**23a-b**). All of the silenes studied in this work exhibit lifetimes of 2-4 μs in hexane, acetonitrile and tetrahydrofuran solution and react with

alcohols, trimethylmethoxysilane, acetone and acetic acid with rate constants in the 10^7-10^9 $M^{-1}s^{-1}$ range. Alcohols and acetone exhibit small primary kinetic isotope effects consistent with rate determining proton transfer, while acetic acid exhibits k_H/k_D values indistinguishable from unity. Reaction rate constants increase with decreasing solvent polarity, which can be attributed to stabilization (through weak complexation) of the silene in the more polar solvent. The reactions afford linear quenching plots consistent with a mechanism that is first order in alcohol, trimethylmethoxysilane, acetone or acetic acid concentration. For alcohol additions, the pathway that is second order in alcohol concentration is not kinetically observable under these conditions because of the low alcohol concentrations employed. Therefore, the reactions with alcohols occur predominantly via the intracomplex proton transfer pathway under the conditions employed for laser flash photolysis experiments.

Solvent polarity has little effect on the UV absorption spectra of the diarylsilenes, although evidence for a 1,1-diphenylsilene-THF complex was observed. The UV spectrum of **12a** is red shifted and much broader in THF than in MeCN. The absolute rate constants for addition of methanol, *t*-butanol and acetic acid are reduced in THF solution, consistent with the formation of a complex which is less reactive than the free silene. An upper limit for the equilibrium constant is *ca.* 0.1 M^{-1} in THF solution. The observation of a silene-THF complex provides indirect evidence for the formation of zwitterionic complexes in the reactions of silenes with alcohols, trimethylmethoxysilane, acetone and acetic acid as well.

The above silenes react with alcohols, acetone and trimethylmethoxysilane to afford the corresponding nucleophilic addition products in high chemical yield, indicating that the course of reactions are not sensitive to variations in substituent within the narrow range studied here. Steady-state competition experiments in which 1,1-diphenylsilene is trapped by various pairs of alcohols, yield product ratios that agree very well with the corresponding relative rate ratios for water, methanol and ethanol addition. Those obtained for methanol/*t*-butanol are significantly different at high alcohol concentrations (>0.05 M), but are in agreement at very low alcohol concentrations such as those used in LFP experiments (<0.01 M). These observations indicate that proton transfer from the complex to a second molecule of alcohol competes with the intracomplex pathway at higher alcohol concentrations for all cases except *t*-butanol and acetic acid. These findings also provide further indirect evidence for the formation of silene-alcohol complexes in these reactions.

The effects of ring substituent on the rate constants, deuterium kinetic isotope effects and Arrhenius parameters for the addition of each of the quenchers listed above are most easily rationalized in terms of two-step reaction mechanisms. The mechanism involves initial reversible formation of a Lewis acid-base complex between the nucleophilic center of the trapping agent and the silenic silicon, followed by transfer of the electrophilic group (H^+ or $SiMe_3^+$) to the silenic carbon. Hammett substituent effect studies reveal that the absolute rate constants for reaction 1,1-diarylsilenes with each of the quenchers listed above increase with increasing electron-withdrawing power of the

aryl-substituent. The corresponding Hammett plots yield small, positive ρ-values in the range of 0.17-1.4. With the exception of acetic acid the reaction constants increase in magnitude with decreasing nucleophilicity of the trap. The positive Hammett ρ-value suggests that it is the initial pre-equilibrium which is primarily responsible for the sensitivity to aryl substitution, since the second step would be expected to exhibit a relatively small ρ-value due to the strong exothermicity involved in product formation and the fact that it involves charge reorganization in a zwitterionic complex. The observed ρ-values are also consistent with the fact that nucleophilic attack precedes proton or $SiMe_3^+$ transfer. The deuterium kinetic isotope effects for methanol and acetone addition to **12a-e** decrease with increasing electron withdrawing ability of the substituent and can be viewed in terms of an increase in the rate constant for proton transfer (k_2) relative to the rate constant for reversion of the complex (k_{-1}) throughout the series.

Arrhenius studies have been carried out on the reactions of methanol, methanol-Od, *t*-butanol and acetic acid in acetonitrile solution, trimethylmethoxysilane in hexane solution and acetone in both acetonitrile and hexane solution. The Arrhenius plots for each of the above quenchers with the exception of acetic acid are characterized by negative activation energies, while acetic acid reacts with a positive activation energy.

The substituent effect studies on Arrhenius activation energies determined for the addition of methanol, acetone and acetic acid addition to the most and least reactive diarylsilenes **12a,e**, and provide by far the most conclusive evidence in favour of the two

step mechanism. Reactions of **12a-e** with methanol and acetone resulted in negative activation energies which decrease in absolute magnitude with increasing electron withdrawing ability of the substituent. The variation in the Arrhenius behaviour and isotope effect as a function of substituent indicate that electron-withdrawing groups at silicon increase the rate constant for complex formation and the rate constant for its collapse to products relative to reversion to starting materials.

Pronounced curvature in the Arrhenius plots is observed with decreasing temperature, for the reactions of **12e** with methanol in acetonitrile solution and acetone in hexane solution, with the curved portion of the line for acetone addition approaching that for diffusion. The curvature observed in the Arrhenius plots is attributed to a change in the rate-determining step as a function of temperature resulting from a variation in the relative rates of collapse of the complex to products and reversion to starting materials with temperature. This change was associated with a transition from reversible complex formation ($k_{-1} >> k_2$) and rate determining collapse to products at high temperatures, to rate determining complex formation at low temperatures ($k_2 >> k_{-1}$). These findings are also in agreement with a decrease in the deuterium kinetic isotope effect for methanol addition to **12a** with decreasing temperature.

A direct comparison of the Arrhenius plots for the addition of methanol and acetone to **12e** in acetonitrile solution indicates that while the former plot shows distinct curvature at temperatures below 13 °C, the latter is quite linear. One can account for this in terms of a difference between the individual rate constants k_1, k_{-1} and k_2 as a function of quencher. The linearity of the plot for addition of acetone to **12e** in MeCN

indicates that the acetone-silene complex reverts to reactants faster than it proceeds to silyl enol ether ($k_{-1}>>k_2$) over the temperature range investigated. On the other hand, the curvature in the plot associated with methanol addition signifies that over the -20-13 °C temperature range, the rate of alkoxysilane formation approaches and then surpasses that of reversion of the complex to reactants. The steeper variation in k_2/k_{-1} for methanol addition in MeCN than acetone addition is presumably due to the higher acidity of the hydroxylic proton in the complex.

1-Silastyrenes **23a-b** are more reactive towards alcohols, trimethylmethoxysilane and acetic acid in hexane and acetonitrile solutions but exhibit isotope effects essentially identical to that observed for **12a**. The higher reactivity towards nucleophilic attack is suggested to result from a reduction in steric bulk at the silenic silicon atom. The rate constants for reaction with acetone are an order of magnitude slower in both hexane and acetonitrile solution than the corresponding reactions with **12a**. Activation parameters obtained for acetone addition to **23b** reveal that the overall reduction in reactivity is due to slower proton transfer within the complex.

Complexation of acetone and the silene involves interactions between the ketone n-orbital and the silenic π-bond, affording a complex in which the silicon lies in the n-orbital plane perpendicular to the carbonyl π-system. It seems reasonable to suggest that the lowest energy pathway for proton transfer is one in which the complex adopts a chair-like transition state which allows for some degree of overlap between the C-H bond and the p-orbital on the carbonyl carbon. The lower reactivity of **23a-b** towards

acetone than **12a** can then be attributed to steric effects on the transition state geometries (eq 4.1). Transfer of a proton from the α-carbonyl carbon will be preferred when it is oriented towards the silenic carbon. Increasing steric bulk at silicon (**12a**), is expected to force the proton in closer proximity to the silenic carbon placing it in the optimum geometry for transfer.

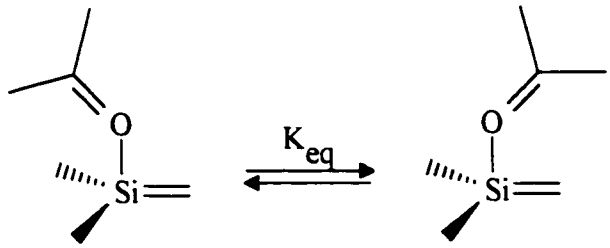

4.1

nonreactive geometry reactive geometry

The above solvent, kinetic isotope, substituent, and temperature effects studies have allowed us to formulate a common detailed mechanism for the reactions of simple silenes with alcohols, trimethylmethoxysilane, acetic acid and acetone in solution (eq 4.2). These reactions occur via stepwise mechanisms involving initial, reversible formation of a zwitterionic complex followed by proton transfer or $SiMe_3^{\cdot}$ transfer. In the case of reactions with alcohols, acetone and trimethylmethoxysilane the second step is rate-determining, while for acetic acid addition, complex formation is rate determining. For methanol, ethanol, and water, proton transfer may also occur by a general-base catalyzed process involving a second molecule of alcohol, which becomes competitive at high alcohol concentrations. Acetone and acetic acid addition most likely involves

complexation at the carbonyl oxygen and in these cases proton transfer occurs via a six-membered transition state.

Alcohols and Alkoxysilanes (L = H, D, or $SiMe_3$)

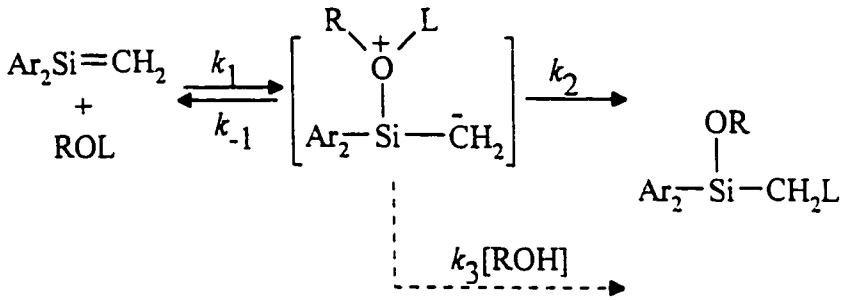

4.2

Carboxylic Acids and Ketones (X = O, CH_2)

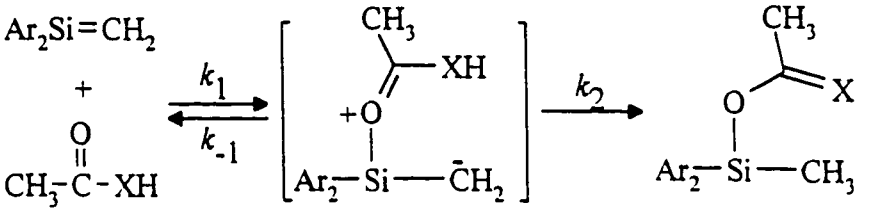

4.2 Future Work

Phenols represent a class of alcohols which have not been employed for study of silene reactions by our group since traditionally all of our silene precursors absorb at wavelengths less than 260 nm and would be screened by the trap. However, silenes such as $Me_2Si{=}C(SiMe_3)_2$ (**29**) may be generated by LFP of $Me_3SiSiMe_2C(N)_2SiMe_3$ at 308

nm,[20] allowing us to determine absolute rate constants for reaction with the aromatic silene traps. A Hammett type study of the reactions of *para*- and *meta*-substituted phenols to **29**, such as that reported for disilenes,[97] would provide valuable additional insight into the mechanism of alcohol additions to silenes. It would be very exciting if a change from rate-determining proton transfer to rate determining nucleophilic addition were observed in the form of a concave Hammett plot.

Several reports on the reactions of epoxides with disilenes have been published, and provide evidence for the involvement of an intermediate (eq 4.3).[109,110] Product ratios were shown to depend on the steric properties of the epoxide and are formed with complete regioselectivity.

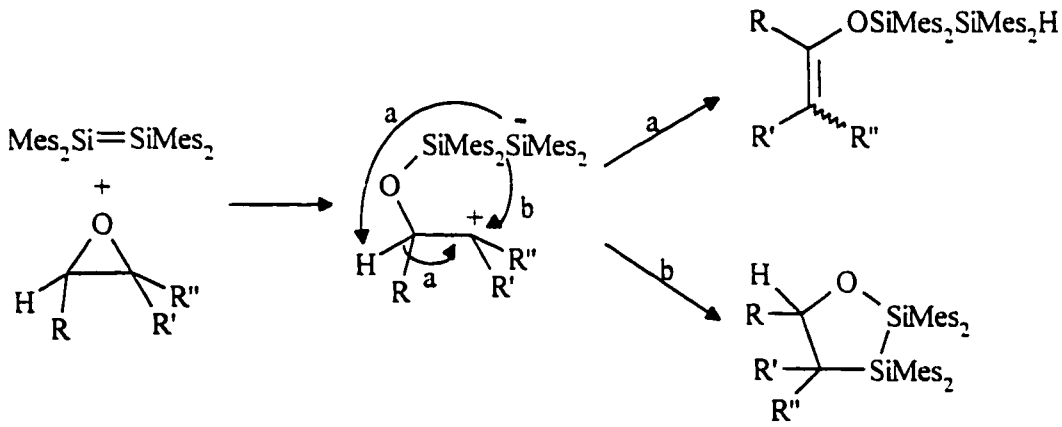

4.3

Silene-epoxide reactions have yet to be explored and would provide a new area of study through both steady-state and nanosecond laser flash photolysis techniques. Evidence of intermediate **30** in the reactions with silenes would provide further indirect

evidence in favour of the two-step mechanism proposed for alcohol, alkoxysilane and carbonyl compound additions to transient silenes.

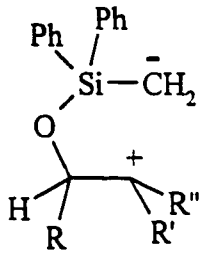

30

Related work which is currently underway in our laboratory includes a study of the (formal) [2+2]-addition of non-enolizable carbonyl compounds, such as pivaldehyde, to **12**. One might predict that these reactions should also proceed through the intermediacy of silene-carbonyl complexes, in which case similar variations in reactivity with substituent and temperature to those presented for the ene-reactions might be expected.

CHAPTER 5

EXPERIMENTAL

5.1 General

NMR spectra were recorded in deuteriochloroform or cyclohexane-d_{12} and referenced to tetramethylsilane. ^{1}H NMR spectra were recorded on Bruker Avance DRX-500 (500 MHz), Bruker AC-300 (300 MHz) and Bruker AC-200 (200 MHz) spectrometers. ^{13}C NMR spectra were recorded on Bruker Avance DRX-500 (125.7 MHz), Bruker AC-300 (75.4 MHz) and Bruker AC-200 (50.3 MHz) spectrometers. ^{29}Si NMR were recorded on a Bruker Avance DRX-500 (99.3 MHz) or using the DEPT pulse sequence[111] on the Bruker AC-300 (59.6 MHz) spectrometer, ^{19}F NMR spectra were recorded on the Avance Bruker DRX-500 (470.4 MHz) spectrometer. Ultraviolet absorption spectra were recorded on Hewlett-Packard HP8451 or Perkin-Elmer Lambda 9 (interfaced to an IBM-PC) spectrometers. Low resolution mass spectra and GC/MS analyses were determined using a Hewlett-Packard 5890 gas chromatograph equipped with a HP-5971A mass selective detector and a DB-1 fused silica capillary column (12m x 0.2mm ; Chromatographic Specialties, Inc.). High resolution electron impact mass spectra and exact masses were recorded on a VGH ZABE mass spectrometer employing a mass of 12.000000 for carbon. Infrared spectra were recorded on a BioRad FTS-40 FTIR spectrometer and are reported in wavenumbers (cm^{-1}).

Analytical gas chromatographic analyses were carried out using a Hewlett-Packard 5890 gas chromatograph equipped with a flame ionization detector, a Hewlett-Packard 3396A recording integrator, a conventional heated splitless injector, and a DB-1 fused silica capillary column (15-m X 0.20-mm; Chromatographic Specialties, Inc.). Semi-preparative GC separations employed a Varian 3300 gas chromatograph equipped with a thermal conductivity detector, and a 6' x 0.25" stainless steel 3% OV-101 packed column on Chromosorb W, HP 80/100 (Chromatographic Specialties).

5.2 Commercial Reagents and Solvents

Acetonitrile (BDH or Caledon Reagent) was refluxed over calcium hydride (Fisher) for several days, distilled under dry nitrogen, and then cycled three times through a 1" x 6" column of neutral alumina (Aldrich) which had been activated by heating under vacuum (ca. 0.05 Torr) at 320 °C for 18-hours (with periodic shaking). The alumina could dry up to 300 mL of acetonitrile per column prior to replacement. Methanol (Sigma, Aldrich HPLC; <0.05% H_2O), ethanol (Aldrich, Spectrophotometric), *i*-propanol (Aldrich, Spectrophotometric), *t*-butyl alcohol (Sigma Aldrich HPLC; <0.05% H_2O) and acetone (Sigma Aldrich) were used as received and stored over activated 4 Å molecular sieves. Diethyl ether (Caledon Reagent) and tetrahydrofuran (BDH Omnisolv) were refluxed for several days over sodium under nitrogen and distilled.

Hexane (EM Science Omnisolv or Caledon Reagent), *i*-octane (EM Science Omnisolv), glacial acetic acid (Caledon Reagent), water (Caledon HPLC), deuterated materials (MSD Isotopes or Isotec, Inc.), bromobenzene (Eastern Chem. Corp.), 1-bromo-

4-methylbenzene (Lancaster), 1-bromo-4-chlorobenzene (Matheson Coleman and Bell), 1-bromo-4-fluorobenzene (Lancaster), 1-bromo-4-(trifluoromethyl)benzene (Aldrich), allyl chloride (Aldrich), trichlorosilane (Aldrich), silica gel (100-200 mesh, Fisher) and magnesium turnings (BDH) were used as received from the suppliers.

5.3 Nanosecond Laser Flash Photolysis

Nanosecond laser flash photolysis experiments employed the pulses (248 nm; *ca.*16 ns; 70-120 mJ) from a Lumonics 510 excimer laser filled with F_2/Kr/He mixtures, and a microcomputer-controlled detection system.[65] The system incorporates a brass sample holder whose temperature is controlled to within 0.1 °C by a VWR 1166 constant temperature circulating bath. Silacyclobutane solutions were prepared at concentrations such that the absorbance at the excitation wavelength (248 nm) was *ca.* 0.7 and were flowed continuously through a 3 x 7 mm Suprasil flow cell connected to a calibrated 100 mL reservoir. Air-saturated solutions were employed since the presence of oxygen had no observable effect on the lifetime or course of reaction with any of the quenchers employed. Solution temperatures were measured with a Teflon-coated copper/constantan thermocouple which was inserted directly into the flow cell. Quenchers were added directly to the reservoir by microlitre syringe as aliquots of neat liquids or standard solutions. Rate constants were calculated by linear least-squares analysis of decay rate-concentration data (6-10 points) which spanned at least 1 order of magnitude in the transient decay rate. Errors are quoted as twice the standard deviation obtained from the least squares analysis in each case.

5.4 Preparation and Characterization of Compounds

The 1,1-diarylsilacyclobutanes **11a-e** were synthesized from 1,1-dichlorosilacyclobutane and the appropriate aryl magnesium bromide using a modification of the procedure of Auner and Grobe.[60] The only difference in the procedure was the reaction time, which increased from 5 hours for **11e** to 8 for **11b**. The silacyclobutanes (**11a-e**) were purified by column chromatography on silica gel (100-200 mesh) with hexanes as the effluent and were obtained as clear, colourless oils, in yields of 50-90%. Each contained less than 0.01% of the corresponding 1,1-biaryl derivative as determined by gas chromatography. 1,1-Dichlorosilacyclobutane used in the synthesis of **11a-e** was prepared from 3-chloropropyltrichlorosilane and both compounds were prepared by following the method of Laane.[112] They exhibited analytical and spectral properties similar to those reported.[60,112]

3-Chloropropyltrichlorosilane: Trichlorosilane (432 g, 3.2 mol) and allyl chloride (253 g, 3.3 mol) were placed in a 500 mL addition funnel. This solution was added dropwise over a period of 8 hours to a 1 L flame dried round-bottomed flask containing 1 mL of H_2PtCl_6, and fitted with a condenser, dry ice trap, and nitrogen inlet. The mixture was refluxed and stirred for two days, after which the reaction was complete. Distillation afforded 3-chloropropyltrichlorosilane (610 g, 2.8 mol, 90%; bp 180-181 °C[60,112]) as a

clear, colourless liquid. ^{1}H NMR ($CDCl_3$, 200 MHz): δ (ppm) = 1.56 (m, 2H), 2.06 (m, 2H), 3.59 (t, 6.3 Hz, 2H)); ^{13}C NMR ($CDCl_3$, 50.3 MHz): δ (ppm) = 21.8, 25.6, 45.7.

1,1-Dichlorosilacyclobutane: 3-Chloropropyltrichlorosilane (109 g, 0.52 mol) was added dropwise to a 3 neck, 2 L round-bottomed flask containing 22.1 g of magnesium turnings and 250 mL of diethyl ether. The flask was fitted with an overhead mechanical stirrer, addition funnel and nitrogen inlet. The reaction mixture was refluxed for one week, over which time the solution became very thick and cloudy due to the formation of $MgCl_2$ salts. Distillation of the reaction mixture yielded 1,1-dichlorosilacyclobutane (39.4 g, 0.28 mol, 54.4 %; bp 113-115 °C[60,112,113]) as a clear, colourless liquid. ^{1}H NMR ($CDCl_3$, 200 MHz): δ (ppm) = 1.91 (m, 4H), 2.08 (m, 2H); ^{13}C NMR ($CDCl_3$, 50.3 MHz): δ (ppm) = 14.0, 27.7.

1,1-Diphenylsilacyclobutane (**11a**): Bromobenzene (8.9 g, 0.057 mol) and 1,1-dichlorosilacyclobutane (4.0 g, 0.028 mol) were dissolved in dry diethyl ether (20 mL) and placed in a 100 mL addition funnel. The solution was added dropwise over two hours to a 250 mL flame dried round-bottomed flask fitted with a reflux condenser, nitrogen inlet, and magnetic stirrer, and containing magnesium turnings (1.7 g, 0.07 mol) in diethyl ether (10 mL). After the addition was complete the resulting mixture was refluxed gently for two hours. The reaction mixture was cooled and gravity-filtered into a 500 mL separatory funnel, washing the salts two times with diethyl ether. The filtrate

was then extracted with saturated aqueous ammonium chloride (3 x 25 mL) and water (3X25 mL), dried over anhydrous magnesium sulphate, and then distilled on the rotary evaporator to yield a light yellow viscous liquid (5.7 g). The liquid was dissolved in a small amount of hexane and chromatographed on a 40 x 2.5 cm silica gel 60 (100 g) column, eluting with hexanes. The purity of fractions containing **11a** (the first component to elute from the column) was determined by GC; those containing >0.001% biphenyl were combined and rechromatographed. 1,1-Diphenylsilacyclobutane was obtained as a colourless oil (3.3 g, 0.0145 mol, 51%; bp= 80°C (0.05 mm Hg); lit bp = 110-115 (0.001 mm Hg).[60] The compound exhibited spectroscopic and analytical properties similar to the reported data.[60] ^{1}H NMR ($CDCl_3$, 200 MHz): δ (ppm) = 1.50 (t, 8.4 Hz, 4H), 2.24 (p, 8.5 Hz, 2H), 7.41-7.53 (m, 5H), 7.55-7.68 (m, 5H); ^{13}C NMR ($CDCl_3$, 50.3 MHz): δ (ppm) = 13.8, 18.3, 127.9, 134.5, 136.4, 139.5; ^{29}Si NMR ($CDCl_3$, 59.6 MHz): δ (ppm) = 6.78; IR, 3080 (m), 2990 (m), 2850 (m), 1490 (m), 1420 (s), 1390 (m), 1300 (m), 1250 (m), 1200 (m), 1100 (s), 1000 (m), 900 (s), 850 (s); MS, m/e (I) = 224 (7), 196 (100), 181 (53), 165 (7), 146 (7), 105 (43), 79 (6), 53 (7); Exact mass, Calcd for $C_{15}H_{16}Si$, 224.1021; found 224.1014.

1,1-Di-(4-methylphenyl)silacyclobutane (**11b**): ^{1}H NMR ($CDCl_3$, 500 MHz): δ (ppm) = 1.45 (t, 8.2 Hz, 4 H), 2.23 (p, 8.4 Hz, 2H), 2.36 (s, 6H), 7.20 (d, 7.8 Hz, 4H), 7.50 (d, 7.7 Hz, 8H); ^{13}C NMR ($CDCl_3$, 75.4 MHz): δ (ppm) = 14.0, 18.3, 21.7, 128.8, 133.0, 134.6, 139.6; ^{29}Si NMR ($CDCl_3$, 99.3 MHz): δ (ppm) = 6.51; IR, 3067 (s), 3035 (s), 3013 (s),

2990 (s), 1603 (s), 1501 (s), 1394 (s), 1121 (s), 1081 (s), 854 (s), 716 (s), 634 (s); MS, m/e (I) = 252 (15), 226 (22), 224 (100), 211 (12), 209 (48), 160 (10) 119 (8); Exact mass, Calcd for $C_{17}H_{20}Si$, 252.1334; found 252.1346. Yield = 90 %.

1,1-Di-(4-fluorophenyl)silacyclobutane (**11c**). ^{1}H NMR ($CDCl_3$, 500 MHz): δ (ppm) = 1.46 (t, 8.3 Hz, 4H), 2.23 (p, 8.3 Hz, 2H), 7.08 (d, 8.7 Hz, 4H), 7.55 (d, 8.7 Hz, 4H); ^{13}C NMR ($CDCl_3$, 125.7 MHz): δ (ppm) = 14.1, 18.1, 115.3, 131.7, 136.5, 164.2; ^{19}F NMR ($CDCl_3$, 470.4 MHz): δ (ppm) = -110.1 (s); ^{29}Si NMR ($CDCl_3$, 99.3 MHz); δ (ppm) = 6.60; IR, 2971 (m), 2928 (m), 2875 (m), 1588 (s), 1500 (s), 1390 (m), 1236 (s), 1162 (s), 1123 (s), 1109 (s), 855 (s), 826 (s), 670 (s), 598 (w), 526 (s); MS, m/e (I) = 260 (5), 233 (20), 232 (100), 231 (43), 219 (20), 217 (62), 183 (8), 165 (20), 164 (6), 152 (9), 151 (18), 150 (14), 123 (40), 75 (6); Exact mass, Calcd. for $C_{15}H_{14}SiF_2$, 260.0833; Found, 260.0852. Yield = 62 %.

1,1-Di-(4-chlorophenyl)silacyclobutane (**11d**). ^{1}H NMR ($CDCl_3$, 500 MHz): δ (ppm) = 1.47 (t, 8.2 Hz, 4 H), 2.25 (p, 8.3 Hz, 2H), 7.37 (d, 8.2 Hz, 4H), 7.50 (d, 8.2 Hz, 8H); ^{13}C NMR ($CDCl_3$, 75.4 MHz): δ (ppm) = 13.9, 18.2, 128.4, 134.2, 135.8, 136.3; ^{29}Si NMR ($CDCl_3$, 99.3 MHz): δ (ppm) = 6.95; IR, 2971 (m), 2927 (m), 1579 (s), 1483 (m), 1381 (m), 1121 (m), 1084 (s), 1015 (m), 853 (s), 713 (m), 677 (m); MS, m/e (I) = 294 (8), 292 (10), 268 (15), 266 (70), 264 (100), 253 (18), 251 (45), 250 (40), 231 (10), 229 (25), 165

(20), 152 (10), 141 (15), 139 (45), 103 (8), 89 (8), 77 (8),65 (28), 63 (78); Exact mass. Calcd. for $C_{15}H_{14}SiCl_2$, 292.0242; Found, 292.0239. Yield = 60 %.

1,1-Di-(4-trifluoromethylphenyl)silacyclobutane (**11e**). ^{1}H NMR ($CDCl_3$, 500 MHz): δ (ppm) = 1.56 (t, 8.3 Hz, 4 H), 2.31 (p, 8.3 Hz, 2H), 7.66 (d, 8.0 Hz, 4H), 7.72 (d, 8.0 Hz, 4H); ^{13}C NMR ($CDCl_3$, 125.7 MHz): δ (ppm) = 13.6, 18.4, 124.1, 124.7, 132.0, 134.7, 140.4; ^{19}F NMR ($CDCl_3$, 470.4 MHz): δ (ppm) = -62.7 (s); ^{29}Si NMR ($CDCl_3$, 99.3 MHz): δ (ppm) = 7.73; IR, 2974 (s), 2931 (s), 1392 (s), 1324 (s), 1166 (s), 1104 (s), 1060 (s), 1019 (s), 827 (s), 704 (s); MS, m/e (I) = 360 (10), 341 (12), 333 (22), 332 (100), 319 (20), 317 (6), 263 (15), 251 (10), 173 (15), 140 (30); Exact mass, Calcd. for $C_{17}H_{14}SiF_6$, 360.0769; Found, 360.0766. Yield = 68 %.

1,1-Di-(4-methoxyphenyl)silacyclobutane (**11f**). ^{1}H NMR ($CDCl_3$, 200 MHz): δ (ppm) = 1.43 (t, 4.2 Hz, 4 H), 2.21 (p, 4.2 Hz, 2H), 3.81 (s, 6H), 6.94 (d, 4.4 Hz, 4H), 7.53 (d, 4.3 Hz, 4H); GC/MS, m/e (I) = 284 (15), 257 (22), 256 (100), 255 (33), 243 (18), 242 (12), 241 (54), 226 (10), 225 (19), 211 (16), 197 (9), 121 (11), 105 (15), 103 (16), 55 (42). Yield = 48 %.

1-Phenyl-1-silacyclobutane (**22a**) was prepared by the reduction of 1-phenyl-1-chloro-1-silacyclobutane as reported by Bertrand and coworkers.[61] In a flame dried, two neck round-bottomed flask fitted with nitrogen inlet and magnetic stirrer were placed 1.30 g (0.034 mol) lithium aluminum hydride and anhydrous ether (15-20 mL). The flask

was cooled to 0 °C in an ice bath and 3.14 g (0.017 mol) of phenylchlorosilacyclobutane in 20 mL of ether was added dropwise. The mixture was maintained at 0 °C and stirred for two hours, after which 2 mL of water was slowly added dropwise followed by 1 mL of 15% NaOH. The white precipitate formed was then filtered and rinsed with ether. The organic layer was dried over magnesium sulfate and concentrated on a rotary evaporator. The residue was distilled to give 1.88 g of **22a** as a clear colorless oil (0.013 mol, 74 %; b.p. 97-100 °C / 20 mmHg); lit. b.p. 85 °C (12 mmHg).[61] ^{1}H NMR ($CDCl_3$, 200 MHz): δ (ppm) = 1.25 (m, 4H), 2.20 (m, 2H), 5.33-5.35 (m, 1H), 7.41 (m, 3H), 7.66 (m, 2H). ^{13}C NMR ($CDCl_3$, 50.3 MHz): δ (ppm) = 12.7, 18.6, 19.7, 128.0, 128.2, 129.9, 134.4, 135.2, 135.8. IR = 2963.0(m), 2924.0(s), 2854.2(s), 2122.6(m), 1731.4(m), 1625.5(s) 1569.4(s), 1510.1(m), 1428.9(m), 1119.5(s), 699.4(s). MS: m/e (I)= 148(30), 120(83), 105(100), 79(15), 67(8), 53(25), 43(8).

1-Methyl-1-phenylsilacyclobutane (**22b**) was prepared by a modification of the method of Auner and Grobe.[60] A solution of phenylchlorosilacyclobutane (0.9 g, 4.9 mmol) in 10 mL of dry ether was added dropwise to a solution of 10 mmol of methylmagnesium bromide in ether at 0 °C (ice bath). The resulting mixture was allowed to warm to room temperature and stirred for 14 hours under anhydrous conditions. The filtrate was extracted with saturated ammonium chloride (3 x 25 ml), and water (3 x 25 ml), dried over anhydrous magnesium sulfate, and then stripped of solvent on the rotary evaporator to yield a light yellow viscous oil. The crude product was purified by column

chromatography (silica gel 100-200 mesh) using hexane as the eluent to yield 0.65g of 1-methyl-1-phenylsilacyclobutane in 82 % yield (bp 62 °C @ 5 mmHg, lit b.p. 61.5-62 °C @ 5 mmHg [62]. ^{1}H NMR ($CDCl_3$, 200 MHz): δ (ppm) = 0.55 (s, 3H), 1.26 (m, 4H), 2.19 (p, 8.2 Hz, 2H), 7.40 (m, 3H), 7.64 (m, 2H). ^{13}C NMR ($CDCl_3$, 50.3 MHz): (ppm) = -1.8, 14.3, 18.2, 127.9, 129.4, 133.5. [114] IR = 2963.8(s), 2856.5(m), 1428.2(s), 1396.3(s), 1249.9(s), 1115.5 (m), 867.2(s), 772.1(s), 732.5 (m), 697.6 (m), 427.7(m). MS: m/e (I)= 162 (10), 134 (100), 119 (45), 105 (20), 93 (7), 79 (5), 53 (10), 43 (13). Exact mass: Calculated for $C_{10}H_{14}Si$: 162.0865 g/mol: found: 162.0874.

Chlorophenylsilacyclobutane used in the synthesis of **22a-b** was prepared from the intramolecular grignard coupling of 3-chloropropyldichlorophenylsilane as reported by Auner and Grobe.[60] The 3-chloropropyldichlorophenylsilane was prepared from the hydrosilylation reaction between allyl chloride and dichlorophenylsilane as described for the synthesis of 3-chloropropyltrichlorosilane.

1-Chloro-1-phenylsilacyclobutane: ^{1}H NMR ($CDCl_3$, 200 MHz): δ (ppm) = 1.68 (m, 4H), 2.05 (m, 1H), 2.35 (m, 1H), 7.45 (m, 3H), 7.72 (m, 2H). bp 120 °C @ 35 mmHg.[114] Yield = 85 %.

3-Chloropropyldichlorophenylsilane: ^{1}H NMR ($CDCl_3$, 200 MHz): δ (ppm) = 1.47 (t, Si-CH_2, 4.8 Hz, 2H), 1.97 (m, CH_2, 2H), 3.56 (t, CH_2Cl, 6.4 Hz, 2H), 7.48 (m, 3H, 7.69 (m, 2H). bp 96 °C @ 0.5 mmHg.[60] Yield = 92 %.

5.5 Steady-State Photolyses

5.5.1 General Methods

Steady-state photolysis experiments were carried out using a Rayonet photochemical reactor equipped with a merry-go-round and five to eight RPR2537 (254 nm) lamps. Photolysis solutions were contained in 25 cm x 1.2 cm, 5 mm x 75 mm or 9 mm x 100 mm quartz tubes which were sealed with rubber septa. Chemical yields were determined by GC analyses relative to the disappearance of the starting silacyclobutane using dodecane or hexadecane as internal standards. The response of the FID detector was calibrated relative to the internal standards by the construction of working curves.

5.5.2 Quantum Yield Determinations

Quantum yield measurements of the photolysis of **11a** (254 nm; 23 °C) were determined by potassium ferrioxalate actinometry,[115] using 0.002 solutions of **11a** in hexane containing 0.02 M methanol and 0.002 M dodecane as the internal standard for starting material. Bunce's method for quantum yield determinations in Rayonet reactors was followed.[116] The quantum yields are reported as the average of triplicate determinations.

5.5.3 Photoproduct Determination and Identification

Compounds **13a-16a** and **21a** were isolated by semi-preparative GC and fully characterized. Photoproducts **24-25** were identified by GC coinjection of the crude photolysates with authentic samples. The remaining photoproducts were identified by a combination of ^{1}H NMR and GC/MS.

Diphenylmethoxymethylsilane (**13a**). ^{1}H NMR ($CDCl_3$, 200 MHz): δ (ppm) = 0.63 (s, 3H), 3.53 (s, 3H), 7.35-7.54 (m, 10H); ^{13}C NMR ($CDCl_3$, 50.3 MHz): δ (ppm) = -3.6, 51.2, 127.9, 129.8, 134.3, 135.6; ^{29}Si NMR ($CDCl_3$, 59.6 MHz): δ (ppm) = -0.90; IR 3080(m), 2990 (s), 2825 (s), 1600 (m), 1420 (m), 1250 (s), 1200 (s), 1100 (s), 1080 (s);

MS, m/e (I) = 228 (9), 213 (100), 183 (27), 151 (9), 121 (12), 105 (11), 91 (7), 59 (10); Exact mass, Calcd. for $C_{14}H_{16}OSi$, 228.0974; Found, 228.0970.

Diphenylethoxymethylsilane (**14a**). ^{1}H NMR ($CDCl_3$, 200 MHz): δ (ppm) = 0.62 (s, 3H), 1.20 (t, 8.5 Hz, 3H), 3.76 (q, 8.4 Hz, 2H) 7.35-7.57 (m, 10H); ^{13}C NMR ($CDCl_3$, 50.3 MHz): δ (ppm) = -2.9, 18.4, 59.2, 127.8, 129.7, 134.3, 136.2; IR 3080(m), 2990 (s), 2970 (m), 1600 (m), 1465 (s), 1400 (m), 1275 (s), 1120 (s), 1080 (s), 950 (m), 790 (s); MS, m/e (I) = 242 (8), 227 (100), 197 (12), 183 (65), 165 (10), 164 (12), 137 (11), 121 (13), 105 (12), 91 (5), 77 (11), 47 (13); Exact mass, Calcd. for $C_{15}H_{18}OSi$, 242.1129; Found, 242.1127.

Diphenyl-t-butoxymethylsilane (**15a**). ^{1}H NMR ($CDCl_3$, 200 MHz): δ (ppm) = 0.66 (s, 3H), 1.25 (s, 9H), 7.33-7.58 (m, 10H); ^{13}C NMR ($CDCl_3$, 50.3 MHz): δ (ppm) = 0.6, 14.0, 32.1, 127.6, 129.3, 134.2, 136.2; IR 3100 (m), 2980 (m), 2900 (m), 1600 (m), 1490 (m), 1420 (m), 1390 (m), 1300 (m), 1210 (s), 1120 (s), 1050 (s), 860 (m), 790 (s); MS, m/e (I) = 270 (4), 255 (44), 199 (100), 181 (8), 137 (25), 105 (9), 77 (6), 47 (6); Exact mass, Calcd. for $C_{17}H_{22}OSi$, 270.1452; Found, 270.1440.

Diphenylisopropoxymethylsilane (**16a**). ^{1}H NMR ($CDCl_3$, 200 MHz): δ (ppm) = 0.62 (s, 3H), 1.19 (d, 7.2 Hz, 6H), 4.08 (p, 7.3 Hz, 1H) 7.35-7.57 (m, 10H); ^{13}C NMR ($CDCl_3$, 50.3 MHz): δ (ppm) = -2.8, 25.7, 65.8, 127.8, 129.6, 134.2, 136.8; IR 3080(m), 2990 (s),

2970 (m), 1600 (m), 1420 (m), 1390 (m), 1250 (m), 1190 (s), 1120 (s), 1000 (s), 790 (s); MS, m/e (I) = 256 (3), 241 (92), 199 (100), 183 (29), 165 (10), 137 (34), 123 (10), 105 (27), 91 (10), 77 (15), 51 (8); Exact mass, Calcd. for $C_{16}H_{20}OSi$, 256.1286; Found, 256.1283.

Diphenylmethylacetylsilane (**18a**). GC/MS, m/e (I) = 256 (2), 242 (20), 241 (100), 200 (16), 199 (93), 197 (17), 181 (13), 180 (15), 179 (78), 165 (5), 138 (10), 137 (84), 105 (10), 91 (14), 78 (8), 77 (30).

Di-(4-methylphenyl)methoxymethylsilane (**13b**). ^{1}H NMR ($CDCl_3$, 500 MHz): δ (ppm) = 0.59 (s, 3H), 2.35 (s, 6H), 3.51 (s, 3H), 7.20 (d, 7.7 Hz, 4H), 7.49 (d, 7.8 Hz, 4H); ^{13}C NMR ($CDCl_3$, 50.3 MHz): δ (ppm) = -3.4, 21.5, 46.2, 128.7, 133.3, 134.8, 139.8; ^{29}Si NMR ($CDCl_3$, 99.3 MHz): δ (ppm) = -0.96; IR, 2959 (s), 2927 (s), 2860 (m), 1601 (m), 1550 (m), 1254 (m), 1112 (m), 1088 (m), 1006 (m), 979 (m); MS, m/e (I) = 256 (6), 242 (21), 241 (100), 212 (5), 211 (23), 165 (11), 131 (11), 119 (13), 105 (8), 93 (6), 91 (7), 65 (5); Exact mass, Calcd. for $C_{16}H_{20}OSi$, 256.1283; Found, 256.1287.

Di-(4-fluorophenyl)methoxymethylsilane (**13c**). ^{1}H NMR ($CDCl_3$, 300 MHz): δ (ppm) = 0.59 (s, 3H), 3.50 (s, 3H), 7.04 (d, 8.7 Hz 4H), 7.50 (d, 8.8 Hz, 4H); ^{13}C NMR ($CDCl_3$, 75.4 MHz): δ (ppm) = -3.6, 46.1, 115.0, 131.1,136.3, 164.1; ^{29}Si NMR ($CDCl_3$, 59.6 MHz): δ (ppm) = -2.49; IR, 2962 (s), 2938 (s), 2835 (m), 1588 (s), 1499 (s), 1388 (s),

1110 (s), 878 (s), 824 (s), 756 (s); MS, m/e (I) = 264 (10), 249 (100), 220 (8), 219 (42), 169 (8), 139 (16), 123 (11), 109 (6), 59 (12); Exact mass, Calcd. for $C_{14}H_{14}F_2OSi$, 264.0782; Found, 264.0782.

Di-(4-chlorophenyl)methoxymethylsilane (**13d**). ^1H NMR ($CDCl_3$, 300 MHz): δ (ppm) = 0.62 (s, 3H), 3.52 (s, 3H), 7.38 (d, 8.3 Hz, 4H), 7.50 (d, 8.4Hz, 4H); ^{13}C NMR ($CDCl_3$, 75.4 MHz): δ (ppm) = -3.6, 51.2, 128.3, 134.2, 135.7, 136.3; ^{29}Si NMR ($CDCl_3$, 59.6 MHz): δ (ppm) = -2.67; IR, 2959 (s), 2928 (s), 2850 (m), 1602 (m), 1550 (m), 1260 (m), 1110 (m), 1088 (m), 1006 (m), 969 (m); MS, m/e (I) = 298 (11), 296 (16), 285 (14), 284 (13), 283 (70), 282 (20), 281 (100), 253 (20), 251 (30), 185 (13), 157 (7), 155 (20), 152 (13), 139 (11), 125 (7), 91 (7), 75 (9), 65 (9), 63 (21), 59 (22); Exact mass, Calcd. for $C_{14}H_{14}Cl_2OSi$, 296.0191; Found, 296.0185.

Di-(4-trifluoromethylphenyl)methoxymethylsilane (**13e**). ^1H NMR ($CDCl_3$, 500 MHz): δ (ppm) = 0.68 (s, 3H), 3.55 (s, 3H), 7.62 (d, 7.8 Hz, 4H), 7.66 (d, 7.7 Hz, 4H); ^{13}C NMR ($CDCl_3$, 50.3 MHz): δ (ppm) = -3.9, 51.3, 124.6, 131.8, 132.1, 134.5, 139.8; ^{29}Si NMR ($CDCl_3$, 99.3 MHz): δ (ppm) = -2.83; IR, 2959 (s), 2929 (s), 2841 (m), 1392 (m), 1325 (s), 1269 (m), 1168 (s), 1132 (s), 1088 (s), 1061 (s), 1019 (s), 909 (m), 813 (s), 760 (s), 735 (s), 703 (m); MS, m/e (I) = 364 (5), 350 (21), 349 (100), 320 (7), 319 (34), 271 (7), 252 (11), 219 (19), 189 (22), 173 (8), 159 (6), 127 (12), 126 (27), 59 (15); Exact mass, Calcd. for $C_{16}H_{14}OSiF_6$, 364.0718; Found, 364.0709.

Di-(4-methoxyphenyl)methoxymethylsilane (**13f**). GC/MS, m/e (I) = 288 (20), 274 (20), 273 (100), 243 (22), 59 (13).

2-(Di-4-methylphenyl)methylsiloxypropene (**20b**): ^{1}H NMR (C_6D_{12}, 500 MHz): δ (ppm): 0.60 (s, 3H), 1.72 (s, 3H), 3.95 (m, 2H), 7.08-7.44 (m, 8H). GC/MS, m/e (I) = 282 (19), 267 (44), 227 (28), 226 (29), 225 (100), 175 (15), 165 (15), 151 (86), 119 (22), 105 (22), 91 (29).

2-Diphenylmethylsiloxypropene (**20a**): ^{1}H NMR (C_6D_{12}, 500 MHz): δ (ppm): 0.65 (s, 3H), 1.74 (s, 3H), 3.96 (m, 2H), 7.24-7.55 (m, 10H). GC/MS, m/e (I) = 254 (13), 239 (36), 197 (78), 165 (18), 137 (100), 105 (33), 91 (15), 77 (20), 43 (17).

2-(Di-4-fluorophenyl)methylsiloxypropene (**20c**): ^{1}H NMR (C_6D_{12}, 500 MHz,): δ(ppm): 0.62 (s, 3H), 1.75 (s, 3H), 3.98 (m, 2H), 7.00-7.51 (m, 8H). GC/MS, m/e (I) = 290 (22), 275 (31), 235 (24), 234 (24), 233 (100), 155 (57), 116 (34), 115 (18), 95 (10), 77 (21).

2-(Di-4-chlorophenyl)methylsiloxypropene (**20d**): ^{1}H NMR (C_6D_{12}, 500 MHz,): δ(ppm): 0.75 (s, 3H), 1.78 (s, 3H), 3.97 (m, 2H), 7.30-7.45 (m, 8H).
GC/MS, m/e (I) = 269 (8), 267 (49), 265 (54), 208 (11), 207 (63), 173 (42), 171 (100), 165 (19), 152 (33), 62 (10).

2-(Di-4-trifluoromethylphenyl)methylsiloxypropene (**20e**): ^{1}H NMR (C_6D_{12}, 500 MHz,): δ (ppm): 0.73 (s, 3H), 1.79 (s, 3H), 4.01 (m, 2H), 7.56-7.66 (m, 8H). GC/MS, m/e (I) = 390 (12), 375 (36), 335 (36), 334 (17), 333 (84), 243 (12), 205 (82), 184 (14), 173 (13), 167 (14), 166 (100), 165 (15), 127 (30), 126 (12).

1,1-Diphenyl-1-methoxy-3,3,3-(trimethylsilylmethyl)silane (**21a**): ^{1}H NMR ($CDCl_3$, 200 MHz,): δ (ppm): -0.10 (s, 3H), 0.39 (s, 2H), 3.46 (s, 3H), 7.38 (m, 5H), 7.59 (m, 5H).[64] ^{13}C NMR ($CDCl_3$, 50.3 MHz): δ (ppm) = 1.0, 13.8, 18.3, 127.8, 129.6, 134.5, 136.4.

Methylphenylmethoxysilane (**24a**) was prepared by the method of Jones and Owen.[32] Phenylmethylchlorosilane (1.5 g, 9.57 mmol) and 3 ml (excess) of trimethylorthoformate were placed in a 10 ml round bottom flask and was stirred at 50 °C overnight. Distillation afforded 0.9 g (5.92 mmol) of **24a**, a clear colorless liquid in 62 % yield; bp 69 °C (35 mmHg). ^{1}H NMR ($CDCl_3$, 200 Mz): δ (ppm) = 0.45 (d, 2.85 Hz, 3H), 3.50 (s, 3H), 4.97 (q, 2.85 Hz, 1H), 7.40 (m, C_6H_5, 3H), 7.60 (m, 2H). ^{13}C NMR ($CDCl_3$, 50.3 MHz): δ (ppm) = -3.2, 52.0, 128.0, 130.2, 133.8, 135.3.[117]

The method of Brook and Dillon [118] was employed for the synthesis of dimethylphenylmethoxysilane (**24b**). Dry dichloromethane (40 mL), excess methanol (0.025 mol), and 0.82 g imidazole (0.012 mol) were placed in a flame dried, 2-necked

round-bottomed flask fitted with an addition funnel, reflux condenser, magnetic stirrer, and nitrogen inlet. To this mixture 1.78 g of chlorodimethylphenylsilane (0.0120 mol) was added dropwise and the resulting white solution was stirred overnight at room temperature. Filtration of the reaction mixture and distillation yielded **24b** as a colourless, liquid (1.31 g, 0.008 mol, 66% yield, bp 75-80 °C / 9 mm Hg [117]). ^{1}H NMR ($CDCl_3$, 200 MHz,): δ (ppm) = 0.46 (s, $Si(CH_3)_2$, 6H), 3.45 (s, OCH_3, 3H), 7.37 (m,C_6H_5, 3H), 7.57 (m, 2H). ^{13}C NMR ($CDCl_3$, 50.3 MHz): δ (ppm) = -2.3, 0.8, 50.6, 127.7, 129.4, 133.2, 139.8. [119] MS: m/e (I)= 166(12), 151(100), 136(5), 121(55), 105(13), 91(15), 59(20), 43(12), 15(4).

The method of Sakurai *et al* [120] was followed for the preparation of the silyl enol ethers **25a** and **25b**. In a dry 50 ml round bottom flask maintained under constant pressure of nitrogen and fitted with a condenser were placed 2.69g (22 mmol) of phenylmethylsilane, 1.16g (20 mmol) of acetone, 0.05g (2.4 mol %) of pyridine and 2.4 mol % of dicobalt carbonyl in CH_2Cl_2. The mixture was stirred and heated at 50 °C for 1 hour after which the reaction was complete. Distillation afforded 1.03g of enol ether **25a** in 13 % yield (bp 79 °C / 22 mm Hg). ^{1}H NMR ($CDCl_3$, 200 MHz): δ (ppm) = 0.51 (d, 2.9 Hz, 3H), 1.80 (s, 3H), 4.07 (s, 1H), 4.12 (s, 1H), 5.15 (q, 2.8, 1H), 7.39 (m, 3H), 7.61 (m 2H). ^{13}C NMR ($CDCl_3$, 50.3 MHz): δ (ppm) = -2.7, 22.3, 91.2, 128.0, 130.3, 133.8, 135.1, 156.3. [121].

(Isopropenyloxy)-dimethylphenylsilane (**25b**): bp 79 °C / 22 mmHg. ^{1}H NMR ($CDCl_3$, 200 MHz): δ (ppm) = 0.45 (s, 6H), 1.76 (s, 3H), 4.02 (m, 2H), 7.37 (m, 3H), 7.59 (m, 2H). ^{13}C NMR ($CDCl_3$, 50.3 MHz): δ (ppm) = -1.2, 22.7, 91.8, 127.8, 129.7, 133.3, 137.6, 155.8.[51]

CHAPTER 6

APPENDIX

6.1 NMR Spectra of Enol Ethers 20a-e

Figure 6.1. ^{1}H NMR spectrum (500 MHz) of a crude reaction mixture from photolysis of a 0.02 M solution of **11a** in C_6D_{12} containing 0.05 M acetone to *ca.* 20 % conversion. Resonances due to **11a** (↓) and **20a** (⇓) are labeled.

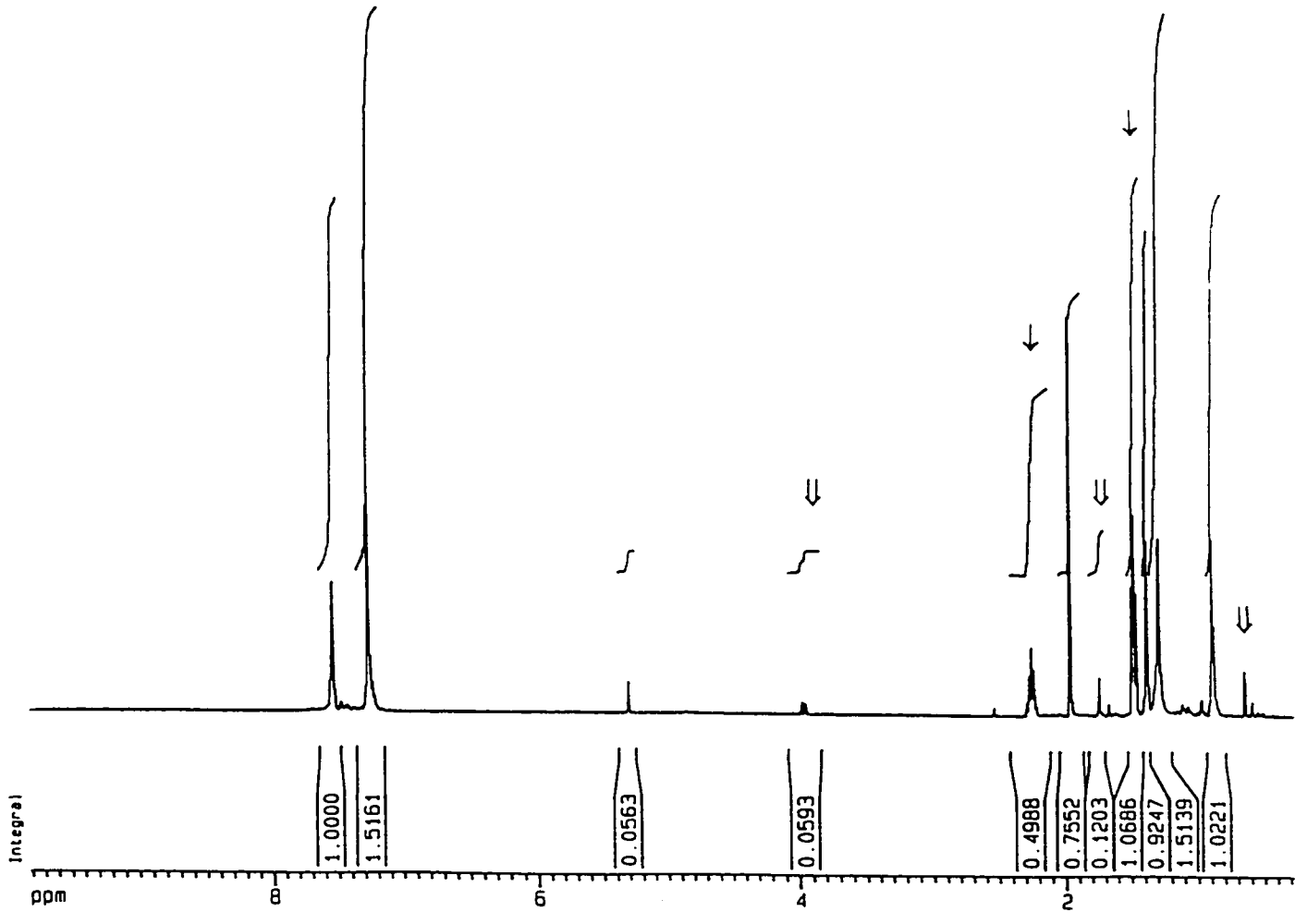

Figure 6.2. ^{1}H NMR spectrum (500 MHz) of a crude reaction mixture from photolysis of a 0.02 M solution of **11b** in C_6D_{12} containing 0.05 M acetone to *ca.* 20 % conversion. Resonances due to **11b** (↓) and **20b** (⇓) are labelled.

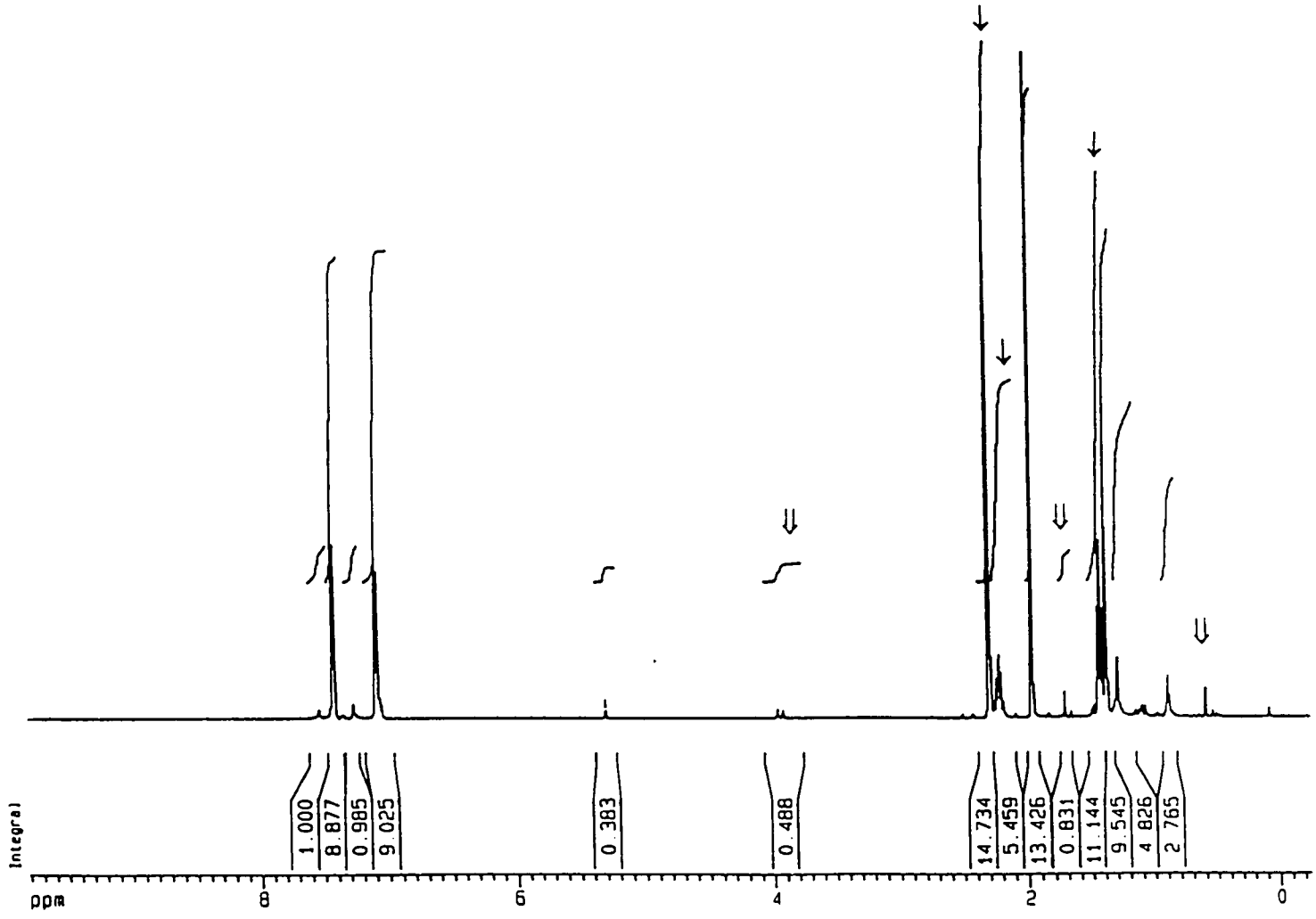

Figure 6.3. ^{1}H NMR spectrum (500 MHz) of a crude reaction mixture from photolysis of a 0.02 M solution of **11c** in C_6D_{12} containing 0.05 M acetone to *ca.* 20 % conversion. Resonances due to **11c** (↓) and **20c** (⇓) are labelled.

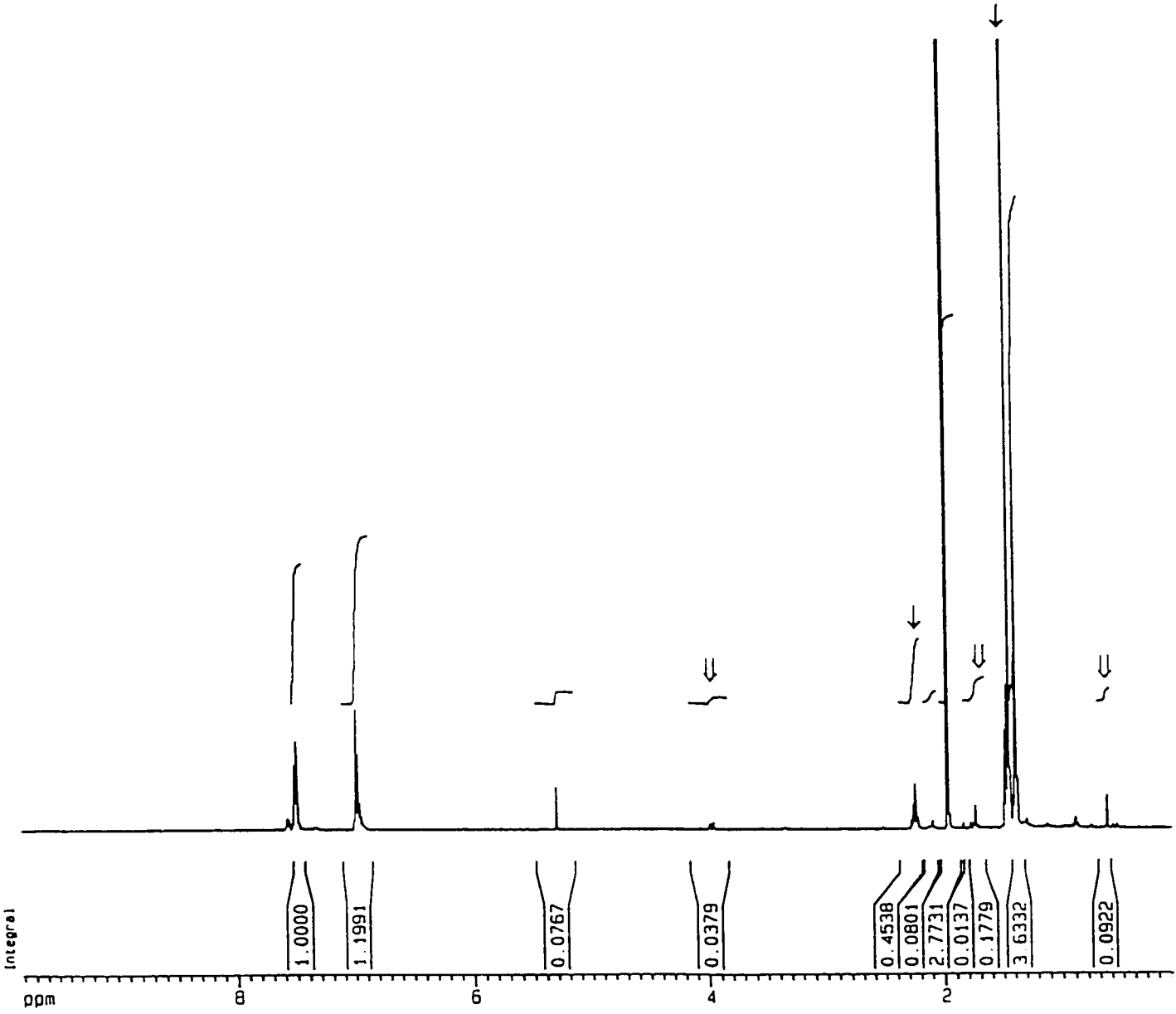

Figure 6.4. ^{1}H NMR spectrum (500 MHz) of a crude reaction mixture from photolysis of a 0.02 M solution of **11d** in C_6D_{12} containing 0.05 M acetone to *ca.* 20 % conversion. Resonances due to **11d** (↓) and **20d** (⇓) are labelled.

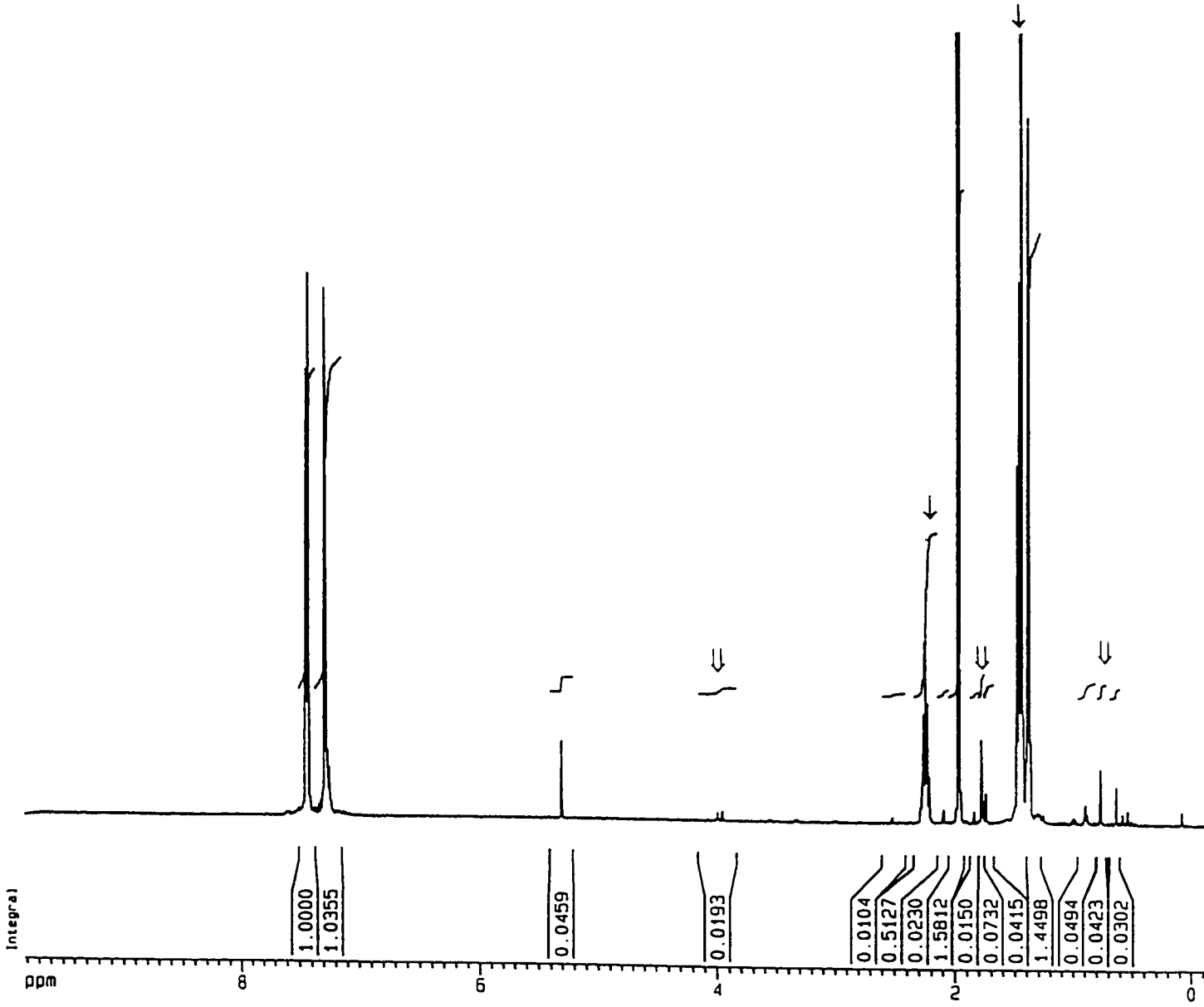

Figure 6.5. ^{1}H NMR spectrum (500 MHz) of a crude reaction mixture from photolysis of a 0.02 M solution of **11e** in C_6D_{12} containing 0.05 M acetone to *ca.* 20 % conversion. Resonances due to **11e** (↓) and **20e** (⇓) are labelled.

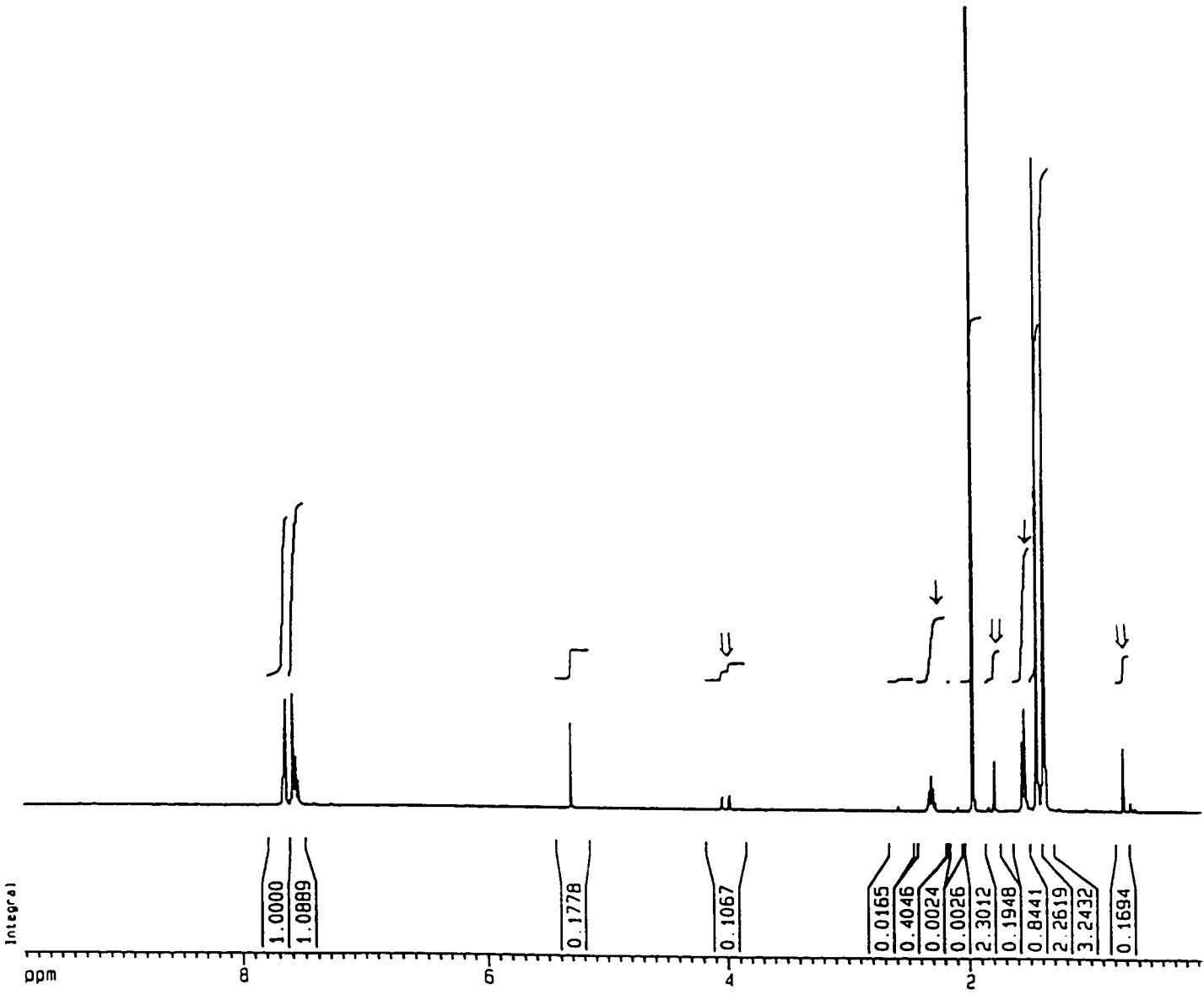

6.2 Transient UV Absorption Spectra of 12b-e

Figure 6.6. Transient absorption spectra obtained from laser flash photolysis of 6.3 x 10^{-3} M **11b** in air saturated *iso*octane solution.

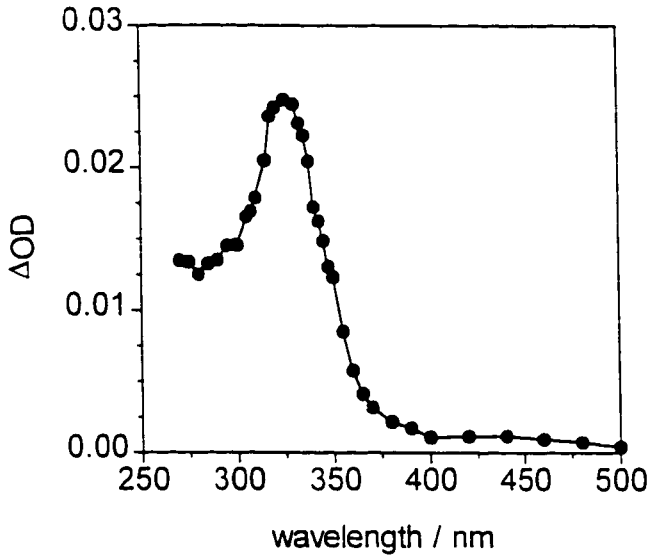

Figure 6.7. Transient absorption spectra obtained from laser flash photolysis of 5.6 x 10^{-3} M **11c** in air saturated *iso*octane solution.

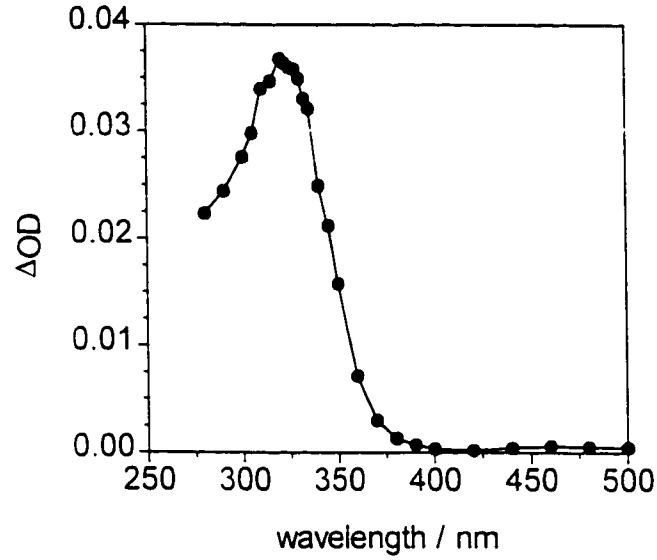

Figure 6.8. Transient absorption spectra obtained from laser flash photolysis of 3.8 x 10^{-3} M **11d** in air saturated *iso*octane solution.

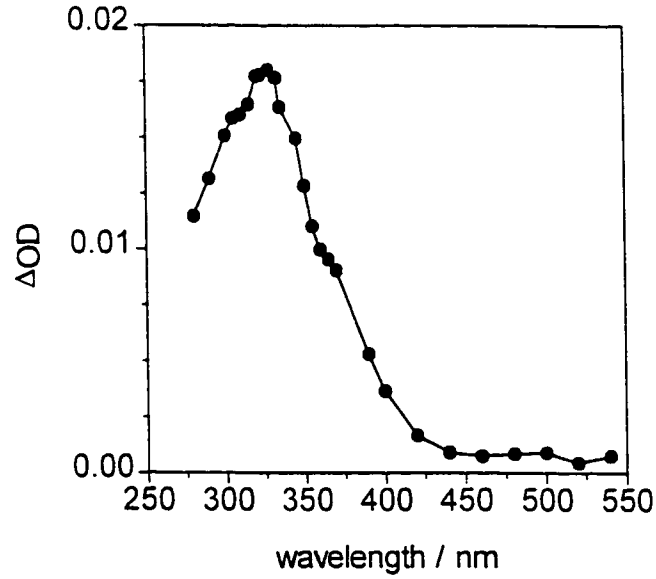

6.3 Quenching Plots and Tables of Rate Constants for Reactions of Silenes 12a-e and 22b with Alcohols, Acetic Acid, Trimethylmethoxysilane and Acetone in Solution at Various Temperatures

Figure 6.9. Plots of k_{decay} versus methanol concentration, from laser flash photolysis of air-saturated solutions 1,1-diphenylsilacyclobutane (**11a**) in acetonitrile solution from -17.2 to 54.9 °C.

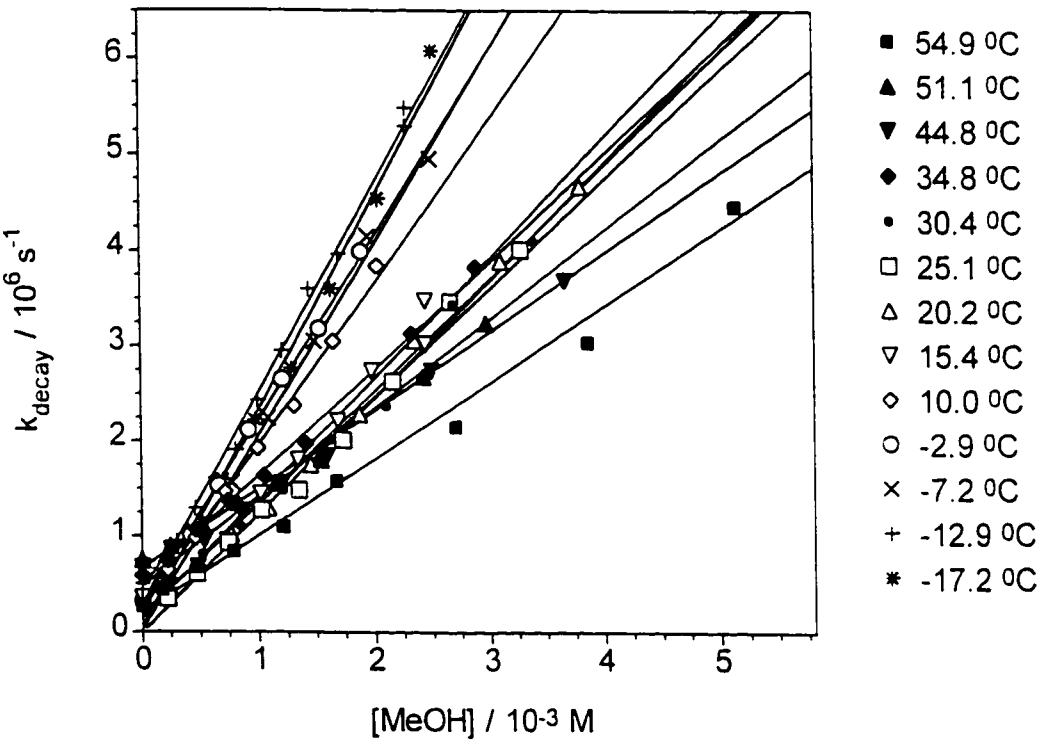

Table 6.1. Rate Constants for the Addition of Methanol to 1,1-Diphenylsilene (**12a**) in MeCN Solution from -17.2 to 54.9 °C.[a]

Disk	Filename	Temperature (°C)	$k_q / 10^9$ ($M^{-1} s^{-1}$)
DAT054	PHSCB0*.058	-17.2 ± 0.3	2.32 ± 0.20
DAT047	PHSCB0*.037	-12.9 ± 0.3	2.26 ± 0.10
DAT054	PHSCB0*.060	-7.2 ± 0.3	1.95 ± 0.09
DAT047	PHSCB0*.010	-2.9 ± 0.3	1.95 ± 0.07
DAT047	PHSCB0*.011	10.0 ± 0.3	1.71 ± 0.09
DAT054	PHSCB0*.053	15.4 ± 0.3	1.43 ± 0.07
DAT054	PHSCB0*.054	20.2 ± 0.3	1.23 ± 0.05
DAT054	PHSCB0*.055	25.1 ± 0.3	1.20 ± 0.05
DAT054	PHSCB0*.052	30.4 ± 0.3	1.15 ± 0.08
DAT047/DAT052	PHSCB0*.012	34.8 ± 0.3	1.13 ± 0.06
DAT036	PHSCB0*.036	44.8 ± 0.3	0.96 ± 0.04
DAT047	PHSCB0*.013	51.1 ± 0.3	0.83 ± 0.06
DAT047	PHSCB0*.038	54.9 ± 0.3	0.82 ± 0.05

[a] Errors are reported as twice the standard deviation of least squares analysis of decay-rate concentration data according to eq 2.10.

Figure 6.10. Plots of k_{decay} versus methanol concentration, from laser flash photolysis of 1,1-diphenylsilacyclobutane (**11a**) in hexane solution from -6.3 to 39.5 °C.

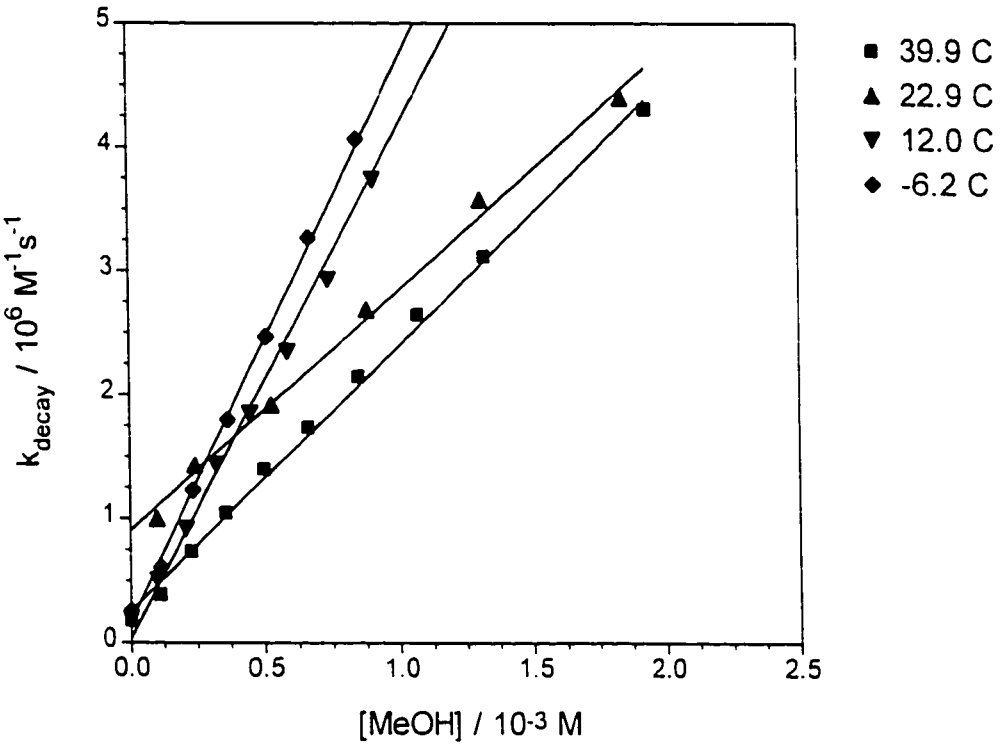

Table 6.2. Rate Constants for the Addition of Methanol to 1,1-Diphenylsilene (**12a**) in Hexane Solution from -6.3 to 39.5 °C.[a]

Disk	Experiment	Temperature (°C)	$k_q / 10^9$ ($M^{-1} s^{-1}$)
DAT054	PHSCB0*.062	-6.3 ± 0.3	4.62 ± 0.15
DAT054	PHSCB0*.065	10.3 ± 0.3	3.63 ± 0.20
DAT054	PHSCB0*.064	39.5 ± 0.3	2.14 ± 0.09

[a] Errors are reported as twice the standard deviation of least squares analysis of decay-rate concentration data according to eq 2.10.

Figure 6.11. Plots of k_{decay} versus methanol-Od concentration, from laser flash photolysis of air-saturated solutions 1,1-diphenylsilacyclobutane (**11a**) in acetonitrile solution from -17.1 to 54.7 °C.

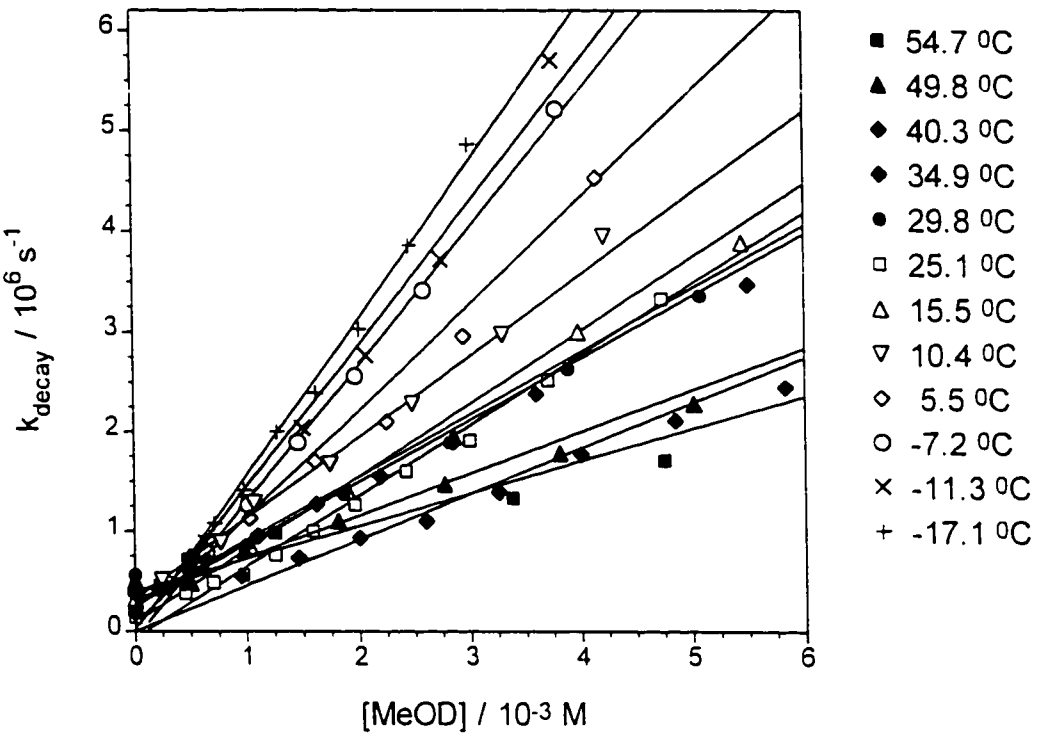

Table 6.3. Rate Constants for the Addition of Methanol-Od to 1,1-Diphenylsilene in MeCN Solution from -17.1 to 54.7 °C.[a]

Disk	Experiment	Temperature (°C)	k_q / 10^9 (M^{-1} s^{-1})
DAT054	PHSCB0*.059	-17.1 ± 0.3	1.56 ± 0.05
DAT054	PHSCB0*.044	-11.3 ± 0.3	1.44 ± 0.10
DAT054	PHSCB0*.061	-7.2 ± 0.3	1.37 ± 0.06
DAT054	PHSCB0*.048	5.5 ± 0.3	1.04 ± 0.09
DAT054	PHSCB0*.045	10.3 ± 0.3	0.81 ± 0.03
DAT054	PHSCB0*.047	15.5 ± 0.3	0.73 ± 0.04
DAT054	PHSCB0*.056	25.1 ± 0.3	0.72 ± 0.03
DAT054	PHSCB0*.046	29.8 ± 0.3	0.66 ± 0.04
DAT054	PHSCB0*.040	34.9 ± 0.3	0.57 ± 0.01
DAT054	PHSCB0*.049	40.3 ± 0.3	0.46 ± 0.02
DAT054	PHSCB0*.050	49.8 ± 0.3	0.43 ± 0.02
DAT054	PHSCB0*.042	54.7 ± 0.3	0.35 ± 0.02

[a] Errors are reported as twice the standard deviation of least squares analysis of decay-rate concentration data according to eq 2.10.

Figure 6.12. Plots of k_{decay} versus *t*-butanol concentration, from laser flash photolysis of air-saturated solutions 1,1-diphenylsilacyclobutane (**11a**) in acetonitrile solution from -21.1 to 50.6 °C.

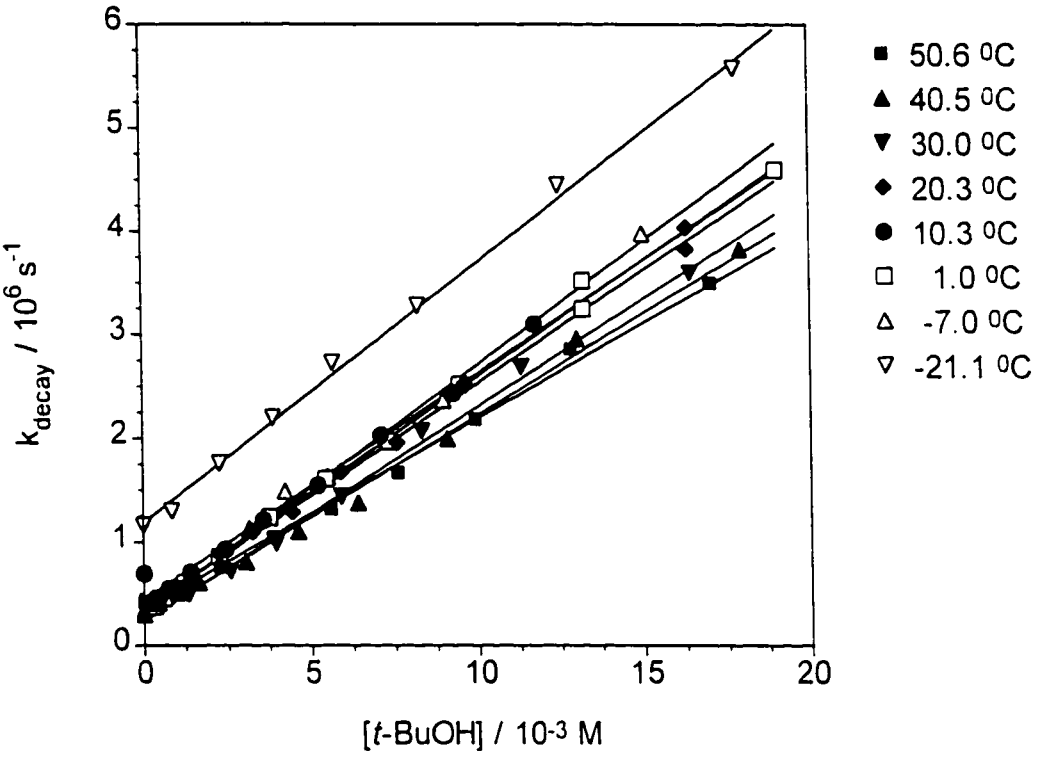

Table 6.4. Rate Constants for the Addition of *t*-BuOH to 1,1-Diphenylsilene (**12a**) in MeCN Solution from -21.1 to 50.6 °C.

Disk	Experiment	Temperature (°C)	$k_q / 10^8$ ($M^{-1} s^{-1}$)
DAT054	PHSCB0*.082	-21.1 ± 0.3	2.54 ± 0.11
DAT054	PHSCB0*.070	-7.0 ± 0.3	2.41 ± 0.10
DAT054	PHSCB0*.071	1.0 ± 0.3	2.33 ± 0.07
DAT054	PHSCB0*.080	10.3 ± 0.3	2.29 ± 0.06
DAT054	PHSCB0*.079	20.3 ± 0.3	2.20 ± 0.08
DAT054	PHSCB0*.081	30.0 ± 0.3	2.09 ± 0.12
DAT054	PHSCB0*.072	40.5 ± 0.3	2.00 ± 0.10
DAT054	PHSCB0*.076	50.6 ± 0.3	1.91 ± 0.09

[a] Errors are reported as twice the standard deviation of least squares analysis of decay-rate concentration data according to eq 2.10.

Figure 6.13. Plots of k_{decay} versus acetic acid concentration, from laser flash photolysis of air-saturated solutions 1,1-diphenylsilacyclobutane (**11a**) in acetonitrile solution from -20.5 to 50.6 °C.

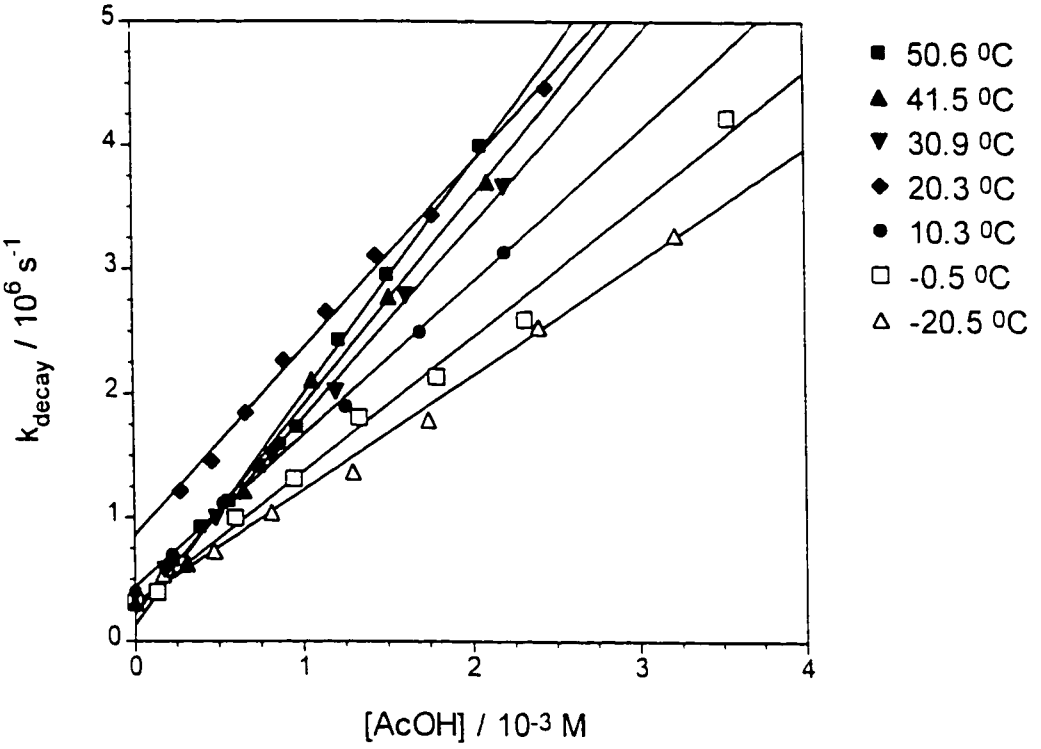

Table 6.5. Rate Constants for the Addition of Acetic Acid to 1,1-Diphenylsilene (**12a**) in MeCN Solution from -20.5 to 50.6 °C.[a]

Disk	Experiment	Temperature (°C)	k_q / 10^9 (M^{-1} s^{-1})
DAT054	PHSCB0*.077	-20.5 ± 0.3	0.92 ± 0.04
DAT054	PHSCB0*.067	-0.5 ± 0.3	1.08 ± 0.06
DAT054	PHSCB0*.068	10.3 ± 0.3	1.22 ± 0.06
DAT054	PHSCB0*.074	20.3 ± 0.3	1.50 ± 0.09
DAT054	PHSCB0*.073	30.9 ± 0.3	1.54 ± 0.06
DAY054	PHSCB0*.069	41.5 ± 0.3	1.68 ± 0.11
DAT054	PHSCB0*.075	50.6 ± 0.3	1.85 ± 0.11

[a] Errors are reported as twice the standard deviation of least squares analysis of decay-rate concentration data according to eq 2.10.

Figure 6.14. Plots of k_{decay} versus methanol concentration, from laser flash photolysis of air-saturated solutions 1,1-di-(4-methylphenyl)silacyclobutane (**11b**) in acetonitrile solution from -15.8 to 56.5 °C.

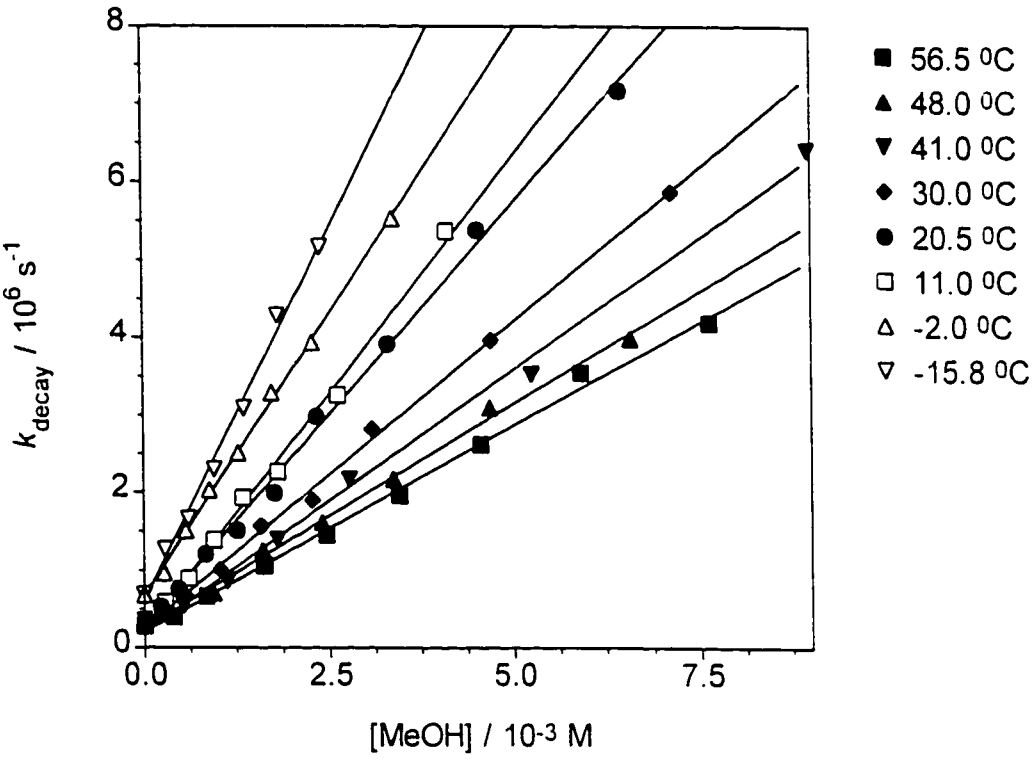

Table 6.6. Rate Constants for the Addition of Methanol to 1,1-Di-(4-methylphenyl)silene (**12b**) in MeCN Solution from -15.8 to 56.5 °C.[a]

Disk	Experiment	Temperature (°C)	$k_q / 10^9$ ($M^{-1} s^{-1}$)
DAT052	4MECB0*.026	-15.8 ± 0.3	1.91 ± 0.14
DAT052	4MECB0*.023	-2.0 ± 0.3	1.45 ± 0.05
DAT052	4MECB0*.024	11.0 ± 0.3	1.14 ± 0.06
DAT052	4MECB0*.027	20.5 ± 0.3	1.09 ± 0.04
DAT052	4MECB0*.025	30.0 ± 0.3	0.83 ± 0.03
DAT052	4MECB0*.022	41.0 ± 0.3	0.68 ± 0.02
DAT052	4MECB0*.021	48.0 ± 0.3	0.58 ± 0.03
DAT070	4MECB0*.035	56.5 ± 0.3	0.53 ± 0.03

[a] Errors are reported as twice the standard deviation of least squares analysis of decay-rate concentration data according to eq 2.10.

Figure 6.15. Plots of k_{decay} versus methanol concentration, from laser flash photolysis of air-saturated solutions 1,1-di-(4-trifluoromethylphenyl)silacyclobutane (**11e**) in acetonitrile solution from -21.0 to 55.0 °C.

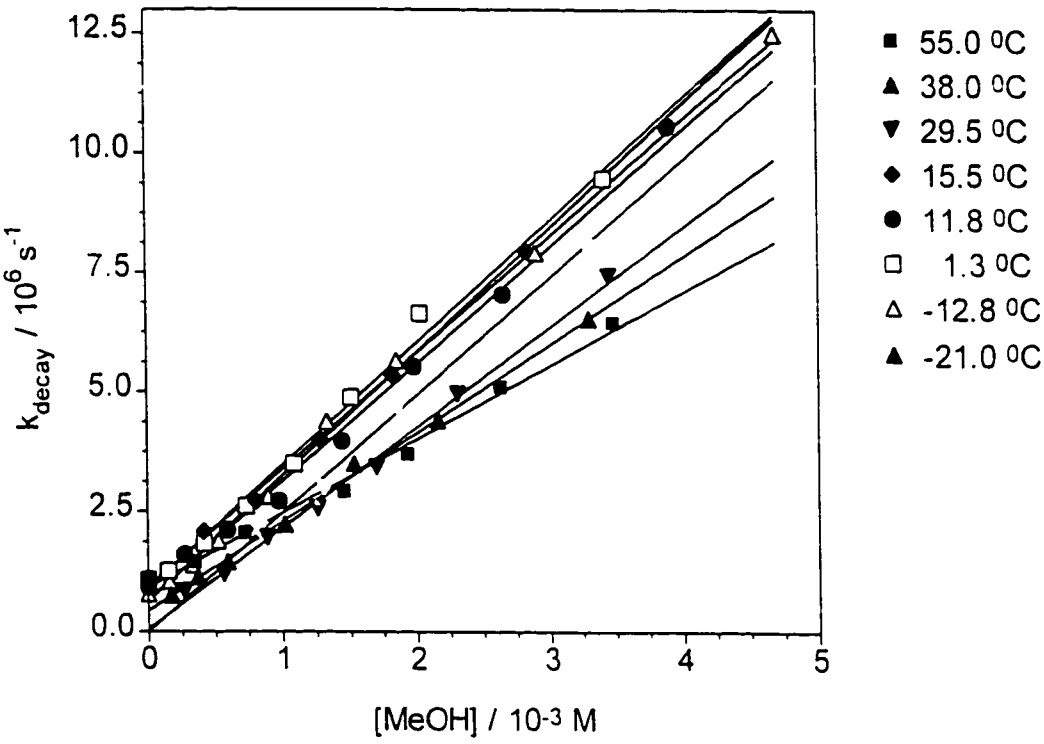

Table 6.7. Rate Constants for the Addition of Methanol to 1,1-Di-(4-trifluoromethylphenyl)silene (**12e**) in MeCN Solution from -21.0 to 55.0 °C.[a]

Disk	Experiment	Temperature (°C)	$k_q / 10^9$ ($M^{-1} s^{-1}$)
DAT052	CF3CB0*.025	-21.0 ± 0.3	2.48 ± 0.20
DAT052	CF3CB 0*.023	-12.8 ± 0.3	2.66 ± 0.16
DAT052	CF3CB0*.024	-12.8 ± 0.3	2.60 ± 0.09
DAT052	CF3CB 0*.020	1.3 ± 0.3	2.57 ± 0.18
DAT052	CF3CB 0*.021	11.8 ± 0.3	2.49 ± 0.17
DAT052	CF3CB 0*.026	15.5 ± 0.3	2.45 ± 0.12
DAT061	CF3CB0*.012	23.0 ± 0.3	2.99 ± 0.16
DAT052	CF3CB 0*.018	29.5 ± 0.3	1.94 ± 0.09
DAT052	CF3CB 0*.019	38.0 ± 0.3	1.86 ± 0.09
DAT070	CF3CB 0*.031	55.0 ± 0.3	1.55 ± 0.12

[a] Errors are reported as twice the standard deviation of least squares analysis of decay-rate concentration data according to eq 2.10.

Figure 6.16. Plots of k_{decay} versus acetic acid concentration, from laser flash photolysis of air-saturated solutions 1,1-di-(4-trifluoromethylphenyl)silacyclobutane (**11e**) in acetonitrile solution from -13.0 to 50.0 °C.

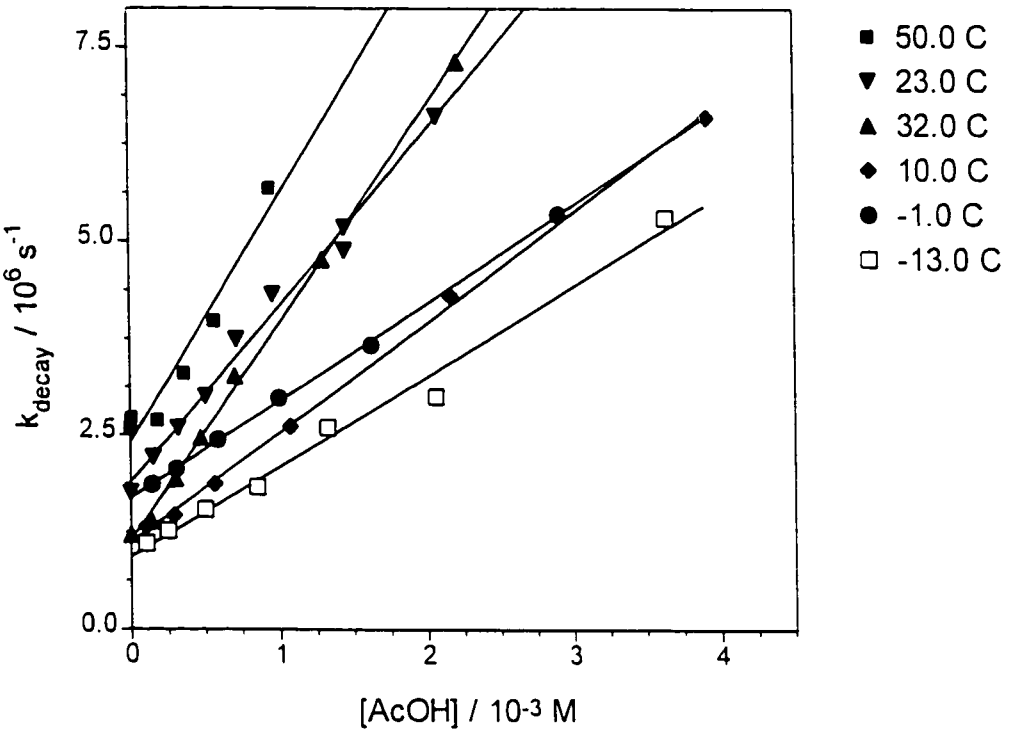

Table 6.8. Rate Constants for the Addition of Acetic Acid to 1,1-Di-(4-trifluoromethylphenyl)silene (**12e**) in Acetonitrile Solution from -13.0 to 50.0 °C.

Disk	Filename	Temperature (°C)	k_q / 10^9 $M^{-1}s^{-1}$
DAT072	CF3CB0*.048	-13.0 ± 0.3	1.17 ± 0.10
DAT072	CF3CB0*.049	-1.0 ± 0.3	1.26 ± 0.03
DAT072	CF3CB0*.047	10.0 ± 0.3	1.74 ± 0.16
DAT 061	CF3CB0*.013	23.0 ± 0.3	2.34 ± 0.10
DAT072	CF3CB0*.050	32.0 ± 0.3	2.81 ± 0.11
DAT072	CF3CB0*.051	50.0 ± 0.3	3.94 ± 0.46

[a] Errors are reported as twice the standard deviation of least squares analysis of decay-rate concentration data according to eq 2.10.

Figure 6.17. Plots of k_{decay} versus acetone concentration, from laser flash photolysis of air-saturated solutions 1,1-diphenylsilacyclobutane (**11a**) in acetonitrile solution from -15.8 to 49.5 °C.

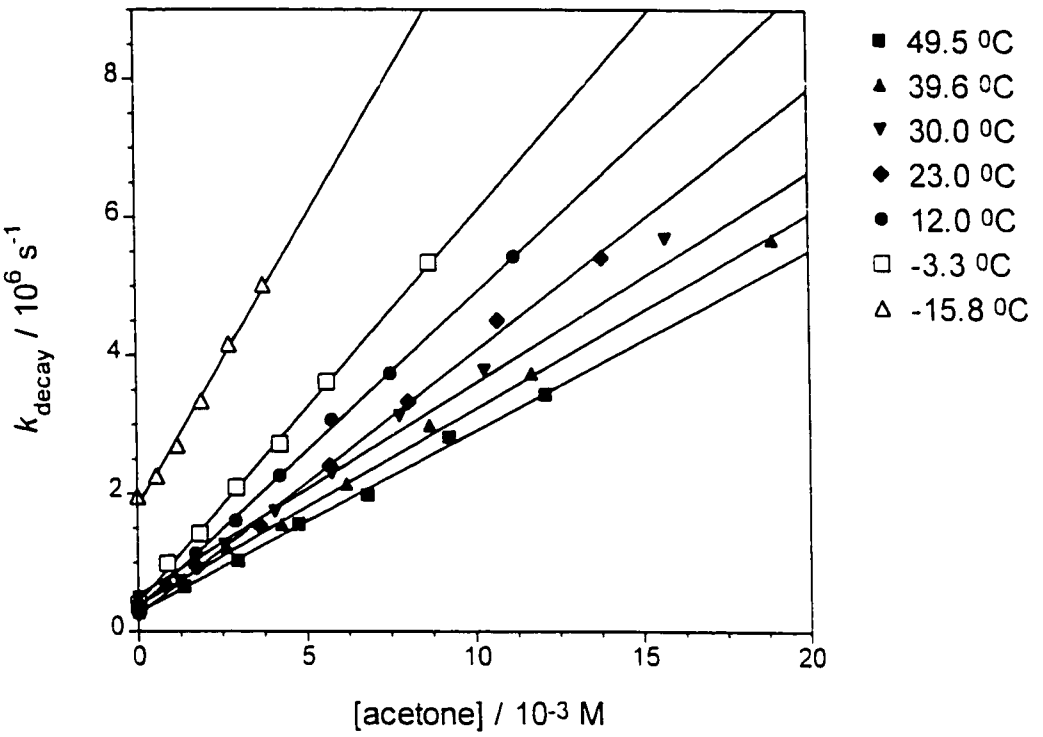

Table 6.9. Rate Constants for the Addition of Acetone to 1,1-Diphenylsilene (**12a**) in Hexane Solution from -15.8 to 49.5 °C.[a]

Disk	Filename	Temperature (°C)	k_q / 10^8 $M^{-1}s^{-1}$
DAT061	PHSICB0*.102	49.5 ± 0.3	2.63 ± 0.13
DAT061	PHSICB0*.101	39.6 ± 0.3	2.84 ± 0.11
DAT061	PHSICB0*.103	30.0 ± 0.3	2.99 ± 0.13
DAT061	PHSICB0*.097	23.0 ± 0.3	3.81 ± 0.16
DAT061	PHSICB0*.105	12.0 ± 0.3	4.55 ± 0.12
DAT061	PHSICB0*.104	-3.3 ± 0.3	5.63 ± 0.16
DAT070	PHSICB0*.112	-15.8 ± 0.3	8.36 ± 0.64

[a] Errors are reported as twice the standard deviation of least squares analysis of decay-rate concentration data according to eq 2.10.

Figure 6.18. Plots of k_{decay} versus acetone concentration, from laser flash photolysis of air-saturated solutions 1,1-diphenylsilacyclobutane (**11a**) in acetonitrile solution from -13.5 to 50.0 °C.

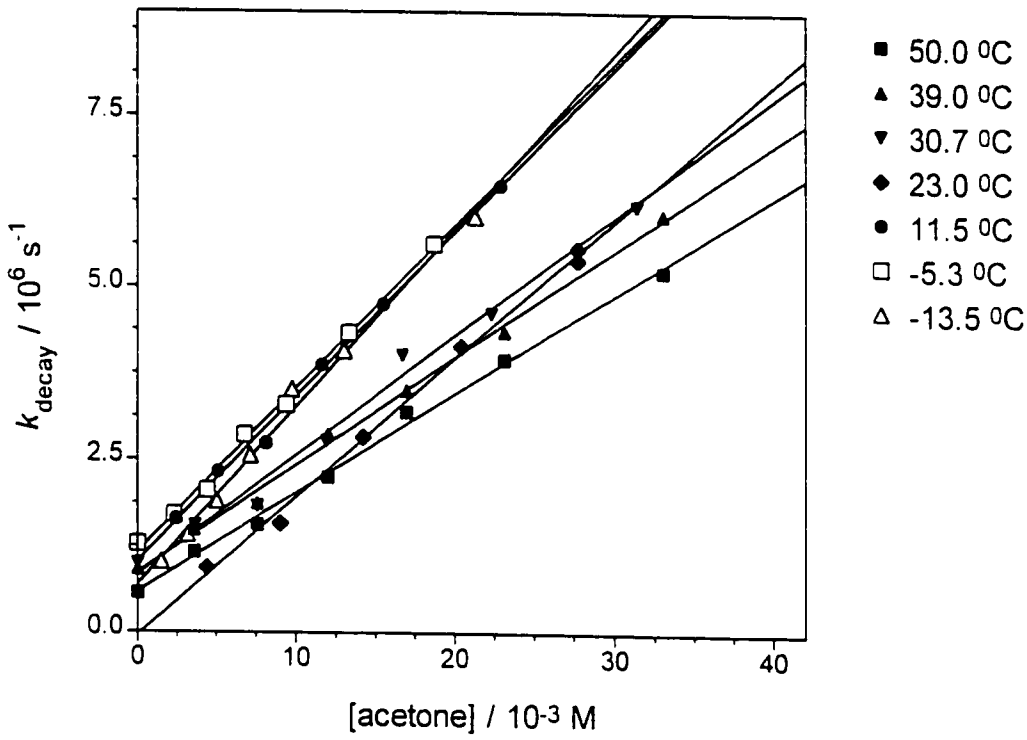

Table 6.10. Rate Constants for the Addition of Acetone to 1,1-Diphenylsilene (**12a**) in MeCN Solution from -13.5 to 50.0 °C.[a]

Disk	Filename	Temperature (°C)	$k_q / 10^8$ $M^{-1}s^{-1}$
DAT061	PHSICB0*.107	50.0 ± 0.3	1.43 ± 0.08
DAT061	PHSICB0*.106	39.0 ± 0.3	1.56 ± 0.09
DAT061	PHSICB0*.108	30.7 ± 0.3	1.73 ± 0.10
DAT034	PHSICB0*.001	23.0 ± 0.3	1.94 ± 0.16
DAT061	PHSICB0*.110	11.5 ± 0.3	2.39 ± 0.15
DAT061	PHSICB0*.109	-5.3 ± 0.3	2.37 ± 0.13
DAT070	PHSICB0*.111	-13.5 ± 0.3	2.57 ± 0.20

[a] Errors are reported as twice the standard deviation of least squares analysis of decay-rate concentration data according to eq 2.10.

Figure 6.19. Plots of k_{decay} versus acetone concentration, from laser flash photolysis of air-saturated solutions 1,1-di-(4-methylphenyl)silacyclobutane (**11b**) in acetonitrile solution from -11.0 to 48.9 °C.

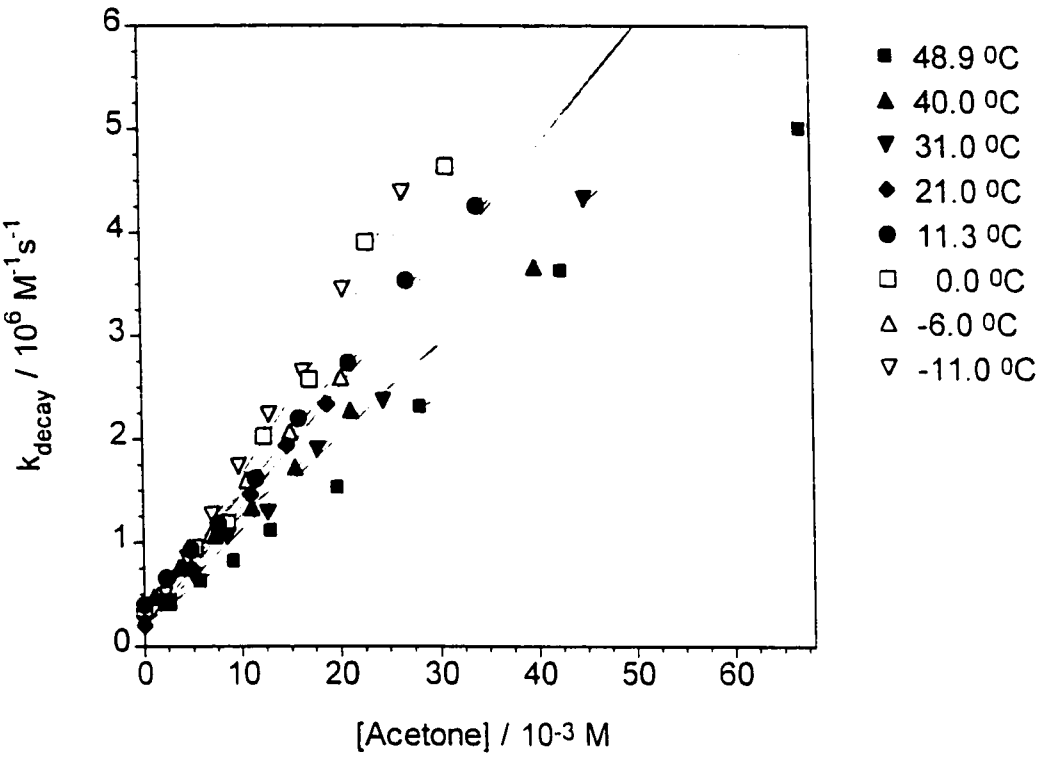

Table 6.11. Rate Constants for the Addition of Acetone to 1,1-Di-(4-methylphenyl)silene (**12b**) in MeCN Solution from -10.8 to 48.9 °C.

Disk	Filename	Temperature (°C)	$k_q/10^8$ $M^{-1}s^{-1}$
DAT052	4MECB0*.031	48.9 ± 0.3	0.74 ± 0.04
DAT052	4MECB0*.030	40.0 ± 0.3	0.82 ± 0.03
DAT052	4MECB0*.032	31.0 ± 0.3	0.91 ± 0.04
DAT052	4MECB0*.033	23.0 ±0.3	1.02 ± 0.14
DAT034	4MECB0*.010	21.0 ± 0.3	1.16 ± 0.32
DAT070	4MECB0*.036	11.5 ± 0.3	1.15 ± 0.04
DAT052 / DAT070	4MECB0*.034	0.0 ± 0.3	1.49 ± 0.15
DAT070	4MECB0*.039	-10.8 ± 0.3	1.59 ± 0.05

[a] Errors are reported as twice the standard deviation of least squares analysis of decay-rate concentration data according to eq 2.10.

Figure 6.20. Plots of k_{decay} versus acetone concentration, from laser flash photolysis of air-saturated solutions 1,1-di-(4-trifluoromethylphenyl)silacyclobutane (**11e**) in acetonitrile solution from -13.2 to 50.1 °C.

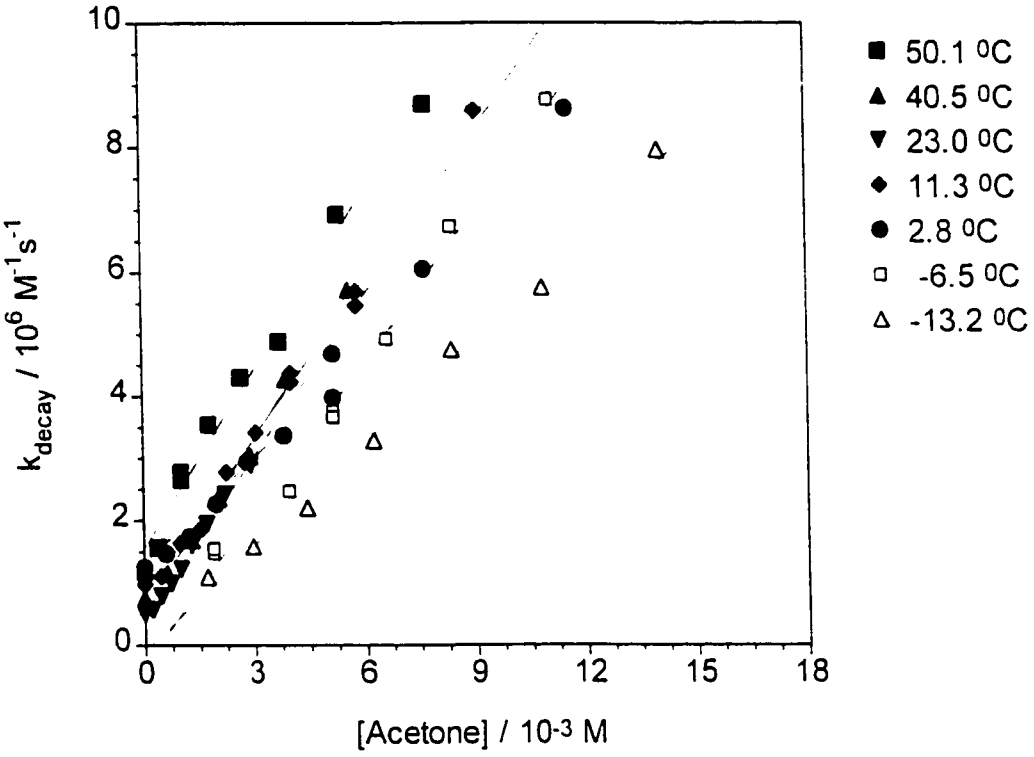

Table 6.12. Rate Constants for the Addition of Acetone to 1,1-Di-(4-trifluoromethylphenyl)silene (**12e**) in MeCN Solution from -13.2 to 50.1 °C.

Disk	Filename	Temperature (°C)	$k_q/10^8$ $M^{-1}s^{-1}$
DAT070	CF3CB0*.030	50.1 ± 0.3	9.66 ± 0.08
DAT070	CF3CB0*.032	40.5 ± 0.3	9.14 ± 0.60
DAT070	CF3CB0*.0	23.0 ± 0.3	8.73 ± 0.50
DAT070	CF3CB0*.029	11.3 ± 0.3	8.51 ± 0.34
DAT070	CF3CB0*.027	-6.5 ± 0.3	7.73 ± 0.70
DAT070	CF3CB0*.035	-13.2 ± 0.3	5.62 ± 0.38

[a] Errors are reported as twice the standard deviation of least squares analysis of decay-rate concentration data according to eq 2.10.

Figure 6.21. Plots of k_{decay} versus acetone concentration, from laser flash photolysis of air-saturated solutions 1,1-di-(4-trifluoromethylphenyl)silacyclobutane (**11e**) in acetonitrile solution from -14.5 to 53.5 °C.

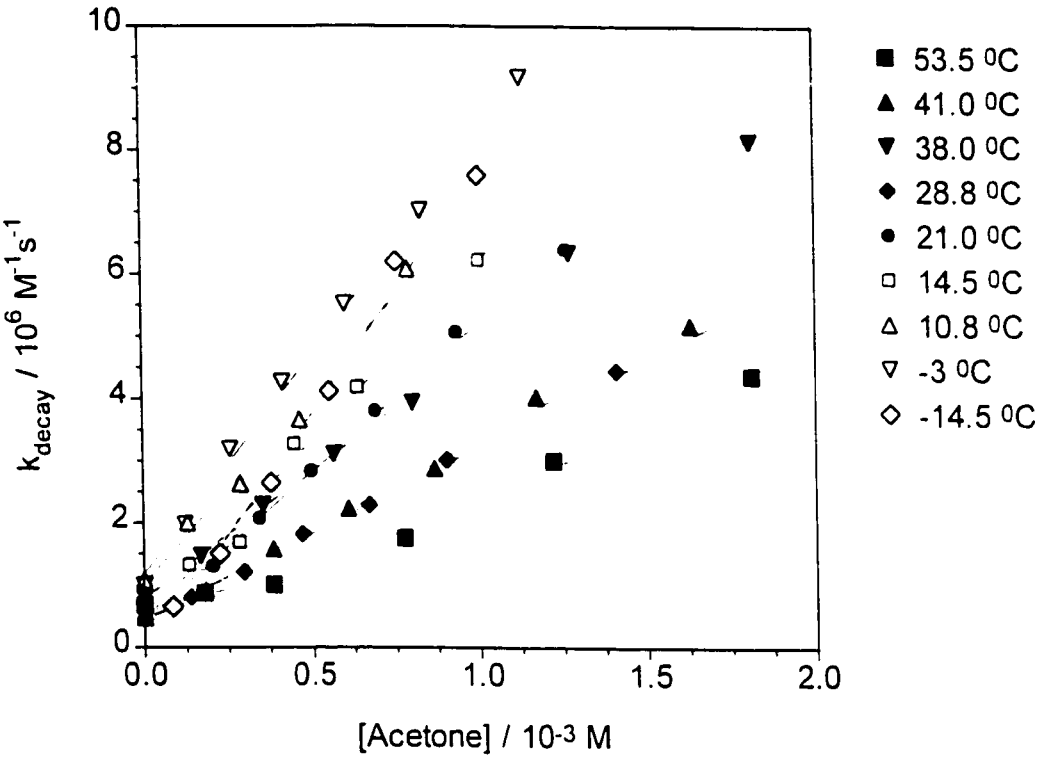

Table 6.13. Rate Constants for the Addition of Acetone to 1,1-Di-(4-trifluoromethylphenyl)silene (**12e**) in Hexane Solution from -14.5 to 53.5 °C.[a]

Disk	Filename	Temperature (°C)	$k_q/10^9$ $M^{-1}s^{-1}$
DAT070	CF3CB0*.036	53.5 ± 0.3	2.09 ± 0.17
DAT070	CF3CB0*.037	38.0 ± 0.3	4.14 ± 0.20
DAT070	CF3CB0*.041	41.0 ± 0.3	2.94 ± 0.13
DAT070	CF3CB0*.040	28.8 ± 0.3	2.82 ± 0.06
DAT070	CF3CB0*.044	21.0 ± 0.3	4.83 ± 0.18
DAT070	CF3CB0*.042	14.5 ± 0.3	5.81 ± 0.06
DAT070	CF3CB0*.039	10.8 ± 0.3	6.20 ± 0.70
DAT070	CF3CB0*.038	-3.3 ± 0.3	7.14 ± 0.28
DAT070	CF3CB0*.043	-14.5 ± 0.3	7.92 ± 0.67

[a] Errors are reported as twice the standard deviation of least squares analysis of decay-rate concentration data according to eq 2.10.

Table 6.14. Rate Constants for the Addition of Acetone to 1-Methyl-1-phenylsilene (**23b**) in Hexane Solution from -13.3 to 48.5 °C.[a]

Disk	Filename	Temperature (°C)	k_q / 10^8 $M^{-1}s^{-1}$
DAT072	MEPHSI0*.032	48.5 ± 0.3	2.37 ± 0.19
DAT072	MEPHSI0*.033	39.6 ± 0.3	2.72 ± 0.15
DAT051	MEPHSI0*.003	23.0 ± 0.3	3.57 ± 0.12
DAT072	MEPHSI0*.034	5.5 ± 0.3	4.63 ± 0.36
DAT072	MEPHSI0*.035	-4.2 ± 0.3	5.17 ± 0.40
DAT072	MEPHSI0*.036	-13.3 ± 0.3	5.13 ± 0.30

[a] Errors are reported as twice the standard deviation of least squares analysis of decay-rate concentration data according to eq 2.10.

Figure 6.23. Plots of k_{decay} versus acetone concentration, from laser flash photolysis of air-saturated solutions 1-methyl-1-phenylsilacyclobutane (**22b**) in MeCN solution from -11.2 to 50.6 °C.

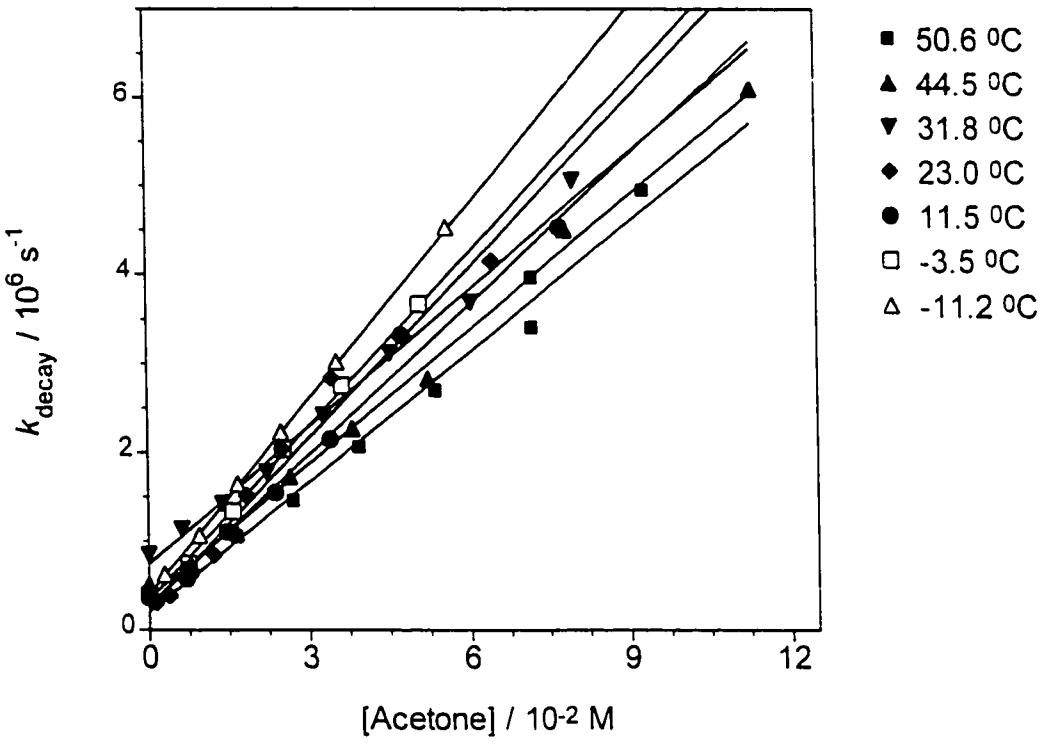

Table 6.15. Rate Constants for the Addition of Acetone to 1-Methyl-1-phenylsilene (**23b**) in MeCN Solution from -11.2 to 50.6 °C.[a]

Disk	Filename	Temperature (°C)	k_q / 10^7 $M^{-1}s^{-1}$
DAT070	MEPHSI0*.024	50.6 ± 0.3	4.92 ± 0.5
DAT070	MEPHSI0*.028	44.5 ± 0.3	5.08 ± 0.25
DAT070	MEPHSI0*.025	31.8 ± 0.3	5.17 ± 0.35
DAT061	MEPHSI0*.020	23.0 ± 0.3	4.80 ± 0.20
DAT070	MEPHSI0*.027	11.5 ± 0.3	6.19 ± 0.7
DAT070	MEPHSI0*.026	-3.5 ± 0.3	6.59 ± 0.26
DAT070	MEPHSI0*.029	-11.2 ± 0.3	7.39 ± 0.09

[a] Errors are reported as twice the standard deviation of least squares analysis of decay-rate concentration data according to eq 2.10.

Figure 6.24. Plots of k_{decay} versus trimethylmethoxysilane concentration, from laser flash photolysis of air-saturated solutions 1,1-diphenylsilacyclobutane (**11a**) in hexane solution from -3.0 to 51.0 °C.

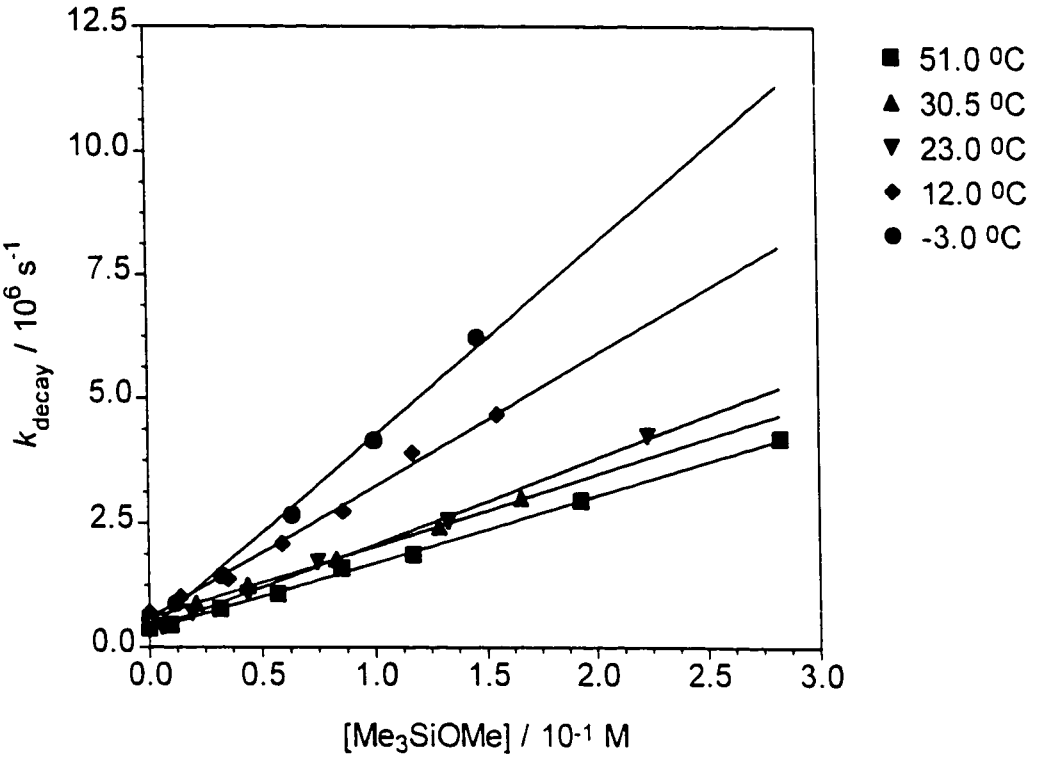

Table 6.16. Rate Constants for the Addition of Trimethylmethoxysilane 1,1-Diphenylsilacyclobutane (**11a**) in Hexane Solution from -3.0 to 51.0 °C.[a]

Disk	Filename	Temperature (°C)	k_q / 10^7 $M^{-1}s^{-1}$
DAT072	PHSCB0*.120	-3.0 ± 0.3	3.80 ± 0.37
DAT072	PHSCB0*.121	12.0 ± 0.3	2.66 ± 0.20
DAT070	PHSICB0*.115	23.0 ± 0.3	1.73 ± 0.07
DAT072	PHSCB0*.122	30.5 ± 0.3	1.33 ± 0.10
DAT072	PHSCB0*.123	40.0 ± 0.3	1.45 ± 0.03
DAT070/DAT072	PHSCB0*.119	51.0 ± 0.3	1.36 ± 0.04

[a] Errors are reported as twice the standard deviation of least squares analysis of decay-rate concentration data according to eq 2.10.

REFERENCES

(1) Gusel'nikov, L. E.; Flowers, M. C. *J. Chem. Soc., Chem. Commun.* **1967**, 864.

(2) Raabe, G.; Michl, J. *Chem. Rev.* **1985**, *85*, 419.

(3) Brook, A. G.; Baines, K. M. *Adv. Organomet. Chem.* **1986**, *25*, 1

(4) Grev, R. S. *Adv. Organomet. Chem* **1991**, *33*, 125.

(5) Brook, A. G.; Brook, M. A. *Adv. Organomet. Chem.* **1996**, *39*, 71.

(6) Wiberg, N. *J. Organomet. Chem.* **1984**, *273*, 141.

(7) Zhang, S.; Conlin, R. T.; McGarry, P. F.; Scaiano, J. C. *Organometallics* **1992**, *11*, 2317.

(8) Leigh, W. J.; Bradaric, C. J.; Sluggett, G. W. *J. Am. Chem. Soc.* **1993**, *115*, 5332.

(9) Sluggett, G. W.; Leigh, W. J. *J. Am. Chem. Soc.* **1992**, *114*, 1195.

(10) Bradaric, C. J.; Leigh, W. J. *Can. J. Chem.* **1997**, in press.

(11) Apeloig, Y.; Karni, M. *J. Am. Chem. Soc.* **1984**, *106*, 6676.

(12) Wiberg, N.; Wagner, G.; Reber, G.; Riede, J.; Muller, G. *Organometallics* **1987**, *6*, 35.

(13) Brook, A. G.; Harris, J. W.; Lennon, J.; El Sheikh, M. *J. Am. Chem. Soc.* **1979**, *83*, 83.

(14) Baines, K. M.; Brook, A. G.; Ford, R. R.; Lickiss, P. D.; Saxena, A. K.;

Chatterton, W. J.; Sawyer, J. F.; Behnam, B. A. *Organometallics* **1989**, *8*, 693.

(15) Strausz, O. P.; Gammie, L.; Theodorakoupoulos, G.; Mezey, P. G.; Csizmadia, I. G. *J. Am. Chem. Soc.* **1976**, *98*, 1622.

(16) Goddard, J. D.; Yoshioka, Y.; Schaefer, H. F. *J. Am. Chem. Soc.* **1980**, *102*, 7644.

(17) Ahlrichs, R.; Heinzmann, R. *J. Am. Chem. Soc.* **1977**, *99*, 7452.

(18) Gordon, M. S.; Koob, R. D. *J. Am. Chem. Soc.* **1981**, *103*, 2939.

(19) Schmidt, M.W. *J. Am. Chem. Soc.* **1985**, *107*, 2585.

(20) Sekiguchi, A.; Ando, W. *Organometallics* **1987**, *6*, 1857.

(21) Vollhardt, K.P.C. *Organic Chemistry*; W.H. Freeman and Company: New York, 1987; pp 206, 740,424.

(22) Nagase, S.; Kudo, T.; Ito, K. *Applied Quantum Chemistry* **1986**, 249.

(23) Boudjouk, P.; Sommer, L. H. *J. Chem. Soc., Chem. Comm.* **1973**, 54.

(24) Steinmetz, M. G.; Udayakumar, B. S. *Organometallics* **1989**, *8*, 530.

(25) Ando, W.; Sekiguchi, A.; Sato, T. *J. Am. Chem. Soc.* **1982**, *104*, 6830.

(26) Ando, W.; Sekiguchi, A.; Sato, T. *Organometallics* **1981**, *103*, 5537.

(27) Sekiguchi, A.; Sato, T.; Ando, W. *Organometallics* **1987**, *6*, 2337.

(28) Jones, P. R.; Lim, T. F. *J. Am. Chem. Soc.* **1977**, *99*, 2013.

(29) Leigh, W. J.; Bradaric, C. J.; Kerst, C.; Banisch, J. A. H. *Organometallics* **1996**, *15*, 2246.

(30) Leigh, W. J.; Sluggett, G. W. *Organometallics* **1994**, *13*, 269.

(31) Jones, P. R.; Bates, T. F. *J. Am. Chem. Soc.* **1986**, *108*, 3122.

(32) Jones, P. R.; Bates, T. F. *J. Am. Chem. Soc.* **1987**, *109*, 913.

(33) Barton, T. J.; Burns, S. A.; Burns, G. T. *Organometallics* **1982**, *1*, 210.

(34) Boudjouk, P.; Roberts, J. R.; Golino, C. M.; Sommer, L. H. *J. Am. Chem. Soc.* **1972**, *94*, 7926.

(35) Sluggett, G. w.; Leigh, W. J. *Organometallics* **1992**, *11*, 3731.

(36) Toltl, N. P.; Leigh, W. J. *Organometallics* **1996**, *15*, 2554.

(37) Sakurai, H.; Kamiyama, Y.; Kakadaira, Y. *J. Am. Chem. Soc.* **1976**, *98*, 7424.

(38) Jutzi, P.; Langer, P. *J. Organomet. Chem.* **1980**, *202*, 401.

(39) Valkovich, P. B.; Ito, T. I.; Weber, W. P. *J. Org. Chem.* **1974**, *39*, 3543.

40) Seidl, E. T.; Grev, R. S.; Schaefer, H. F. *J. Am. Chem. Soc.* **1992**, *114*, 3643.

(41) Bernardi, F.; Bottoni, A.; Olivucci, M.; Venturini, A.; Robb, M. A. *J. Chem. Soc. Faraday Trans.* **1994**, *90*, 1617.

(42) Brook, A. G. In *The Chemistry of Organic Silicon Compounds*; Patai, S., Rappoport, Z., Eds.; John Wiley & Sons Ltd.: 1989; pp 965-1005.

(43) Sekiguchi, A.; Maruki, I.; Sakurai, H. *J. Am. Chem. Soc.* **1993**, *115*, 11460.

(44) Leigh, W. J.; Sluggett, G. W. *J. Am. Chem. Soc.* **1994**, *116*, 10468.

(45) Bradaric, C. J.; Leigh, W. J. *J. Am. Chem. Soc.* **1996**, *118*, 8971.

(46) Brook, A. G.; Safa, K. D.; Lickiss, P. D.; Baines, K. M. *J. Am. Chem. Soc.* **1985**, *107*, 4339.

(47) Kira, M.; Maruyama, T.; Sakurai, H. *J. Am. Chem. Soc.* **1991**, *113*, 3986.

(48) Fink, M. J.; Puranik, D. B.; Johnson, M. P. *J. Am. Chem. Soc.* **1988**, *110*, 1315.

(49) Sluggett, G. W. Ph.D. Thesis, McMaster University, 1993.

(50) Davidson, I. M. T.; Wood, I. T. *J. Chem. Soc., Chem. Commun.* **1982**, 550.

(51) Ishikawa, M.; Nishimura, Y.; Sakamoto, H. *Organometallics* **1991**, *10*, 2701.

(52) Roark, D. N.; Sommer, L. H. *J. Chem. Soc., Chem. Comm.* **1973**, 167.

(53) Golino, C. M.; Bush, R. D.; Sommer, L. H. *J. Organomet. Chem.* **1974**, *66*, 29.

(54) Brook, A. G.; Chatterton, W. J.; Sawyer, J. F.; Hughes, D. W.; Vorspohl, K. *Organometallics* **1987**, *6*, 1246.

(55) Brook, A. G.; Hu, S. S.; Saxena, A. K.; Lough, A. J. *Organometallics* **1991**, *10*, 2758.

(56) Brook, A. G.; Hu, S. S.; Chatterton, W. J.; Lough, A. J. *Organometallics* **1991**, 2752.

(57) Wiberg, N.; Preiner, G.; Scheida, O. *Chem. Ber.* **1981**, *114*, 3518.

(58) Steinmetz, M. G.; Bai, H. *Organometallics* **1989**, *8*, 1112.

(59) Banisch, J.H. M.Sc. Thesis, McMaster University, 1995.

(60) Auner, N.; Grobe, J. *J. Organomet. Chem.* **1980**, *188*, 25.

(61) Bertrand, G.; Dubac, J.; Mazerolles, P.; Ancelle, J. *Nouveau Journal de Chimie* **1982**, *6*, 381.

(62) Damrauer, R. *Organomet. Chem. Rev. A*, **1972**, *8*, 67.

(63) Leigh, W.J.; Banisch, J.H., unpublished results.

(64) Devine, A. M.; Griffin, P. A.; Haszeldine, R. N.; Newlands, M. J.; Tipping, A. E. *J. Chem. Soc., Dalton Trans.* **1975**, 1822.

(65) Leigh, W. J.; Workentin, M. S.; Andrew, D. J. *J. Photochem. Photobiol. A: Chem.* **1991**, *57*, 97.

(66) Bradaric, C. J.; Leigh, W. J. *Organometallics* **1997**, in press.

(67) Sluggett, G. W.; Leigh, W. J. *Organometallics* **1994**, *13*, 1005.

(68) Izutsu, K. *Chemical Data Series* **1990**, *35*, 1-37.

(69) Melander, L.; Saunders, W. H. *Reaction Rates of Isotopic Molecules*; Wiley Interscience: New York, 1980

(70) Scaiano, J. C. In *CRC Handbook of Photochemistry, Vol III*; Scaiano, J.C., Eds. CRC Press: Boca Raton, 1989; pp 343-346.

(71) Moss, R. A. *Acc. Chem. Res.* **1989**, *22*, 15.

(72) Turro, T. J.; Cha, Y.; Gould, I. R. *Tettrahedron Lett.* **1985**, *26*, 5951.

(73) Griller, D.; Nazran, A. S.; Scaiano, J. C. *J. Am. Chem. Soc.* **1984**, *106*, 198.

(74) Zupancic, J. J.; Grasse, P. B.; Lapin, S. C.; Schuster, G. B. *Tetrahedron* **1985**, *41*, 1471.

(75) Turro, T. J.; Okamoto, M.; Gould, I. R.; Moss, R. A.; Lawrynowicz, W.; Hadel, L. M. *J. Am. Chem. Soc.* **1987**, *109*, 4973.

(76) Moss, R. A.; Lawrynowicz, W.; Turro, T. J.; Gould, I. R.; Cha, Y. *J. Am. Chem. Soc.* **1986**, *108*, 7028.

(77) Turro, T. J.; Lehr, G. F.; Butcher, Jr.; Moss, R. A.; Guo, W. *J. Am. Chem. Soc.* **1982**, *104*, 1754.

(78) Jackson, J. E.; Soundararajan, N.; Platz, M. S.; Doyle, M. P.; Liu, M. T. H. Te*trahedron Lett.* **1989**, *30*, 1335.

(79) Mayr, H.; Schneider, R.; Grabis, U. *J. Am. Chem. Soc.* **1990**, *112*, 4460.

(80) Blitz, M. A.; Frey, H. M.; Tabbutt, F. D.; Walsh, R. *J. Phys. Chem.* **1990**, *94*, 3294.

(81) Becerra, R.; Walsh, R. *Int. J. Chem. Kin.* **1994**, *26*, 45.

(82) Houk, K. N.; Rondan, N. G. *J. Am. Chem. Soc.* **1984**, *106*, 4293.

(83) Houk, K. N.; Rondan, N. G.; Mareda, J. *J. Am. Chem. Soc.* **1984**, *106*, 4291.

(84) Nagase, S.; Kudo, T.; Ito, K. *Applied Quantum Chemistry*; D. Reidel: Dordrecht, 1986; pp 249-267.

(85) Melander, L. *Acta. Chem. Scand.* **1971**, *25*, 3821.

(86) Chiltz, G.; Eckling, P.; Goldfinger, P.; Huybrechts, G.; Johnstonnn, H.S.; Meyers, L. Verbcke, G. *J. Chem. Phys.* **1963**, *38*, 1053.

(87) Caldin, E.; Gold, V. *Proton-Transfer Reactions*; Chapman and Hall: London, 1975; pp 250-254.

(88) McClure, D. S.; Blake, N. W.; Hanst, P. L. *J. Chem. Phys.* **1954**, *22*, 255.

(89) Ermolaev, V. L.; Svitashev, K. J. *Opt. Spect.* **1959**, *7*, 399.

(90) Patai, S. In *The Chemistry of Alkenes*; Patai, S. Eds.; Interscience Publishers:, Great Britain 1964; pp 481-491.

(91) Gross, Z.; Hoz, S. *J. Am. Chem. Soc.* **1988**, *110*, 7489.

(92) Bernasconi, C. F.; Renfrow, R. A.; Tia, P. R. *J. Am. Chem. Soc.* **1986**, *108*, 4541.

(93) Kamlet, M. J.; Glover, D. J. *J. Am. Chem. Soc.* **1956**, *78*, 4556.

(94) Gorman, A. A.; Lovering, G.; Rodgers, M. A. J. *J. Am. Chem. Soc.* **1979**, *101*, 3030.

(95) Maharaj, U.; Winnik, M. A. *J. Am. Chem. Soc.* **1981**, *103*, 2328.

(96) Kirk, .; Othmer, D.F. *Encyclopedia of Chemical Technology*; Herman, F.; Othmer, D.F.; Overberger, C.G.; Seaborg, G., Eds.; John Wiley & Sons: U.S.A, 1983; pp 388-390.

(97) Apeloig, Y.; Nakash, M. *J. Am. Chem. Soc.* **1996**, *118*, 9798.

(98) Bertrand, G.; Dubac, J.; Mazerolles, P.; Ancelle, J. *J. Chem. Soc., Chem. Comm.* **1980**, 382.

(99) Krempner, C.; Hoffman, D.; Oehme, H.; Kempe, R. *Organometallics* **1997**, *16* 1828.

(100) Sluggett, G. W.; Bradaric, C. J.; Venneri, P.; Leigh, W. J.; Conlin, R. T. *J. Organomet. Chem.* **1997**, in press.

(101) Sakamoto, H.; Ogasawara, J.; Sakurai, H.; Kira, M. *J. Am. Chem. Soc.* **1997**, *119*, 3405

(102) Voronkov, M. G.; Mileshkevich, V. P.; Yuzhelevskii, Y. A. *The Siloxane Bond Physical Properties and Chemical Transformations*; Consultants Bureau: New York, 1978; pp 55-74.

(103) HYPERCHEM 4.0. Hypercube Inc., 419 Philip Street, Waterloo, ON N2L 3X2, Canada.

(104) March, J. *Advanced Organic Chemistry*; John Wiley and Sons: New York, 1992; pp 269-271.

(105) Briggs, J. P.; Yamdagni, R.; Kebarle, P. *J. Am. Chem. Soc.* **1972**, *94*, 5128.

(106) Arnett, E. *Acc. Chem. Res.* **1973**, *6*, 404.

(107) Kebarle, P. *Ann. Rev. Phys. Chem.* **1977**, *28*, 445.

(108) Werstiuk, N. H.; Leigh, W. J. **1997**, unpublished results.

(109) Mangette, J. E.; Powell, D. R.; Firman, T. K.; West, R. *J. Organomet. Chem.* **1996**, *521*, 363.

(110) Mangette, J. E.; Powell, D. R.; Calabrese, J. C.; West, R. *Organometallics* **1995**, *14*, 4064.

(111) Blinka, T.A.; Helmer, B.J.; West, R. *Adv. Organomet. Chem.* **1984**, *23*, 193.

(112) Laane, J. *J. Am. Chem. Soc.* **1967**, *89*, 1144.

(113) Vdovin, V. M.; Nametkin, N. S.; Grinberg, P. L. *Dokl. Akad. Nauk. SSSR* **1963**, *150*, 799.

(114) Krapivin, A. M.; Magi, M.; Svergun, V. I.; Zaharjan, R. Z.,Babich *J. Organomet. Chem.* **1980**, *190*, 9.

(115) Hatchard, C. G.; Parker, C. A. *Proc. R. Soc.* **1956**, *235A*, 518.

(116) Bunce, N. J.; LaMarre, J.; Vaish, S. P. *Photochemistry and Photobiology* **1984**, *39*, 531.

(117) Rakita, P. E.; Srebro, J. P.; Worsham, L. S. *J. Organomet. Chem.* **1976**, *104*, 27.

(118) Brook, A. G.; Dillon, P. J. *Can. J. Chem.* **1969**, *47*, 4347.

(119) Caseri, W.; Pregosin, P. S. *Organometallics* **1988**, *7*, 1373.

(120) Sakurai, H.; Miyoshi, K.; Nakadaira, Y. *Tetrahedron Lett.* **1977**, *31*, 2671.

(121) Wang, W. D.; Eisenberg, R. *J. Am. Chem. Soc.* **1990**, *112*, 1833.